Effects of episodic sediment supply on channel adjustment of an experimental gravel bed

by

Maria A. Elgueta Astaburuaga

BA, Geography, Universidad de Chile, 2006

MSc, Geography, The University of British Columbia, 2014

A THESIS SUBMITTED IN PARTIAL FULFILLMENT
OF THE REQUIREMENTS FOR THE DEGREE OF

Doctor of Philosophy

in

THE FACULTY OF GRADUATE AND POSTDOCTORAL STUDIES
(Geography)

The University of British Columbia
(Vancouver)

March 2018

Abstract

A flume experiment was conducted to study channel adjustment of gravel beds to episodic sediment supply. The bed and sediment feed included grains 0.5–64 mm with geometric mean size 5.7 mm. Flow discharge was constant and every 40 h, 300 kg of sediment was supplied through different feed regimes. Sediment transport and storage, bed slope, and bed surface texture responded to sediment supply regime. The preferential storage of grains $> 8\,\mathrm{mm}$ caused a cumulative increase in bed slope, which probably increased transport efficiency. Within a run, sediment transport rate q_b and bed-surface texture were controlled by the magnitude and frequency of sediment feed and not the total mass. Constant feed promoted gradual increases in q_b and small changes in bed surface texture, whereas large infrequent sediment pulses caused pronounced increases in q_b and strong surface fining, followed by monotonic decreases in q_b as surface re-coarsened. Pronounced trends caused stronger memory in bedload time series for runs with episodic feed than in those for runs with constant feed, although within each run, the structure of memory varied. Long memory was observed for periods when bedload rate was nearly stable, which indicates that it could result from local changes in storage. Patterns of grain-size dependence were not affected by sediment feed and the limit for full-mobility was stable around 8 mm. Scaling statistics for total bedload were similar to those for fine gravel, which was fully-mobile and dominated bedload. A decrease in the frequency of movement with size for gravel fractions caused a reduction in the memory strength of fractional bedload signals. Size-selective transport promoted the storage of coarse grains upstream and downstream fining on the bed surface. Although fully-mobile, more than 60% of the sand fed got stored in the bed, probably because of its high potential to infiltrate and get caught within larger grains. Memory was weaker for sand bedload rates than for fine gravel, which indicates that sand mobility was more influenced by short-term stochastic dynamics (e.g., clustering) and less affected by long-term processes like the evolution of large bedforms and sediment pulses.

Lay summary

Sediment supply is a first order control in channel morphology and sediment transport regime in mountain streams. Although streams usually receive sediment episodically through natural and human induced mechanisms such as landslides, physical models have mostly used constant sediment feed to analyze the adjustments of gravel beds to changes in sediment supply regime. Here, the importance of the magnitude and frequency of sediment supply regimes is assessed by comparing the adjustments of an experimental gravel-bed to changes in sediment feed under constant water discharge. The experiment included constant feed and different episodic feed regimes for comparisons. The limitations of assuming constant feed in experiments and the scales and situations for which the assumption would be correct are discussed. Experimental runs were conducted as a sequence, in which some feed regimes were run twice to explore the effects of the initial bed on its adjustment.

Preface

The experiment was conducted in partnership with Claudia vonFlotow under the supervision of Marwan Hassan. All the analyses and writing in this manuscript were conducted by the author while working toward a PhD. A version of Chapter 2 has been published as *Elgueta-Astaburuaga and Hassan* (2017). For that paper, I conducted the analyses and wrote the manuscript, for both of which, Marwan Hassan provided guidance. A version of Chapter 3 has been submitted as *Elgueta-Astaburuaga et al.* (2017). Here, I was again responsible for data analyses and writing. Marwan Hassan, Matteo Saletti, and Garry Clarke provided guidance for methods, analyses, discussion, and writing. Chapter 4 was written as a paper to be submitted, in which I will be the first author and Marwan Hassan the second author. In this chapter, I completed the analyses and writing under M. Hassan's supervision.

Table of contents

List of tables

List of figures

List of symbols and acronyms

Roman symbols

Symbol	Definition
a	intercept for log–linear relation
AIC	Akaike information criterion
AR(1)	autoregressive order 1
b	slope for log–linear relation
b'	rate of decrease in sediment transport rate for Run 7
b_{1-4}	slopes for general least-squares model
c_τ	autocovariance at time lag τ
c_0	autocovariance at time lag $\tau = 0$
Cumulative $\overline{\delta}\eta_d$	cumulative mean change in bed elevation
Cumulative Δ_{T_n}	cumulative mass balance
d	chronological order of DEM
d_f	duration of sediment feed
D	total number of DEMs available
DEM	digital elevation model

D_g	geometric mean grain size
$D_{g\,(\text{bulk})}$	geometric mean grain size for bedload
$D_{g\,(\text{bulk})}$	geometric mean grain size for bulk sediment
$D_{g\,(\text{surface})}$	geometric mean grain size for bed surface
D_i	grain size i
D_{max}	maximum grain size
D_{16}	16th percentile of grain size distribution
D_{75}	75th percentile of grain size distribution
D_{90}	90th percentile of grain size distribution
f_i	grain size distribution for bulk sediment
g	acceleration of gravity
H	Hurst exponent
L-ratio	likelihood ratio
n	exponent for power law between variance σ_T^2 and time scale T
N	number of observations
p	p-value
p_e	probability of exceedance
$P_{i[bursts]}$	proportion of sediment with size i in large sediment bursts

$P_{i[bulk]}$	proportion of sediment with size i in bulk bedload
q_b	total sediment transport rate per unit channel width
$\overline{q}_b$	mean sediment transport rate per unit channel width
q_{bi}	fractional transport rate for grain size i per unit channel width
$[q_b]_i$	total sediment transport rate per unit channel width at time instant i
q_{ref}	reference transport rate
q_0	intercept for exponential fit
Q_f	sediment feed rate
$\overline{Q}_b$	mean sediment transport rate
R_h	hydraulic radius
R1–R7	experimental runs
R^2	coefficient of determination
SD_g	geometric standard deviation
S	best fit slope on log-log scale
S_w	water surface slope
t	time
T	aggregation time scale
T_i	time of first significant increase in sediment transport rate after a sediment pulse

$T_{\max(\rho_1)}$	time scale with highest autocorrelation ρ for time lag $\tau = 1$
T_p	time in between sediment pulses
T_r	relaxation time
T_{r1}	relaxation time obtained from an exponential fit
T_{r2}	relaxation time obtained from a log–linear fit
$[x, y]$	DEM coordinates
Y	time series
$\overline{Y}$	mean for time series
Y_t	value for time series Y at time t
$Y_{t-\tau}$	value for time series Y at time t minus time lag τ

Greek symbols

Symbol	Definition
α	level of statistical significance
$\delta\eta_{[x,y]}$	change in bed elevation for coordinates [x,y]
$\overline{\delta}\eta$	mean change in bed elevation
Δ_T	mass balance for time period T
η	bed elevation
Λ	rate of decay for exponential fit
ρ_s	sediment density
ρ_w	water density

ρ_τ	autocorrelation coefficient for time lag τ
ρ_1	autocorrelation coefficient for time lag 1
ρ_{1_T}	autocorrelation coefficient for time lag 1 and aggregation time scale T
σ_{q_b}	standard deviation for bedload
σ_T	standard deviation for aggregation time scale T
σ_η	standard deviation for bed elevation
σ_T^2	variance for aggregation time scale T
τ	time lag
τ_b	mean boundary shear stress
τ_{ci}	critical shear stress for grain size i
τ_{ci}^*	critical Shields number

Aknowledgements

The experiment was conducted in the Mountain Channel Hydraulic Experimental Laboratory at the University of British Columbia and funded by NSERC. The studies of the first author have been funded by Becas Chile (Conicyt). Data was collected in partnership with Claudia vonFlotow and Tobias Müller. I want to aknowledge the work of Marwan Hassan, Garry Clarke, and Rob Millar in my supervisory committee. Marwan generously shared his knowledge on sediment transport and helped me come up with research questions and hypotheses of study. He supervised my work in a critical but very constructive way. Garry Clarke was always available for advice and his careful revisions of manuscripts improved them significantly. He assisted me in time series analyses and instructed me on scientifc writing. Rob Millar helped me to complete my comprehensive exam and provided me with useful suggestions for my research. The following people were supportive and their comments, advice, and questions helped me improve my research: Carles Ferrer, Matteo Saletti, Tobias Müller, Shawn Chartrand, Katie DeRego, Leonora King, Dave Reid, NianNian Fan, Eva Crego, and Dan Moore. WRR Associate Editor, Jon Major, and an anonymous person reviewed the version of Chapter 2 published in WRR. Helena Trajic sieved some sediment samples and Eric Leingerber assisted with some figures.

Dedication

This manuscript is dedicated to my ancestors, who taught me the value of knowledge for knowledge's sake.

Chapter 1

Introduction

Sediment transport and channel morphology in mountain streams are affected by unsteady and non-uniform flow conditions (*Hassan et al.*, 2006), the wide range of shapes and sizes of grains (*Einstein*, 1950; *Wilcock*, 1992), the arrangement of grains on the bed surface (*Parker and Klingeman*, 1982; *Wilcock and Detemple*, 2005), and changes in sediment supply regime, which has been proposed as a first order control (*Hassan et al.*, 2006, 2008). At a reach scale, the channel responds to imbalances between sediment supply and flow transport capacity by adjusting its width, slope, and the arrangement of grains on the bed surface. Channels for which transport capacity exceeds sediment supply are considered as supply-limited, whereas those for which sediment supply exceeds capacity are considered as transport-limited (*Montgomery and Buffington*, 1997). The intensity of transport in supply-limited streams is usually low because of the development of a coarse bed surface with structures that counteract bed degradation (*Parker et al.*, 1982; *Dietrich et al.*, 1989; *Church et al.*, 1998; *Venditti et al.*, 2008; *Nelson et al.*, 2009). Instead, under the same slope and flow conditions, sediment transport is more intense in transport-limited streams, which develop a finer bed surface and an aggraded bed (*Lisle and Madej*, 1992; *Madej et al.*, 2009; *Pryor et al.*, 2011).

Mountain streams are subjected to episodic sediment supply, which can cause them to shift between relatively high and low supply regimes. Sediment supply comes from multiple sources and enters the channel at discrete locations and through different mechanisms like debris flows, landslides (*Hovius and Stark*, 2006), or the release of large wood jams (e.g. *Hassan et al.*, 2005). The texture of sediment inputs and flow competence will dictate which grains are potentially mobile and those that are not will likely be deposited in situ. Flow capacity will dictate how much sediment can be transported and the channel bed will condition sediment mobility by promoting efficient paths for sediment transport, as well as deposition fronts (*Gaeuman et al.*, 2017). The sediment that gets deposited can entrain at later stages due to larger floods or because of changes in the bed configuration (e.g., increase in bed slope, destruction of bed structures). All of these processes and factors cause bedload transport to vary at multiple temporal and spatial scales.

Data collection in the field is limited by technology, time, and accesibility, so flumes have been used to study channel adjustment to changes in sediment supply under controled environments (e.g., *Dietrich et al.*, 1989; *Lisle and Church*, 2002; *Curran and Wilcock*, 2005; *Eaton and Church*, 2004, 2009; *Madej et al.*, 2009; *Nelson et al.*, 2009; *Venditti et al.*, 2010; *Pryor et al.*, 2011). Changes in the sediment supply regime are followed by adjustments of the channel and sediment transport–storage relations. Reductions in sediment supply have been linked to bed degradation, which can be counteracted by the expansion on the bed of coarse fixed patches that limit sediment transport (*Dietrich et al.*, 1989; *Nelson et al.*, 2009). Sediment transport–storage relations are also affected by changes in sediment supply (*Lisle and Church*, 2002) and can exhibit complex patterns of hysteresis during aggradation–degradation cycles (*Madej et al.*, 2009; *Pryor et al.*, 2011; *Luzi*, 2014). The nature of stream boundaries influences channel adjustment to changes in sediment supply (*Eaton and Church*, 2004, 2009). Unconstrained channels primarily adjust channel sinuosity and slope, whereas constrained channels adjust particle size and bed state. The content of sand (*Curran and Wilcock*, 2005) and texture of sediment feed relative to bed texture (*Venditti et al.*, 2010) affect critical conditions for gravel entrainment. Most experiments have used constant feed and only few have used episodic feed regimes like those found in mountain streams (*Cui et al.*, 2003; *Sklar et al.*, 2009; *Venditti et al.*, 2010; *Johnson et al.*, 2015).

Experimental studies using episodic sediment feed have mostly analyzed the importance of textural differences between the bed and feed for: pulse propagation (*Cui et al.*, 2003; *Sklar et al.*, 2009), pulse–bed interactions (*Venditti et al.*, 2010), and bed surface texture (*Johnson et al.*, 2015). Experiments indicated that sediment pulses transmit downstream by dispersion if the bed and feed material have similar texture, whereas pulse translation occurs if the feed material is considerably finer (*Cui et al.*, 2003; *Sklar et al.*, 2009). Field gravel augmentations (*Gaeuman et al.*, 2017) have revealed that pulses can propagate by fragmentation into smaller pulses and that the time it takes to propagate depends on the state of intervening sediment reservoirs. The interaction between sediment pulses and the bed can increase if sediment supply has a finer texture (*Venditti et al.*, 2010). Beds have even been reported to become coarser and rougher after fine sediment pulses (*Johnson et al.*, 2015). Besides these studies, the roles of the magnitude and frequency of sediment pulses on channel adjustment remain as open questions and the suitability of constant feed regimes for modeling mountain streams has not been thoroughly discussed.

Gravel-bed streams exhibit a wide range of grains sizes, which can sort in all directions and at different scales as a result of sediment transport (*Parker*, 1992; *Powell*, 1998). Sediment mixtures influence the mobility of specific grain sizes through the hiding effects of relatively large particles on smaller particles (*Einstein*, 1950), the relative exposure of large grains to the flow (*Fenton and Abott*, 1977), and the effects of sand on the entrainment of gravels (*Wilcock and Crowe*, 2003; *Curran and Wilcock*, 2005). Usually, part of the bed is transported during bankfull flows capable of mobilizing a wide range of grain sizes, but with different intensities. Finer material is fully mobile and its proportion in bedload is the same as in the bed, whereas coarser material affected by size-selectivity is partially mobile and its proportion in bedload is less than in the bed (*Wilcock and McArdell*, 1993). Specific grain sizes are important at different scales and for different processes. Coarse material increases channel stability (*Zimmermann*, 2010; *Waters and Curran*, 2012; *Mackenzie and Eaton*, 2017), gravels provide fish spawning habitat (e.g., *Kondolf and Wolman*, 1993; *Hassan et al.*, 2008), and fine sediment affects water quality (e.g., *Jones*, 2012; *Mathers et al.*, 2017). As different grain sizes move by different transport regimes, their temporal patterns of mobility are not the same and are not necessarily represented by those of total bedload transport (e.g., *Saletti et al.*, 2015), which should also influence sediment storage. Whereas fully-mobile grains are frequently entrained and easily transported downstream, coarser partially-mobile grains move occasionally and are preferentially stored when supplied.

Here, the main objective is to study the effects of episodic sediment supply on channel adjustment of an experimental gravel bed (Figure 1.1). The research is guided by the following questions:

1. Which episodic sediment feed regimes could be represented by constant feed and at which time scales?
2. How do bed history and bed state affect channel response to changes in sediment feed regime?
3. What are the consequences of size-selective bedload transport on this response?

To isolate the effects of sediment feed, flow discharge was held constant throughout the experiment and 300 kg of sediment was introduced every 40 h using different feed regimes in a sequence of seven runs. We included runs without feed and with constant feed as references, and three different episodic feed regimes to assess the roles of the magnitude and frequency of sediment pulses. Many experiments start all their runs from flat well-mixed beds because it facilitates direct comparisons among them. This experiment was conducted as a sequence of runs, which started one after the other, to develop a complex bed topography that resulted from a long history of flow and sediment supply. Runs with constant feed and without feed were conducted twice within the sequence to explore the effects of initial bed conditions and bed history on channel adjustment to changes in supply. Although the importance of bed state for transport–storage relations has been mentioned (e.g., *Madej et al.*, 2009; *Pryor et al.*, 2011), a meticulous assessment of the effects of bed characteristics and configuration in the response of a channel to changes in sediment feed is still missing.

The wide range of grain sizes in the bed and feed (0.5–64 mm) promoted sediment sorting and allowed the bed to armor, which influences sediment transport (*Parker and Klingeman*, 1982; *Parker et al.*, 1982). Given the flow and sediment texture, partial sediment transport was expected over the bed and the effects of sediment mixtures (*Einstein*, 1950; *Fenton and Abott*, 1977; *Curran and Wilcock*, 2005) were expected to be strong. Fractional sediment transport data

Figure 1.1: Flume experiment in progress at the Mountain Channel Hydraulic Experimental Laboratory (UBC). Sediment was colored by grain size to facilitate the identification of bed surface texture on photographs. The image was taken after the first run. The flow had just started at a very low rate to wet the bed after a scan and photographs (water flows from back to front). Sediment is prepared to be fed upstream during the second run. In subsequent runs, sediment was introduced manually.

was collected during the 280-h long experiment to study the effects of the wide range of sizes and size-selective entrainment on the temporal patterns for fractional bedload transport and storage at multiple scales and how they relate to those for total bulk bedload.

The study is organized around three main topics regarding the effects of sediment feed regime on channel adjustment and the influence of initial bed conditions. The first topic is the effects of sediment feed on the temporal adjustments of total bedload transport, for which the following hypotheses are proposed.

- (T1-H1) Adjustment of a gravel bed to sediment supply is significantly affected by the magnitude and frequency of sediment feed.

- (T1-H2) If the time between sediment pulses is less than the time needed for the sediment transport rate to relax to a low value after a pulse, the response could be similar to constant feed regimes.
- (T1-H3) Large pulses, which result in greater sediment availability, produce stronger responses in the transport rate and have longer relaxation times than small pulses.
- (T1-H4) The temporal adjustment of sediment transport rates to changes in the supply regime is conditioned by the initial bed slope, surface grain-size distribution, and sediment storage.

The second topic is the patterns of grain-size dependence on bedload transport, and more specifically, on the memory of bedload rate signals under changing sediment supply regimes. Under partial transport, as expected during the experiment, aggregated bedload patterns are not representative of all grain sizes. Given that the relevance of grains of different sizes is varied in river studies and projects (e.g., *Hassan et al.*, 2008; *Mackenzie and Eaton*, 2017; *Mathers et al.*, 2017), it is interesting to evaluate the responses to sediment feed of specific grain sizes and how they relate to the response of total bulk bedload patterns. Three hypotheses are formulated.

- (T2-H1) Bedload transort rate time series for runs with constant sediment feed have weaker memory than those for runs with large infrequent sediment pulses which can cause pronounced trends in bedload transport.
- (T2-H2) The memory structure of total bedload reflects that of fully-mobile grain sizes, which dominate sediment transport and exhibit strong memory in their bedload signals.
- (T2-H3) Grain-size dependence in bedload transport increases with sediment feed because the movement of fully-mobile sediment is more responsive to feed than that of partially-mobile grain sizes.

The last topic is the effects of sediment feed regime and bed history on temporal and spatial patterns of sediment storage, and how they relate to fractional bedload transport. As preferential storage of coarse sediment is expected under partial transport, the following hypotheses are proposed.

- (T3-H1) Preferential deposition of coarse partially-mobile gravels near the feed source promote increased storage upstream and downstream fining on the bed surface.
- (T3-H2) Constant feed, which makes sediment available more gradually, promotes larger sediment storage than sediment pulses because of a greater probability for sediment being sequestered in the bed.
- (T3-H3) Hysteresis in sediment transport-storage relations largely depends on differences in bed surface texture and sediment availability.

Chapter 2

Experiment on temporal variation of bedload transport in response to changes in sediment supply in streams

2.1 Summary

A flume experiment was conducted to study channel adjustment to episodic sediment supply in mountain streams. The bulk sediment used for the bed and feed included grain sizes 0.5–64 mm with geometric mean $D_{g\,(\mathrm{bulk})}$ of 5.7 mm. Water discharge was held constant for 40 h, and 300 kg of sediment was supplied through a range of scenarios. Bed slope, sediment storage, sediment transport and bed surface texture responded to sediment supply. During the first of seven runs, bed slope decreased from 0.022 m/m (flume slope) to 0.018 m/m due to sediment starvation. Bed slope increased beginning in the second run as the bed aggraded due to preferential storage of grains > 8 mm. Transport rate and bed-surface particle size were significantly affected by the magnitude and frequency of sediment feed. Under constant feed, transport rate increased gradually and $D_{g\,(\mathrm{surface})}$ ranged between 12–15 mm. Instead, sediment pulses caused a pronounced increase in sediment transport rate and surface fining, trends that were inverted as sediment evacuated. At the run-scale, sediment transport and storage behaved as with constant feed if pulse relaxation time exceeded time between pulses. The increase in transport rate and surface fining were proportional to pulse size. After the 300 kg pulse, transport rate reached $100\,\mathrm{g\,m^{-1}\,s^{-1}}$ and $D_{g\,(\mathrm{surface})}$ was $<$10 mm. After 75 kg pulses transport rate reached $\sim$$10\,\mathrm{g\,m^{-1}\,s^{-1}}$ and $D_{g\,(\mathrm{surface})}$ was $>$12 mm. Textural differences on the initial bed surface influenced the patterns of sediment transport. Channel adjustment was controlled by the magnitude and frequency of sediment feed and not by total feed.

2.2 Introduction

Mountain streams are commonly subjected to episodic inputs of sediment through bank collapse, landslides, debris flows, and other kinds of natural or anthropogenic disturbances (*Madej and Ozaki*, 1996; *Benda and Dunne*, 1997; *Dadson et al.*, 2004; *Hovius and Stark*, 2006; *Lancaster*, 2008). Depending on the amount and size composition of sediment, the introduced material can be transported downstream, or can remain in place and act as a persistent source of sediment (*Jackson and Beschta*, 1982; *Goff and Ashmore*, 1994; *Lane et al.*, 1995; *Sutherland et al.*, 2002; *Reid and Dunne*, 2003). In the longer term, the supply regime for mountain streams is defined by the frequency and magnitude of the sediment inputs, which affect stream morphology.

Mountain river channels exhibit a wide variety of morphologies that reflect variable sediment transport patterns. At the reach scale, stream morphology has been linked to magnitude of transport capacity relative to sediment supply, distinguishing between supply-limited and transport-limited conditions (*Montgomery and Buffington*, 1997). At slopes around 0.02 m/m, rapids and riffle-pool channels can shift between supply-limited and transport-limited conditions, which will be reflected in the degree of armoring and prevalence of bed structures. Field evidence and experimental observations indicate supply-limited channels develop coarse, well-structured beds, with sediment transport rates below transport capacity (*Parker et al.*, 1982; *Dietrich et al.*, 1989; *Lisle et al.*, 1993; *Church et al.*, 1998; *Ryan*, 2001; *Venditti et al.*, 2008; *Nelson et al.*, 2009). Under the same flow and slope conditions, transport-limited streams aggrade, develop fine bed surfaces with little or no surface structure, and sediment transport rates near transport capacity due to greater sediment availability (*Lisle and Madej*, 1992; *Madej et al.*, 2009). Given the difficulties of data collection in the field and advances in laboratory instrumentation, physical modeling commonly has been used to study the effects of disturbances in streams (*Yager et al.*, 2015).

Flume experiments have been used to study the role of sediment supply, among other controls, on bedload transport and bed surface evolution. Observations indicate fine mobile patches and coarse fixed patches coexist on gravel beds under high sediment supply. As supply is reduced, coarse fixed patches expand and limit the areas of the bed where sediment transport occurs (*Dietrich et al.*, 1989; *Nelson et al.*, 2009). The content of sand in sediment feed affects entrainment conditions over gravel beds (*Wilcock and Crowe*, 2003; *Curran and Wilcock*, 2005). In systems that lack sand, sediment transport is affected by the size ratio between the feed and bed material (*Venditti et al.*, 2010). Sediment transport–storage relations respond to reductions in sediment supply (*Lisle and Church*, 2002), and the way in which this response occurs is strongly influenced by previous bed conditions (*Pryor et al.*, 2011). An aggraded channel responds with initial decrease in storage, followed by decline of transport rate as bed armors. A channel at equilibrium with low supply rates instead does not adjust the storage and there is only decline of transport rate. The influence of the nature of stream boundaries on channel adjustment to changes in sediment supply has been tested in flumes as well (*Eaton and Church*, 2004, 2009). Results indicate unconstrained channels primarily adjust channel sinuosity and slope, whereas constrained channels first adjust particle size and bed state (surface texture and structures, see *Hassan et al.* (2008)).

For simplicity, most flume experiments have analyzed response of gravel bed streams to sediment supply using constant feed rates, and only a few studies have used episodic supply rates typically observed in mountain streams (*Cui et al.*, 2003; *Sklar et al.*, 2009; *Venditti et al.*, 2010; *Johnson et al.*, 2015). Experiments using episodic feed rates show dispersion and translation are the principal mechanisms of sediment pulse evolution, and the relation between sediment feed particle size and bed particle size determines which mechanism dominates. When the bed and feed material have similar particle size dispersion dominates, but if the feed material is considerably finer than the bed significant translation can occur (*Cui et al.*, 2003; *Sklar et al.*, 2009). The interaction between sediment pulses and bed sediment is influenced by the pulse grain size relative to the bed, and by the magnitude and frequency of pulse inputs (*Venditti et al.*, 2010). More recently, flume studies of step-pool-like channel beds point out that channel beds can become coarse and rougher in response to pulses of finer gravel (*Johnson et al.*, 2015). These studies give insights on the effects of episodic sediment supply, but especially on pulse propagation and the role of relative sediment texture.

Here, we study channel adjustment under episodic sediment supply by introducing various volumes and frequencies of sediment over a poorly sorted gravel bed. The high resolution of data systematically collected during the 280-hour long experiment allowed us to examine temporal variation of bedload transport in a way that to our knowledge has not been done before. We were able to develop a bed that resembled those found in mountain streams, with complex topography and surface organization, as a result of the extended history of flow and sediment supply. The use of both constant feed and sediment pulses provided an opportunity to evaluate the use of constant feed for the study of sediment transport in mountain streams, and explore the temporal scales and cases for which it might be valid.

The goal of this study is to test four hypotheses related to the impact of episodic sediment supply on channel adjustment and sediment mobility: (H1) adjustment of a gravel bed to sediment supply is significantly affected by the magnitude and frequency of sediment feed; (H2) if the time between sediment pulses is less than the time needed for the sediment transport rate to relax to a low value after a pulse, the response could be similar to constant feed regimes; (H3) large pulses, which result in greater sediment availability, produce stronger responses in the transport rate and have longer relaxation times than small pulses; and (H4) the temporal adjustment of sediment transport rates to changes in the supply regime is conditioned by the initial bed slope, surface grain-size distribution, and sediment storage.

2.3 Materials and methods

2.3.1 Experimental design

The flume experiment was conducted in the Mountain Channel Hydraulic Experimental Laboratory at the University of British Columbia (UBC). The flume is 18 m long, 1 m wide and 1 m deep, with a slope of 0.022 m/m. It is a generic model of riffle-pool reaches in East Creek, a mountain stream in the UBC Malcolm Knapp Research Forest. Flume dimensions and flow were not scaled. Water discharge was kept constant at 65 $\mathrm{L\,s^{-1}}$, which was able to mobilize most sediment size fractions and is similar to the scaled bankfull discharge in the prototype stream. The bed and feed were composed of poorly sorted sand and gravel (1:3 bed grain size distribution in East Creek), which ranged from 0.5 to 64 mm with geometric mean $D_{g\,(\mathrm{bulk})}$ of 5.7 mm (Figure 2.1). More details on experimental settings can be found in *Elgueta* (2014).

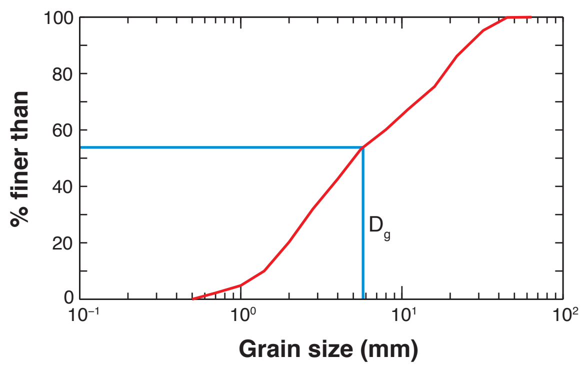

Figure 2.1: Grain size distribution of the bulk sediment that constituted bed and feed material.

A sequence of seven runs was conducted with no feed, constant feed, and episodic feed regimes (Figure 2.2). Each run lasted 40 hours. The initial bed of the first run was well-mixed and flat, whereas subsequent runs inherited bed conditions from the previous runs. The sequence of runs made direct comparisons more difficult, but gave time for the bed to evolve under more realistic conditions and to develop complex channel morphology as observed in natural rivers. Run 1 (R1) was conducted under no feed to condition the bed. As a reference, in Run 2 (R2), 300 kg of sediment was introduced at a constant feed rate (2.1 $\mathrm{g\,m^{-1}\,s^{-1}}$) over 40 h. To examine the response of the system to an abrupt supply, in Run 3 (R3) all the material was introduced during the first hour. Run 4 (R4) and Run 5 (R5) were designed to analyze the role of size and frequency of episodic inputs, so the 300 kg was split in four pulses with duration = 0.25 h and two pulses with duration = 0.5 h respectively. Finally, to explore the importance of the initial bed on the response to supply; Run 6 (R6) had the same constant feed regime as R2, and Run 7 (R7) had no feed, as in R1. The feed rate used to supply all pulses was 83 $\mathrm{g\,m^{-1}\,s^{-1}}$, which is similar to the average transport capacity of the experiment (79 $\mathrm{g\,m^{-1}\,s^{-1}}$). The feed rate was established from several preliminary runs.

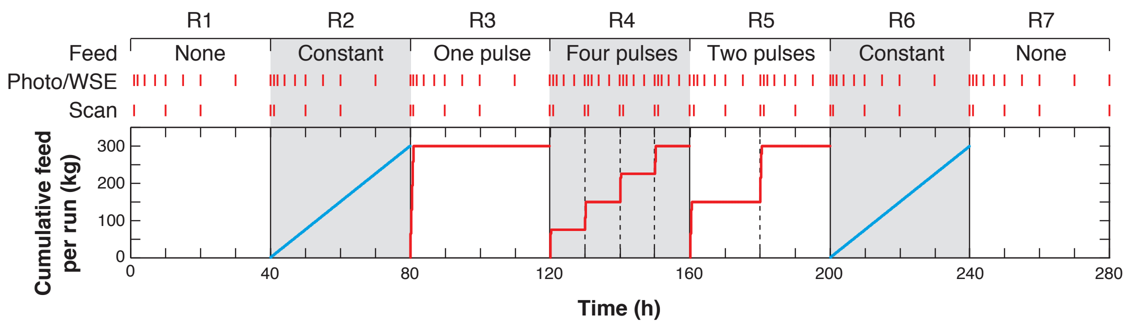

Figure 2.2: Sequence of feed regimes followed during the experiment. Cumulative feed is plotted as a function of time for constant feed (blue) and three types of episodic feed regimes (red). The time at which bed surface photos, water-surface elevation (WSE), and bed scans were acquired are displayed with red bars.

2.3.2 Data collection

Detailed information on flow properties, bed elevation, bed-surface particle-size organization and sediment transport was collected systematically during the experiment (Figure 2.2). Water depth was estimated as the difference between the bed-surface and water-surface elevation, measured on the side of the flume every 0.5 m, and mean depth was 0.077 m over the experiment. Water depth measurements were used to compute water-surface slopes and shear stresses.

Bed properties were measured from laser scans and photographs of the bed surface under no flow. Digital elevation models (DEMs) were obtained by scanning the bed with a video camera that recorded the reflectance location of a green laser beam, with a resolution of 2 mm in the longitudinal and horizontal direction and 1 mm in the vertical. Bed-surface grain-size distributions were obtained from point counts on four photos over 2 m^2 in the center of the flume, 6 to 8 m upslope from the downstream end of the flume. A sample grid of 36$\times$14 points with a cell size of 65 mm (largest particle size) was superimposed on each photo. Grains smaller than 2.8 mm were difficult to recognize and were grouped in one class.

Sediment transport was estimated using video-based measurements with a light table. The method follows the same principles as *Zimmermann et al.* (2008), but we improved the design significantly by detecting grains as small as 1 mm. Grains that exited the flume were recorded using a video camera (at frequency 27–32 frames per second) over a light table and images were post-processed in Labview Software to compute sediment transport information on a per second basis. The required conversion to weight based on measured projected particle area and b-axis was calibrated by recording stones of known dimensions and weights, and obtaining best fit linear regression relations (recorded minor axis against known b axis, recorded projected particle area against known weight). To check the results sediment was collected in a trap placed at the downstream end of the flume.

2.3.3 Data analysis

Sediment transport capacity was estimated using a modified version of Meyer-Peter and Müller (MPM) equation (*Wong and Parker*, 2006). Bed slope was estimated along the thalweg using DEMs. Only data between 4–11.8 m were included to avoid upstream and downstream boundary effects observed in flow profiles. Particle size data were used to calculate grain size statistics such as the geometric mean (D_g), geometric standard deviation (SD_g), and the grain size percentiles (e.g., D_{90} and D_{16}). This was done for both the bedload and bed surface.

To analyze the temporal variability of sediment transport rates over each run and the effects of changes in the sediment feed, cumulative departures from the long-term mean were computed over each run using

$$\sum_{i=1}^{N}\left([q_b]_i - \bar{q}_b\right); \quad N = 1, 2, 3, ..., \tag{2.1}$$

where $[q_b]_i$ is sediment transport rate at time instant i, $\bar{q}_b$ is the mean sediment transport rate over a run, and N is the number of observations over a run. Data were averaged every 15 min to reduce noise. The mean sediment transport rate of a run was subtracted from each observation for normalization, and the cumulative departure from the mean was evaluated as a function of time.

To test our hypothesis regarding differences and similarities among sediment transport signals of each run and the importance of the initial bed state, a statistical model of sediment transport rate was built using the R programming language. After trying different nested versions, we used a general least-squares model (method of maximum likelihood), for which a full version included: run as a factor, a time polynomial of degree 4 ($b_1 t + b_2 t^2 + b_3 t^3 + b_4 t^4$, where t is time and b_i are the slopes of the model), interactions between run and time variables, and an autoregressive order 1 (AR(1)) error term. Likelihood L-ratio tests were used to compare goodness of fit among nested models. The Akaike information criterion AIC (*Akaike*, 1974) was used to penalize complexity (number of free parameters) in model assessment. Including run as a factor allows changes in the intercept of the model (initial sediment transport rate) with run number. Adding the interactions between run and time variables accounts for changes in the temporal trend of sediment transport rate (slopes of the model) with run number. L-ratios were used to test the significance of the full model against: (1) a reduced version in which the intercept and slopes of the model are not allowed to change with run, and (2) a partly reduced version in which only the intercept is allowed to adjust with run. The significance level α was set to 0.05. Because the main interest was in long-term trends, the data were averaged. Resolutions ranging from 5–60 min were used to explore the scales at which differences appeared. The 5 min resolution limit was selected to avoid random fluctuation in the bedload transport, while early adjustments might be lost above 60 min. The averaged transport rates were log-transformed to approach normality.

To assess the effects of pulses of different magnitudes, relaxation times were estimated using the relations obtained from an exponential fit and a log–linear fit to the sediment transport rate data (T_{r1} and T_{r2} respectively) as

$$T_{r1} = \frac{\ln(q_{ref}/q_0)}{-\Lambda} \tag{2.2}$$

$$T_{r2} = 10^{(\log_{10}(q_{ref})-a)/b} \tag{2.3}$$

In equation (2.2), q_{ref} is the low reference transport rate, q_0 is the intercept, and Λ is the rate of decay. This type of function has been used to model changes in storage under degradation (*Lisle and Church*, 2002). In equation (2.3), a is the intercept and b is the slope of the linear relation. The log–linear fit was used because it resembled more closely the decrease in sediment transport rate, especially after the large and medium-sized pulses.

2.4 Results

To address the four hypotheses formulated in the introduction, we present our results as follows:

- Summary of the observations from each run, including sediment transport, hydraulics, bed-slope evolution, particle size adjustments, and sediment storage.
- Assessment of temporal patterns of variability in sediment transport rate under the different feed regimes.
- Results of statistical tests for significant differences in the trend of sediment transport rate among runs at different temporal resolutions.
- Relaxation times T_r and sediment output until T_r for pulses of different size.

2.4.1 Observations

To assess the effects of feed regime on channel adjustment we comment on the evolution of sediment transport rate (Figure 2.3), Shields number (Figure 2.4a), bed slope (Figure 2.4b), and grain size statistics of the bed surface and bedload (Figure 2.4c–e). A summary of observations towards the end of each run is presented in Table 2.1. To emphasize comparisons among and within the different supply regimes, observations over each run are presented by feed regimes.

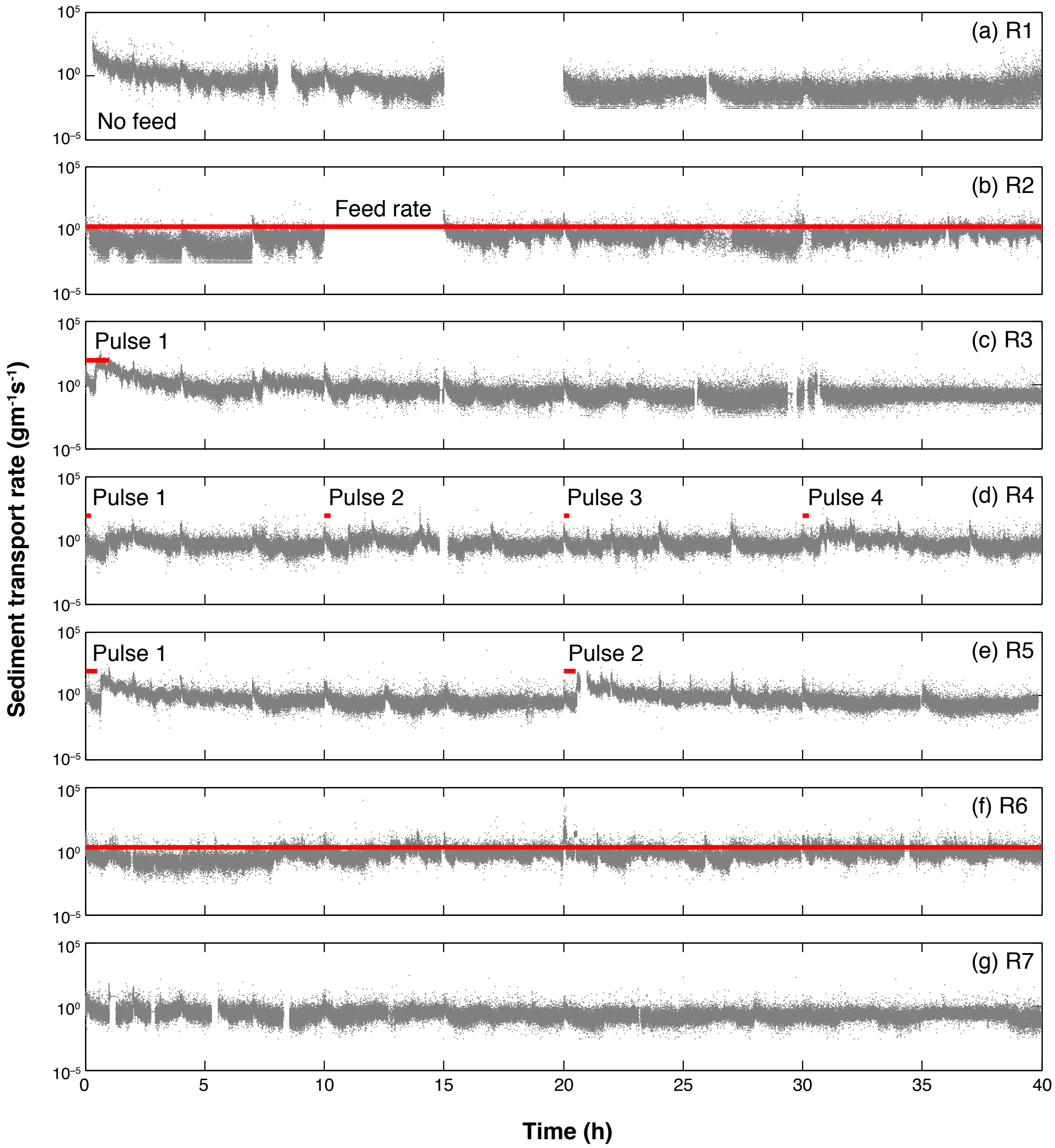

Figure 2.3: Time series of total bedload rate estimated by processing images recorded over a light table at the end of the flume. Red lines indicate sediment feed rates. The high resolution of the method allowed computing fractional mass and number of grains that exited the flume at every second. Gaps in the data are due to technical problems.

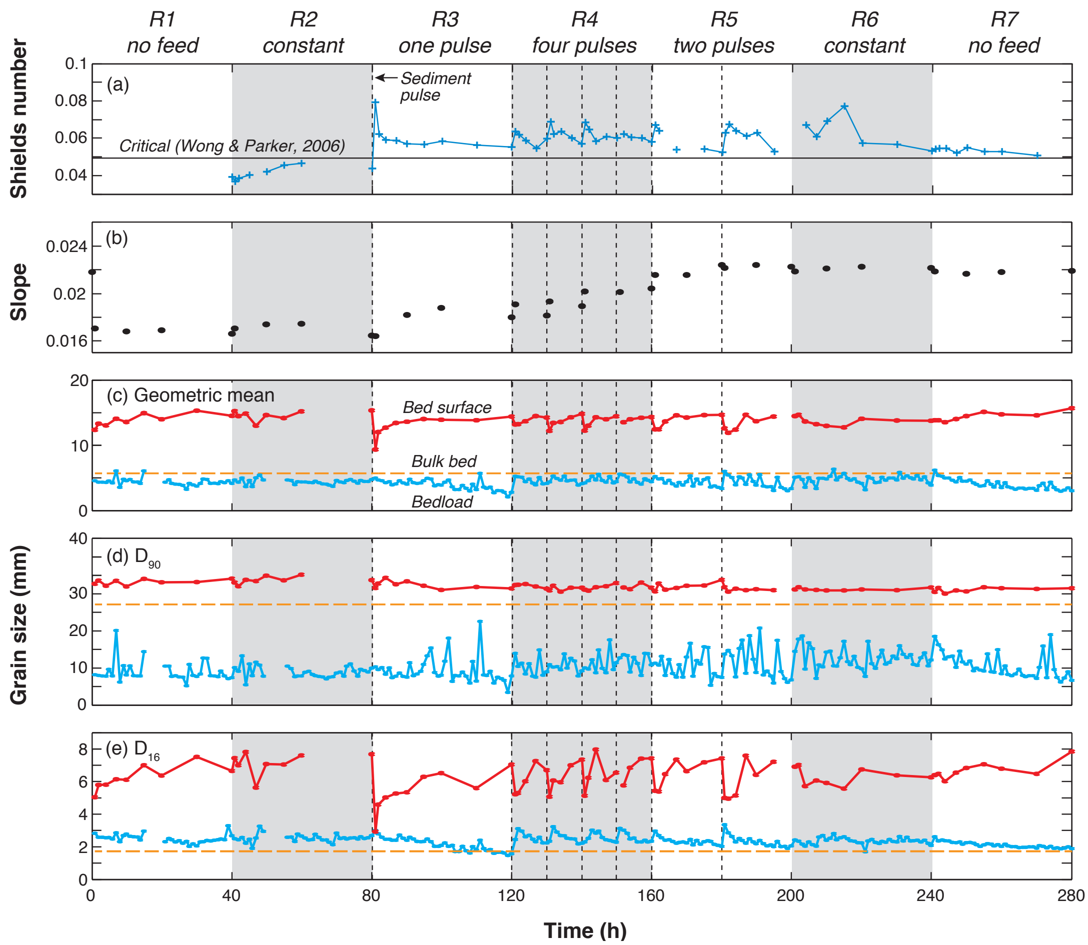

Figure 2.4: (a) Shields number. (b) Thalweg slope (m/m). Grain size statistics of the bed surface (red dots), bedload (blue dots) and bulk sediment that constituted the original bed and feed (horizontal dashed lines): (c) geometric mean particle size, (d) D_{90}, and (e) D_{16}. Sediment pulses are indicated with vertical dashed lines.

Table 2.1: Sediment feed characteristics and observations towards the end of each run

Run	1	2	3	4	4	6	7
Feed type	no feed	constant	episodic	episodic	episodic	constant	no feed
Feed rate $g\,m^{-1}\,s^{-1}$	0	2.1	83.3	83.3	83.3	2.1	0
Number of pulses	-	-	1	4	2	-	-
Water discharge $l\,s^{-1}$	65	65	65	65	65	65	65
Mean water depth m	-	0.073	0.08	0.083	0.072	0.075	0.073
Water-surface slope m/m	-	0.017	0.019	0.020	0.020	0.020	0.020
Froude number	-	1.11	0.84	0.75	1.15	1.02	1.11
Reynolds number	-	241564	294823	318700	260404	275292	264978
Bed slope m/m	0.017	0.016	0.018	0.020	0.022	0.022	0.022
$D_{g\,(\mathrm{surface})}$ mm	14.5	15.3	14.4	14.3	14.4	13.8	15.7
$SD_{g\,(\mathrm{surface})}$	2.2	2.0	2.1	2.0	2.0	2.1	1.9
$D_{90\,(\mathrm{surface})}$ mm	34.1	33.7	31.5	31.6	31	31.7	31.5
Roughness scale k_s m	0.0716	0.0708	0.0662	0.0664	0.0651	0.0666	0.0662

Both R1 and R7 were conducted with no feed, but differed in their initial beds. R1 started from a well-mixed plane bed that was not yet worked by water, had a slope of 0.022 m/m and $D_{g\,(\text{surface})}$ = 4.7 mm. The transport rate was high initially, decreased two orders of magnitude over the first five hours, and more gradually thereafter (Figure 2.3). No hydraulic data are available for this run. Bed slope changed subtantially during the first hour, but varied little thereafter (Figure 2.4). Bedload fining was unclear, whereas bed surface coarsening was significant. Net degradation (157 kg) was equivalent to erosion of a 4.3 mm deep uniform layer. By the end of the run, a well-developed channel thalweg was present with no bedforms apparent. R7 was conducted on an armored bed that was the result of the six preceding runs. Its well-developed channel morphology included sediment wedge and riffle-pool sequences upstream, and lateral bars toward the middle and lower parts of the flume. The transport rate was generally low and the decrease was less pronounced than in R1 (Figure 2.3). The Shields number was near the critical value of 0.05 (*Wong and Parker*, 2006), which can be associated with a low transport regime (Figure 2.4). There was slight variation in bed slope and mild adjustments of particle size. Overall, the bedload texture became finer as the bed surface coarsened. Net degradation of 59 kg corresponded to 1.6 mm of erosion.

R2 and R6 received constant feed. R2 started from an armored bed with no bedforms, a slope of 0.017 m/m, and $D_{g\,(\text{surface})}$ = 14.5 mm. During the first seven hours sediment transport rate was well below the feed rate most of the time. Since then, transport rate showed an increase. The rate of increase became milder with time as sediment transport rate approached the feed rate. By the end of the run, sediment transport rate fluctuated within two orders of magnitude. The largest values surpassed the feed rate, and the smallest rates were less than 0.1 $\mathrm{g\,m^{-1}\,s^{-1}}$ (Figure 2.3). The Shields number was below the nominal critical at the beginning, but approached the threshold value toward the end of the run (Figure 2.4). The bed slope increased during the first 20 h, but decreased after that. Bedload grain size statistics varied without clear trends and the bed surface coarsened slightly. At the end of the run, alternating bars were visible and net aggradation was 218.95 kg (5.7 mm deposition).

The initial bed of R6 was armored and had a slope of 0.022 m/m. This run yielded transport patterns similar to those obtained for R2; transport rate was well below the feed rate during the first hours, then increased markedly at around 8 h into the run (Figure 2.3). Shields number varied from near critical to twice this value, considerably larger than in R2 (Figure 2.4). There was variability in bedload texture, which coarsened slightly during the run. The surface got finer during the first 10–20 h, and coarsened after that. Nonetheless, the bed slope was relatively stable during this run. A mid-channel and a lateral bar disappeared by the end, while change in storage (122 kg) was only half the aggradation estimated during R2.

At the beginning of R3, a 300 kg pulse entered the flume, producing an increase of two orders of magnitude in the transport rate after 0.5 h (Figure 2.3). Thereafter, the rate decreased monotonically, but exhibited considerable variability. Another, albeit milder, rise in sediment transport rates was evident at around 7 h. Shields number exhibited a trend similar to transport rate, and by the end of the run it was slightly above the critical value (Figure 2.4). The bed slope first increased, but then decreased. A gradual fining in the bedload texture through the experiment was evident. The bed surface exhibited significant fining one hour after the feed, followed by sharp coarsening within the next 7–10 h. Regardless of the large sediment output during this run, there was relatively little change in storage, and only 78 kg of aggradation (1.6 mm deposition).

With initial conditions inherited from R3, the sediment transport rate in R4 exhibited a similar response after each sediment feed pulse, except after the third one (Figure 2.3). Shields number clearly increased following the first three pulses, but after the last pulse it remained stable (Figure 2.4). Bed slope and grain size statistics clearly responded to all four pulses. Net aggradation was 160 kg (4.3 mm deposition). R5 began with a relatively coarse bed, a 0.020 m/m slope, and lateral bars. Transport rate (Figure 2.3), Shields number, and bed surface and bedload texture adjusted to each pulse in a way similar to that described for R3 and R4. Bed slope increased after the first pulse, but changed little thereafter (Figure 2.4). By the end of the run, the bed aggraded 132 kg (3.5 mm deposition).

The bulk sediment used for the original bed and feed included a wide range of sizes that moved at different rates (Figure 2.5). While sand and fine gravel exhibited nearly continuous movement (Figure 2.5b–d), coarser gravel motion was sporadic (Figure 2.5e–f) as reflected in the intermittency of the signal. Grains between 22–32 mm exhibited periods of no mobility that lasted up to 5 h, coarser particles (not displayed here) were immobile even longer. Irrespective of the observed size selectivity on sediment transport, effects of sediment supply were evident for all fractions. The frequency of movement of all grain sizes increased with introduction of sediment pulses, bu s) exhibited temporal trends that resembled those of total transport (Figure 2.5a–d). The behavior observed during R5 is representative of all runs.

All sediment pulses moved downstream by dispersion (no evidence of translation). Part of the feed was stored upstream in a wedge (especially coarser fractions that moved less frequently), acting as a source of sediment and dispersing during the experiment.

2.4.2 Temporal patterns of variability in sediment transport rate under different supply regimes

To examine shifts in the sediment transport rate due to changes in the sediment supply regime, we performed cumulative departure analysis using equation (2.1). This analysis assumes that inflections in the cumulative departure curve (Figure 2.6) indicate the timing and response to changes in feed conditions. An increasing trend in the departure curve indicates a period of high transport rate relative to the mean, whereas persistently negative departure represents low sediment-transport phases. A flat curve indicates a period when transport rate approaches the mean. Our main interest is in long-term changes in transport rate, which are likely associated with sediment pulses. Changes in feed conditions produce inflections in the slope of the cumulative departure trend. The start of sediment feed produces a shift from a negative slope,

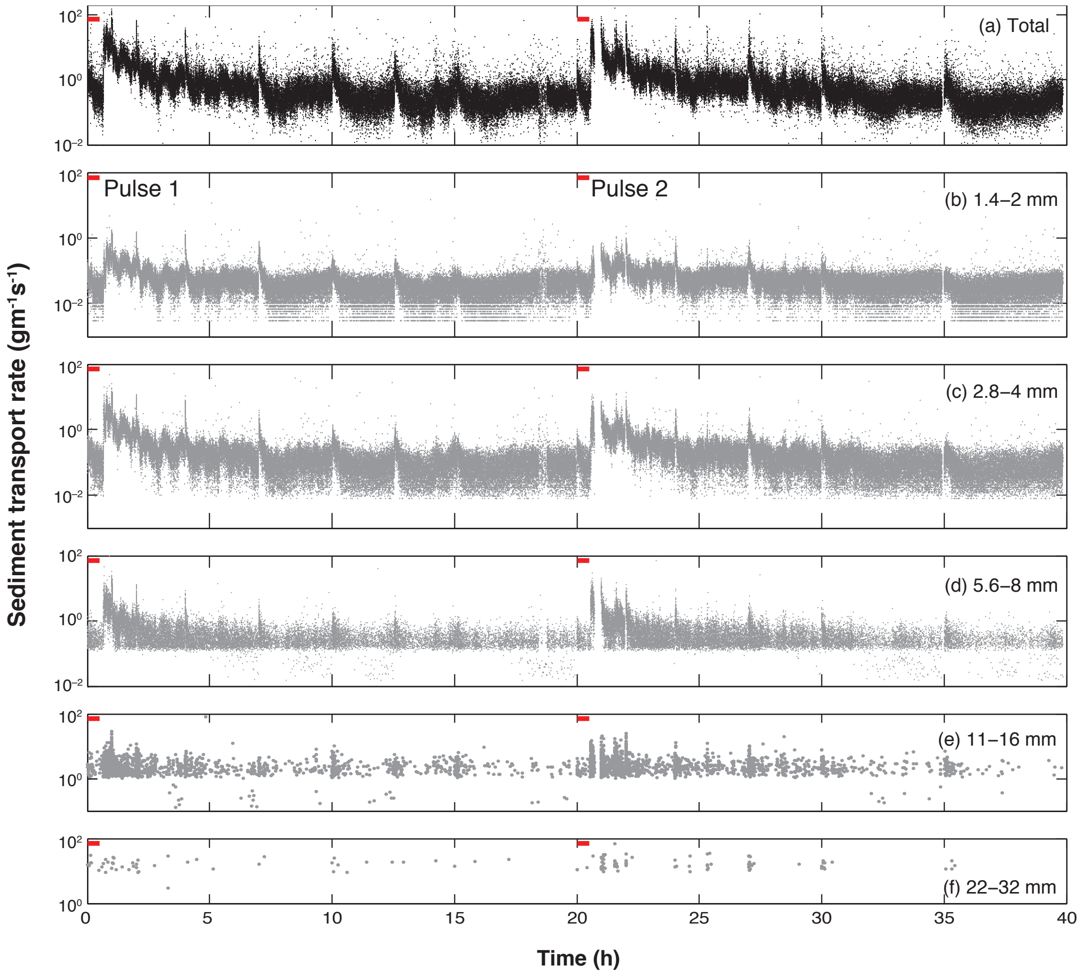

Figure 2.5: Total sediment transport rate and fractional rate of four grain size classes during R5. Red lines indicate sediment feed rate.

which represents low transport conditions previous to the feed, to a positive slope characteristic of more intense transport stages promoted by the feed. No feed produces an inflection from a positive slope or a nearly horizontal curve, when sediment feed effects are still strong, to a negative slope when transport rate falls below average after sediment starvation.

The two runs with no feed (R1 and R7) show cumulative departure curves with similar shape (Figure 2.6a and g). In both cases there is initial exponential increase, followed by continuous decrease. The major inflection observed occurs earlier in R1 than in R7, which could be related to sediment storage during runs previous to R7. It could be associated with the high transport rates during the first hours of R1 which raise the mean over the run, causing observations to fall below it earlier in the run.

In comparison to no feed runs, different trends are obtained for constant feed. In both these runs, transport rates initially fall below average values until 7–8 h into the run when there is a major inflection in the departure curve slope. Thereafter, the curve exhibits intermittent

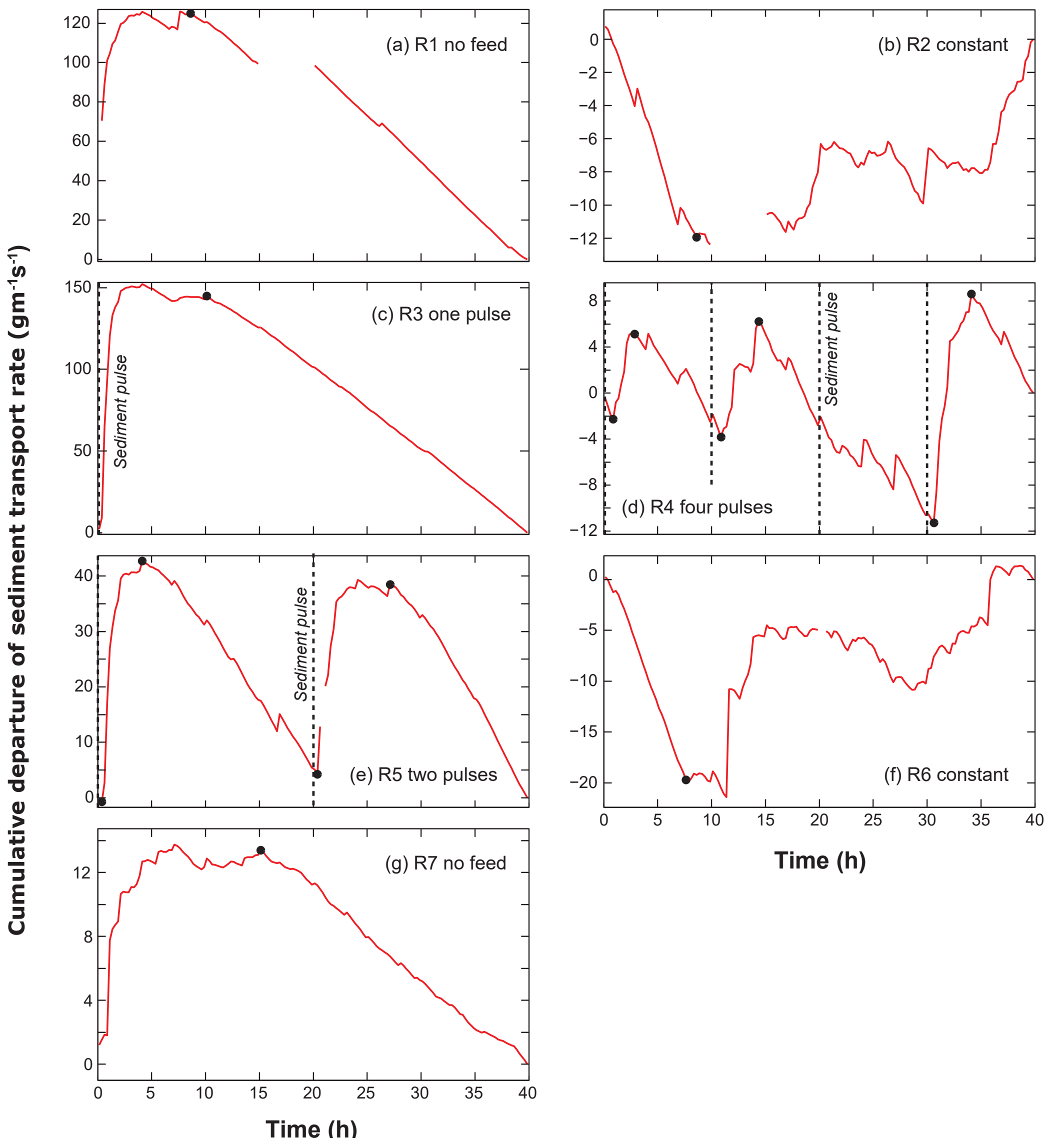

Figure 2.6: Variation of sediment transport rate over each run. The mean transport rate of a run is subtracted from each observation for normalization, and the cumulative departure from the mean is plotted as a function of time. Sediment inputs are represented with vertical dashed lines and major trend inflections are identified with black dots.

periods of flat, positive, or negative slopes, within an overall increasing trend.

In multiple pulse runs, the departure curve varies as a function of the number of pulses. It can increase and decrease in sequences related to changes in the feed. The absence of a clear inflection in the curve after the third pulse in R4 is due to the weaker response observed in the transport time series (Figure 2.3d). The span of total departure (Figure 2.7a) is greatest in runs with larger infrequent pulses such as R3 (or R1 in which the well-mixed initial bed could be considered as a big isolated pulse as well). The range of departure decreases as the feed magnitude during first hour becomes smaller and the range observed with 75 kg pulses is similar to constant feed.

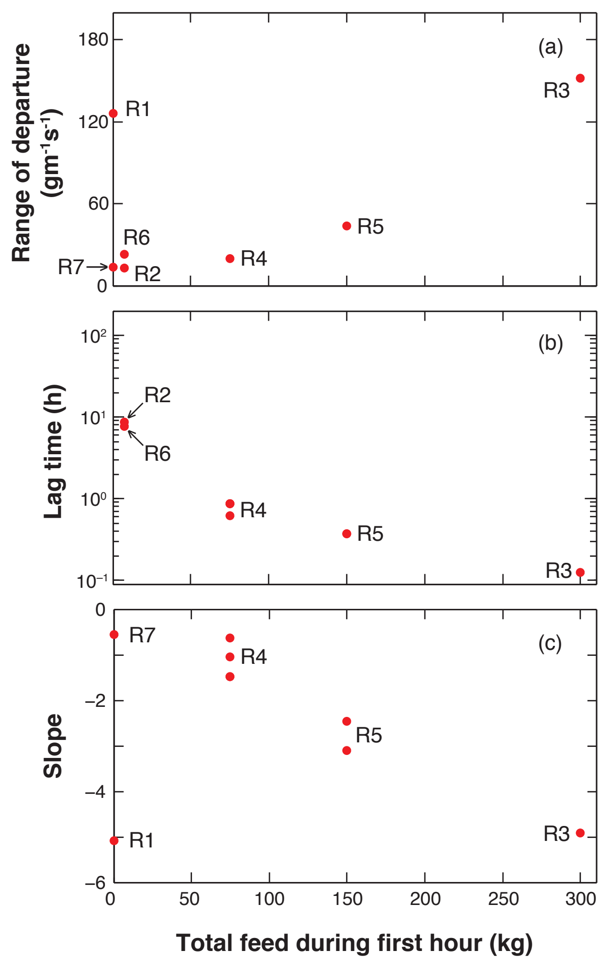

Figure 2.7: Characteristics of cumulative departure from mean transport rate against feed regimes. (a) Range of cumulative departure. (b) Lag time between starts of feed and associated inflections in the curve. (c) Slope of decreases related to stops in feed. (c) The amount of feed received during the first hour of each experiment is used to represent feed regime as a quantitative variable in the x-axis.

To describe the strength of the effects of changes in sediment feed on the cumulative departure curve, the lag time between start of feed and associated slope inflection (Figure 2.7b), and the rate of decrease in the departure curve during periods of no feed (Figure 2.7c) are presented as a function of total feed during first hour of experiment. The lag time in the response of the cumulative departure as a function of feed regime is related to the time that it takes the sediment to move downstream. The lag time decreases with feed magnitude and is considerably longer under constant feed. The rate of decrease in the departure curve is used to represent low sediment transport regimes during sediment starvation and was estimated as the slope of the best fit line through the points between two inflections, or from one inflection to the end of the run. Larger pulses exhibit steeper decreases, but there is considerable variability within pulses of the same size that might be related to difference in pre-pulse bed conditions. The importance of bed conditions can be appreciated by the significant differences in the slope of the cumulative departure curve for no feed runs. While in R7 the slope is gentle, R1 behaves in a manner similar to that of the single large pulse, R3.

2.4.3 Statistical modelling of sediment transport rate series

To examine how sediment supply regime impacted the temporal variability of sediment transport, a least squares model was fit to the averaged sediment transport rate time series. Significant differences in the evolution of sediment transport rate were detected among the seven runs at 60 min resolution using likelihood L-ratio tests ($p < 0.0001$). To identify differences between runs, the models were fit to include one pair of runs at a time. This was repeated until completing all possible pairs (21 in total). In most cases, L-ratio tests indicated model slopes were significantly affected by run style (Table 2.2). Curiously, significant differences appeared between R1 and R7, which had the same no feed regime. This is probably related to their differing initial conditions as discussed subsequently.

Changes in the slopes and intercept of the model were non-significant at 60 min averaging in only three pairs of runs. The first case corresponded to R1 and R3. The lack of differences when using 60 min averages was not too surprising since both runs presented relatively high transport rates during the first hours because one started with a well-mixed bed and the other received the largest pulse (Figure 2.3). However, differences in slopes appeared when increasing the temporal resolution to 30 min averages (Table 2.3). Runs with constant feed were the most similar, exhibiting no significant changes in model parameters even when increasing the resolution to 5 min averages. Because sediment feed in R4 was better distributed over time in four small pulses, we expected to find similarities between this run and constant feed. Instead, significant differences were indicated between the four pulses (R4) and constant feed run R2; whereas between R4 and constant feed run R6, no significant differences were detected with averaging periods larger than 15 min. As a group, no differences were found among R4 and constant feed runs with 60 min averages; differences emerged only when the temporal resolution was increased to 30 min.

Table 2.2: p-values from L-ratio tests

Run	Test	R2	R3	R4	R5	R6	R7
R1	F/R*	<.0001	**0.25**	<.0001	0.0002	<.0001	<.0001
	F/PR**	<.0001	-	<.0001	0.0001	<.0001	<.0001
R2	F/R	-	<.0001	0.02	0.0002	**0.8**	<.0001
	F/PR	-	<.0001	0.008	0.0001	-	<.0001
R3	F/R	-	-	<.0001	0.01	<.0001	0.0001
	F/PR	-	-	<.0001	0.004	<.0001	0.0001
R4	F/R	-	-	-	0.002	**0.19**	0.03
	F/PR	-	-	-	0.0006	-	0.02
R5	F/R	-	-	-	-	0.001	0.008
	F/PR	-	-	-	-	0.0005	0.004
R6	F/R	-	-	-	-	-	0.001
	F/PR	-	-	-	-	-	0.0005

* L-ratios were estimated between the full and reduced model (F/R). ** L-ratios were estimated between the full and partly reduced model (F/PR). Initially, the 21 possible pairs of runs were tested using 60 min averaged data. Statistically sgnificant differences indicated with bold font.

Table 2.3: p-values from L-ratio tests using 5 different temporal resolutions

Runs	Test	Temporal Resolution				
		60 min	30 min	15 min	10 min	5 min
R1-R3	F/R	0.25	0.003	-	-	-
	F/PR	-	0.02	-	-	-
R2-R6	F/R	0.81	0.63	0.52	0.42	0.32
	F/PR	-	-	-	-	-
R4-R6	F/R	0.19	0.07	0.027	-	-
	F/PR	-	-	0.013	-	-
R2-R4-R6	F/R	0.12	0.02	-	-	-
	F/PR	-	0.006	-	-	-

2.4.4 The effects of pulses of different sizes on sediment transport

To evaluate the persistence and strength of the effects of the different pulses on sediment transport rate, we estimated relaxation times T_r and total sediment output until T_r (Table 2.4). The relaxation time T_r is the time required for the transport rate to adjust to a relatively stable low mean value equivalent to no feed conditions. We used the mean transport rate over the last 20 h of no feed in run R7 as a reference of low transport ($0.27\,\mathrm{g\,m^{-1}\,s^{-1}}$). This period was chosen because time series plots (Figure 2.3) indicate the transport rate fluctuated around a nearly constant mean, which is supported by cumulative departures that display a nearly constant slope over this period (Figure 2.6). Such transport behavior is consistent with reported times for particle adjustment (*Church et al.*, 1998; *Hassan and Church*, 2000; *Hassan et al.*, 2006). Even though it was expected that the system would have adjusted to even lower transport values if more time had been given, we assumed this would happen at very slow rates relative to the run scale. Similar to the cumulative departure analysis, data were averaged every 15 min because of a good signal-to-noise relation.

Table 2.4: Persistence and strength of pulse effects

Run-pulse ID	Mass (kg)	Exponential fit				Log–linear fit				Output to T_{r2} (kg)	
		q_0	Λ	R^2	T_{r1} (h)	10^a	b	R^2	T_{r2} (h)	raw	adjusted
R3p1	300	1.9	0.07	0.52	27.2	9.4	-1.11	0.74	24.9	208.5	195.7
R5p1	150	2.1	0.11	0.45	18.4	5.4	-0.99	0.65	20.5	89.1	82.9
R5p2	150	2.9	0.15	0.74	16.2	7.1	-1.13	0.84	17.6	76.6	73.2
R4p1	75	1.8	0.15	0.43	12.6	2.4	-0.72	0.5	20.8	32.0	30.2
R4p2	75	2.0	0.18	0.45	11.3	2.6	-0.79	0.45	17.6	33.5	27.5
R4p3	75	0.8	0.03	0.03	30.8	1.4	-0.07	0.02	4.1×10^{10}	-	-
R4p4	75	3.1	0.23	0.63	10.7	4.3	-1.02	0.72	12.1	42.4	37.3

The relation between T_r of a pulse and the time between pulses (T_p) defined the dominance of discrete or cumulative effects of episodic supply over a run and the recovery of ambient transport rate. With the large pulse in R3 $T_r < T_p$, indicating relaxation occurred within the run (Table 2.4). With the pair of medium sized pulses (R5), $T_r \leq T_p$. The experiment using multiple small pulses (R4) contrasts with $T_r > T_p$, indicating transport rate had not fully relaxed before a new input entered. There was no evident relation between pulse mass and relaxation time (Figure 2.8a). The variability within pulses of the same size was as large as variability among pulses of different size.

The strength of the effects of a pulse on sediment transport rate was evaluated by computing the total sediment output over the response time as follows

$$\text{Total Output} = \sum_{i=T_i}^{T_p} [q_b]_i + \int_{T_p}^{T_{r2}} 10^a T^b \tag{2.4}$$

Here, T_i is the time of the first significant increase in transport rate after a pulse, T_{r2} is the relaxation time estimated with (2.3), T_p is the time between sediment pulses, $[q_b]_i$ is the observed sediment transport rate at time i, and a and b are the coefficients from (2.3). These coefficients are used to predict the output beyond T_p, for those cases in which $T_p < T_{r2}$ (see Figure 2.8a). T_{r2} was used instead of T_{r1} because the log–linear fit better resembled the decrease in sediment transport rate, especially after small and medium sized pulses; and because it had higher coefficients of determination R^2 (Table 2.4).

To account for differences in the transport rate previous to a pulse, we predicted the sediment output under no feed conditions and subtracted it from the estimated output as

$$\text{Adjusted Output} = \text{Total Output} - \int_{T_i}^{T_{r2}} 10^{\overline{q}_b} T^{b'} \tag{2.5}$$

Here $\overline{q}_b$ is the mean sediment transport rate estimated over three hours before the input and b' is the rate of decrease in sediment transport rate, estimated with equation (2.3) for R7. If $\overline{q}_b \leq q_{ref}$, the effects of the transport regime previous to the pulse were considered negligible.

A positive trend was clear between the size of the pulse and the magnitude of the response (Figure 2.8b). There was variability in the total output within pulses of the same size, but it was considerably less than the variability observed among pulses of different sizes. With small pulses the output varied between 30–45 kg, whereas with the medium-sized pulses the output was twice as much (between 70–90 kg). Finally, after the single large pulse ~200 kg of sediment had left the flume by the time transport rate relaxed to the no feed condition.

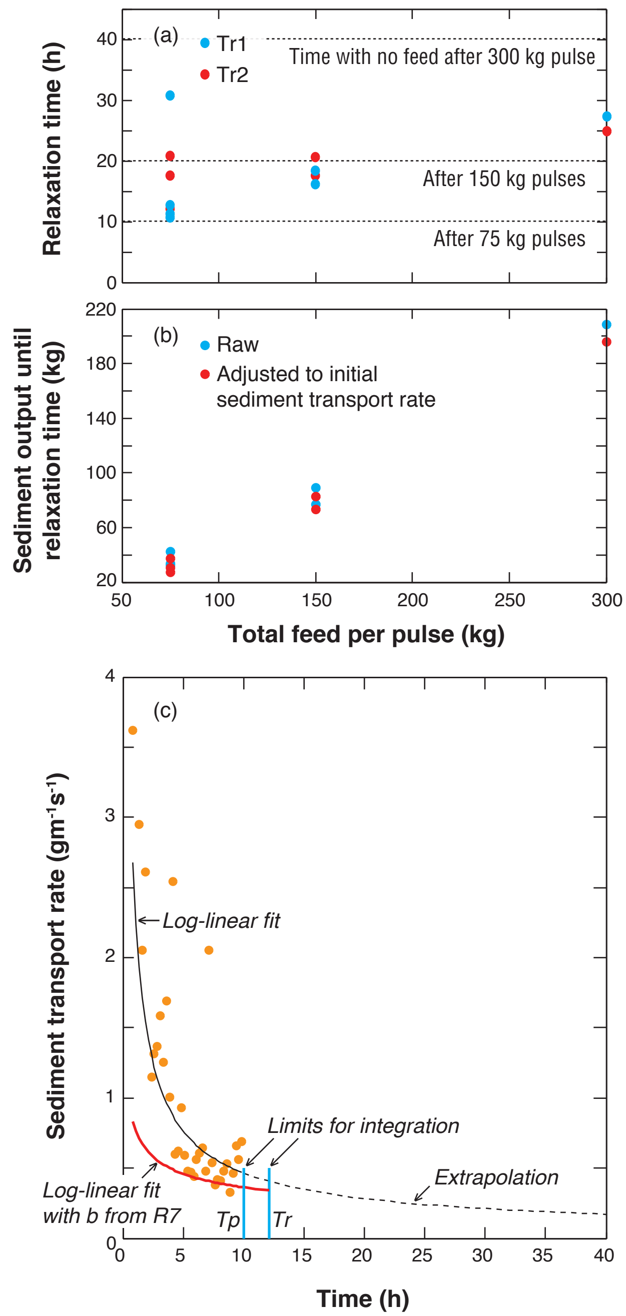

Figure 2.8: Persistence and strength of the effects of supply episodes of different size on sediment transport. (a) Relaxation time T_{r1} estimated with equation 2.2 (exponential fit), and T_{r2} estimated with equation 2.3 (log–linear fit). (b) Total sediment output until T_{r2}. (c) Estimation of total output until T_r for the last small pulse.

2.5 Discussion

In the following section, we discuss the four hypotheses presented. Channel adjustment is evaluated in terms of sediment transport rate, bed surface and bedload particle size, sediment storage, and bed slope.

2.5.1 Hypothesis 1: The adjustment of a gravel bed to sediment supply is significantly affected by the magnitude and frequency of sediment feed

This hypothesis was verified after comparing the results under episodic and constant feed. All the runs with feed showed overall aggradation, which was considerably greater under constant feed or with small frequent pulses than with larger rare pulses. The evolution of sediment transport rate was consistent with particle size adjustments on the surface. As bed surface coarsened, sediment transport rate decreased (see Figures 2.3 and 2.4c-e). As bed surface got finer, transport rate increased. Sediment feed caused surface fining and increased transport rate as described in previous studies (*Dietrich et al.*, 1989; *Venditti et al.*, 2008; *Madej et al.*, 2009; *Nelson et al.*, 2009); the intensity of change in transport was related to the supply regime. Sediment pulses promoted stronger and faster, but more transient, responses than did constant feed. In time the system behaved as if sediment starved after sediment pulses passed. Sharp increases in transport rate caused by one or few large pulses (R3, R5) can be explained by surface fining that occurred initially, which provided great availability of fine sediment for transport as well as a decrease of bed roughness at the grain scale. As the pulse dispersed and fine sediment was evacuated, the bed surface coarsened and reorganized, and transport rate decreased. Our observations support the idea that dispersion is the dominant mechanism of pulse evolution when the bed and feed material have similar particle size (*Cui et al.*, 2003; *Sklar et al.*, 2009). However, some adjustments cannot be explained simply by the supply regime. These include cumulative storage observed under episodic sediment supply, overall increase in bed slope, and little variability of bed slope following the last pulse fed in R5 until the end of the experiment.

Cumulative storage and the general increase in bed slope over the experiment could be related to the coarse grain-size distribution of the bulk sediment that constituted the original bed and feed material. Roughly 40% of the bulk sediment was coarser than 8 mm, which moved at lower intensities and more intermittently than the finer fractions. A significant fraction of coarse material was stored in a sediment wedge that developed near the upstream end of the bed. The wedge increased local slope and caused the bed slope to increase as the wedge grew and expanded. Such behavior could have promoted the mobilization of stored sediment at later stages. With most sediment pulses, bed slope increased, but did not return to its pre-pulse value before more sediment was supplied. The cumulative increase in bed slope can be explained by bed armoring and structuring, which could have counteracted degradation once the sediment feed was exhausted. This would explain as well the stability of channel slope under no feed during R7, and is consistent with previous observations that constrained channels primarily respond to changes in flow or sediment supply by adjusting surface particle size (*Eaton and Church*, 2009). Interestingly, by the middle of run R5 the slope became nearly constant at 0.02 m/m, which is similar to the flume slope. It is difficult to establish why the slope did not change with the second pulse in R5 or during R6 which had constant feed. In these cases, bed slope stability could be a result of bedforms or the fact that the upstream end of the bed was not included in bed slope estimations.

In summary, the significance of the magnitude and frequency of sediment supply was evident in particle size adjustments and the evolution of sediment transport rate. Cumulative storage and changes in bed slope were conditioned by the grain-size distribution of the feed, which coarse fractions remained as partially mobile during the experiment.

2.5.2 Hypothesis 2: If the time between sediment pulses is less than the time needed for the sediment transport rate to relax ($T_p < T_r$), the response can be similar to constant feed regimes

This hypothesis is supported by similarities between constant feed regimes and run R4 which introduced multiple small sediment pulses. R4 had $T_p = 10\,\mathrm{h}$, with estimated $T_r > T_p$ (Figure 2.8). During R4 sediment storage was considerably greater than during the run that received the large sediment pulse and more similar to the constant feed runs. The departure curve of R4 was similar to that of constant feed runs. The span of cumulative variability in R4 was relatively small, similar to those for constant feed. That similarity may relate to a smaller increase in transport rate relative to those produced by larger pulses. Finally, L-ratio tests suggest similarities with constant feed regimes can emerge from high-frequency episodic inputs.

But at time-scales shorter than 10 h, channel adjustments after the small pulses in R4 were similar to those following infrequent, large pulses. The timing with which the transport rate at the end of the flume responded to small pulses was similar to the response time for larger, less frequent pulses and much faster than the response under constant feed. The same was noted for particle size adjustments, for which responses following small pulses resembled those following large pulses, but in a less pronounced way.

2.5.3 Hypothesis 3: Large sediment pulses produce stronger responses in the transport rate and require longer time for relaxation than small pulses

Estimated sediment outputs until T_r (Figure 2.8b) support the hypothesis that infrequent large pulses produce stronger effects in transport rate; however, there was no clear relation among T_r following different sized pulses (Figure 2.8a). The largest pulse delivered more than twice the material delivered following medium-sized inputs, and more than five times the amount of sediment transported following multiple small pulses. Variability observed within pulses of similar size was considerably less than differences among pulses of distinct magnitudes. Differences in bed configurations previous to a pulse, which affected mean sediment transport rates, defined how far from q_{ref} (low reference sediment transport rate) the system deviated before the pulse and could have caused differences in T_r. In addition, differences in the degree of armoring and slope of the bed could affect the value at which mean sediment transport rate would become stable after a pulse. At lower bed slopes and coarser bed surfaces sediment transport rate could become stable at smaller values than with higher bed slopes and finer bed surfaces. The steady state of sediment transport rate under no sediment feed in this study was defined as q_{ref}, which was constant and added error to T_r estimations.

2.5.4 Hypothesis 4: The temporal adjustment of sediment transport rates to changes in the supply regime is conditioned by the initial bed slope, surface grain-size distribution, and sediment storage

Comparisons among results from runs with identical feed regimes are used to discuss the important influence of initial bed conditions in sediment transport rate. The L-ratios indicate there were no significant differences in the intercept and slopes of the statistical model fit to sediment transport rates between runs with constant feed (even at 5 min resolution), whereas significant differences were encountered at one hour averages between runs with no feed.

These differences are explained by initial bed conditions. Because runs were sequential and supply regimes varied, initial sediment storage was considerably different for runs with similar feed regimes. Constant feed runs (R2, R6) had different initial bed slopes but similar surface-size compositions and degree of armoring. The initial beds of R1 and R7 (no feed) instead had similar slopes, but very different surface textures. In R1, the primary surface was well-mixed and had the same grain-size distribution as the feed, whereas in R7 the bed was armored. Even though differences in the initial bed conditions were not tested statistically; we think the different bed conditions between R1 and R7 were important for sediment transport because of a disparity in the availability of easily transportable fine material. The great availability of fine sediment at the beginning of R1 made it more similar to the run with a large sediment pulse (R3) than to R7 which also received no feed. From the bedload transport rate time series (Figure 2.3), we observe that despite an initial period of high transport in R1, sediment transport rate evolution in both runs without feed (R1, R3) was similar. In the case of constant feed regimes (R2, R6), differences in slope were less than 1% and relate to transport capacity. The rather small effects produced by differences in bed slope could have been counteracted by surface armoring and structuring. In summary, only large textural differences in the initial bed significantly affected the trend of sediment transport rates over runs.

2.6 Conclusions

Observations on an experimental gravel bed under steady flow but variable feed conditions indicate that the magnitude and frequency of sediment supply are important controls on bed surface organization and temporal patterns of sediment transport rate. These results point out that the assumption of constant feed might not be suitable to model streams that are subjected to large, infrequent sediment pulses. Under these regimes, the channel changed significantly shortly after a pulse, but became relatively stable as sediment evacuated and the bed armored. Instead, the use of constant feed might be appropriate to study channels that receive more frequent pulses (as in run R4), and over long time scales (i.e., $>$ one event). In overall, temporal patterns of sediment transport rate and sediment storage during the four frequent, small pulses in R4 were like under constant feed.

The use of poorly sorted sediment, which coarse fractions remained as partially mobile during the experiment, promoted bed surface armoring and structuring between sediment pulses and counteracted degradation, resulting in cumulative sediment storage. Infrequent, larger pulses caused stronger short-term ($<$10 h) effects on surface fining and sediment output than frequent smaller pulses, and caused less sediment storage over a run.

The experimental design used helped to develop a realistic bed with different types of channel morphologies, which evolution reflected the history of flow and feed conditions. The bed degraded during the first run, but then aggraded because of net storage during subsequent runs, and developed complex topographies. Detailed analysis of bed topography and structures (using DEMs and bed photos) would improve our understanding of bedform evolution under the different supply regimes.

The initial bed surface texture and bed structures influenced significantly sediment transport rates during a run, whereas initial bed slope and cumulative storage played a minor role. Results were likely conditioned by the sequence of runs used and it would be interesting to explore other experimental designs. Channel adjustment could have been different if each run had started from the same flat well-mixed bed or if the sequence of runs had followed a different order.

Chapter 3

The effect of sediment supply regime on bedload scaling and sediment mobility

3.1 Summary

The effect of sediment supply regime on bedload scaling and mobility was analyzed for a poorly sorted (0.5–64 mm) experimental bed. Water discharge was held constant and, during each run, 300 kg of sediment was supplied in a different way. Total bedload transport rate and D_g of bed surface responded consistently to sediment feed. Constant feed caused gradual increases in bedload rate. In contrast, large sediment pulses caused pronounced increases as the bed surface got finer, followed by monotonic declines as the surface coarsened. Pronounced trends caused stronger memory in bedload time series for runs with episodic feed than in those for runs with constant feed. Autocorrelation coefficients ρ_τ were higher and the duration of a memory stage of fluctuation was larger. Over shorter periods of time (5-h) within each run, memory (Hurst exponent H) exhibited considerable variation. Long-term memory ($H \approx 1$) was observed during periods with strong decays in bedload rate and during periods when bedload rate was stable around a constant mean. This behavior indicates that memory can result from bedform evolution at different scales and local changes in sediment storage and transport. Patterns of grain-size dependence persisted regardless of sediment feed. Memory strength always decreased with grain size for gravels, as fractional transport became more intermittent. The movement of sand exhibited more stochasticity than that of fine gravel (2–8 mm), but not due to intermittency. Scaling statistics for total bedload were similar to those for fine gravel, which was fully-mobile and dominated bedload.

3.2 Introduction

Understanding sediment transport patterns is important for river engineering design, habitat maintenance, and river restoration projects (*Parker*, 2008). The movement of specific grain sizes is relevant for a variety of physical and biological processes in gravel-bed streams. As examples, coarse material is important for channel stability (e.g., *Zimmermann*, 2010; *Waters and Curran*, 2012; *Mackenzie and Eaton*, 2017), gravels are relevant for fish spawning habitat (e.g., *Kondolf and Wolman*, 1993; *Hassan et al.*, 2008; *Riebe et al.*, 2014; *Hassan et al.*, 2015), and fine sediment can affect water quality and macroinvertebrates (e.g., *Jones*, 2012; *Mathers et al.*, 2017).

Sediment transport and channel stability in mountain streams are strongly affected by: unsteady and non-uniform flow conditions (*Hassan et al.*, 2006), bed surface armor and structures (*Parker and Klingeman*, 1982; *Wilcock and Detemple*, 2005), the wide range of shapes and sizes of grains (*Einstein*, 1950; *Wilcock*, 1992), and changes in the texture and amount of sediment supply (*Curran and Wilcock*, 2005; *Hassan et al.*, 2008). At the reach scale, stream morphology responds to imbalances between the magnitude of transport capacity and that of sediment supply, and streams can be classified as supply-limited if transport capacity exceeds sediment supply or transport-limited if sediment supply exceeds transport capacity (*Montgomery and Buffington*, 1997). Supply-limited channels commonly develop a coarse, well-structured bed surface, with low intensity of sediment transport (e.g., *Parker et al.*, 1982; *Dietrich et al.*, 1989; *Lisle et al.*, 1993; *Church et al.*, 1998; *Venditti et al.*, 2008; *Nelson et al.*, 2009). Under the same flow and slope conditions, transport-limited streams aggrade and develop a fine, poorly-structured bed surface, with sediment transport rates near transport capacity (e.g., *Lisle and Madej*, 1992; *Madej et al.*, 2009; *Pryor et al.*, 2011). Most experimental work on the effects of changes in sediment supply on channel adjustment have used constant sediment feed and only a few experiments have introduced the sediment in isolated episodes as observed in mountain streams (*Cui et al.*, 2003; *Sklar et al.*, 2009; *Venditti et al.*, 2010; *Johnson et al.*, 2015). Flume studies that use episodic sediment supply have primarily examined the mechanisms of sediment pulse propagation and the effects of relative sediment texture, but with few exceptions the role of the magnitude and frequency of sediment supply has received little attention (*Elgueta-Astaburuaga and Hassan*, 2017).

Field and flume observations indicate that sediment transport is a stochastic process that varies intermittently in space (*Nelson et al.*, 2009; *Heyman et al.*, 2014) and time (*Heyman et al.*, 2013; *Ghilardi et al.*, 2014). Variability appears at different scales, ranging from grain mobility to bedform evolution, even under steady flow and constant sediment feed. Studies that analyze the effect of sediment supply regime on the scales of bedload variability are missing. The use of probabilities to account for the stochastic and intermittent nature of bedload transport started with *Einstein* (1937, 1950). In the past decade, numerous probabilistic approaches have been developed to describe fluctuations in bedload transport, which include: microstructural descriptions of bedload transport (*Ancey et al.*, 2006) and their implications on larger scales

(*Ancey and Heyman*, 2014), quantification of roughness and intermittency on bedload signals (*Singh et al.*, 2009), deriving probability distribution functions for bedload transport (*Turowski*, 2010; *Furbish et al.*, 2012), and analyzing the dependence of bedload statistics on temporal scales (e.g., *Ganti et al.*, 2009; *Campagnol et al.*, 2012; *Ma et al.*, 2014; *Saletti et al.*, 2015), which is the approach that we will use in this study.

The scaling properties of bedload transport fluctuation are important for the design of measurement programs, comparisons among data sets, testing bedload transport models, and connecting the results from short-term studies to long-term evolution of stream morphology (*Singh et al.*, 2009; *Foufoula-Georgiou and Stark*, 2010; *Recking et al.*, 2012). One important aspect is the relationship between the variance of bedload flux σ_T^2 and the aggregation time scale T at which the signal is sampled. This relationship has been characterized as both a power law (e.g., *Einstein*, 1937; *Ancey et al.*, 2006) and a more complex relation (e.g., *Campagnol et al.*, 2012). Using experimental data, *Ma et al.* (2014) proposed three stages of fluctuation in bedload transport rate: intermittent, invariant, and memoryless. The intermittent stage occurs at short T with the variance σ_T^2 decaying as a power law with exponent $n = -1$, indicating no memory. The invariant stage occurs at intermediate T with constant σ_T^2, indicating memory. At long T, σ_T^2 decays with $n = -1$, the autocorrelation vanishes, and as for short T the process has no memory. The authors suggest that to avoid underestimating σ^2 (shorter T) or overestimating it (longer T) bedload statistics should be computed within the invariant stage. The classification proposed by *Ma et al.* (2014) is based on three experiments under steady flow and constant sediment feed. Two of them used unisize particles (*Ancey et al.*, 2006; *Heyman et al.*, 2013) and the other used two separate groups of grain diameters (*Singh et al.*, 2010). In this paper, we assess the effects of episodic feed regimes, as in natural rivers, on the stages of bedload fluctuation. Unlike *Ma et al.* (2014), we used poorly sorted sediment in our experiment to recreate more realistic conditions like the development of bed armor and bed structures.

The dependence of the current state on system history characterizes the system memory. If there is no dependence (e.g., white noise process), there is no memory. Short-term persistence occurs if the current state depends only upon the recent past (e.g., Markovian process). Long-term persistence occurs if the current state depends upon the entire history. The Hurst exponent H, describing the relationship between the standard deviation σ_T of a process and aggregation time scale T, has been used to quantify memory in time series of hydrological variables (*Hurst*, 1951; *Koutsoyiannis and Montanari*, 2007), suspended sediment load (*Shang and Kamae*, 2005), and bedload sediment transport (*Saletti et al.*, 2015). Using experimental data of step-pool morphologies under unsteady flow (*Zimmermann*, 2009, 2010), *Saletti et al.* (2015) found that, in the absence of feed, periods with intense transport exhibited stronger memory than periods with low transport. They also found that memory strength (sample autocorrelation ρ_τ and H) varied with grain size. Our experimental design allowed us to test the effect of sediment feed regime on the memory of bedload time series and to assess the effects of grain-size dependence over sand-sized fractions, which were not present in the experiments analyzed by *Saletti et al.* (2015), and over longer time periods than the 1-h intervals used by them. The bed morphologies developed over our experiment differed considerably from those reported in *Saletti et al.* (2015), which could cause differences in the scales of the processes governing sediment transport (e.g., step arrangement vs. armoring and cluster dynamics) that would show in the memory structure of bedload transport.

Gravel-bed streams, composed of poorly sorted sediment, exhibit grain-size dependence of their transport patterns under moderate (e.g., bankfull) flow conditions. Sediment enters a stream as episodic inputs through bank collapse, landslides, debris flows, and other disturbances (*Dadson et al.*, 2004; *Hovius and Stark*, 2006; *Lancaster*, 2008). The introduced material can be immediately transported downstream or get deposited and become a source of sediment (*Jackson and Beschta*, 1982; *Goff and Ashmore*, 1994; *Lane et al.*, 1995; *Sutherland et al.*, 2002; *Reid and Dunne*, 2003). When mobilized, bed sediment can sort in the longitudinal, transverse, and vertical directions (e.g., *Parker*, 1992; *Powell*, 1998) with different grain sizes relating to specific processes of bed evolution. Despite studies that report on fractional bedload transport (e.g., *Wilcock and McArdell*, 1993; *Hassan and Church*, 2000), our data provide an opportunity to assess the temporal variability of bedload transport at 1 s resolution for the multiple grains size fractions in our experimental bed, which included sand between 0.5–2 mm and gravels in the range 2–64 mm.

We examine the effect of sediment supply regime on bedload scaling and sediment mobility for a poorly sorted experimental gravel bed, which developed under steady flow but changing sediment supply. Constant flow discharge allowed us to isolate the effects of changes in sediment feed. We used no feed and constant feed regimes as references, and three types of episodic supply regimes to evaluate the effects of the magnitude and frequency of occasional sediment pulses. The same 300 kg was fed over each run to compare among them. The data available allowed us to test if the three stages of bedload fluctuations proposed by *Ma et al.* (2014) hold under more realistic conditions (episodic sediment feed, wide grain-size distribution) and if the memory structures described by *Saletti et al.* (2015) are also noticed for bed morphologies that occur at milder slopes and have finer textures. Our experiment was conducted as a sequence of consecutive runs so that the bed had an extended history of flow and sediment supply as in natural streams. We repeated no feed and constant feed regimes twice within the sequence to assess the importance of bed history and initial bed conditions in the results.

The study aims to evaluate the following hypotheses related to the effects of sediment feed on the memory structure of bedload rates and the grain-size dependence of bedload patterns: (H1) bedload rate time series for runs with constant sediment feed have weaker memory than those for runs with large infrequent sediment pulses, which can cause pronounced trends in bedload transport; (H2) the memory structure of total bedload reflects that of fully-mobile grain sizes, which dominate sediment transport and exhibit strong memory in their bedload signals; (H3) grain-size dependence in bedload transport increases with sediment feed because the movement of fully-mobile sediment is more responsive to feed than that of partially-mobile grain sizes.

3.3 Methods

3.3.1 Experiment

The data were collected in a flume experiment conducted at the Mountain Channel Hydraulic Experimental Laboratory, University of British Columbia (UBC). The flume was 18 m long, 1 m wide, and 1 m deep, with a slope of 0.022 m/m (*Elgueta-Astaburuaga and Hassan*, 2017). The bed and feed sediment were poorly sorted and ranged from 0.5 to 64 mm, with ∼20% sand, geometric mean $D_g = 5.7$ mm, and percentiles $D_{16} = 1.6$ mm and $D_{90} = 27$ mm. The experiment consisted of a sequence of seven runs, denoted R1–R7, under constant flow discharge (65 $\mathrm{L\,s^{-1}}$), but combining multiple feed regimes. Except for the first run, which started from a flat and well-mixed bed, the initial bed conditions for each run were inherited from the previous runs. For R2–R6, 300 kg of sediment was introduced over 40 h. The magnitude and frequency of sediment feed varied among runs (Table 3.1). R1 had no feed to condition the bed and R2, which served as a reference, received constant feed. In R3, a large sediment pulse was introduced at the beginning to test the bed response to large infrequent episodes. To assess the roles of pulse magnitude and frequency, R4 and R5 received smaller, but more frequent sediment pulses than R3. Finally, to explore the importance of bed history, the constant feed regime of R2 was repeated in R6, and R7 was conducted under no feed as for R1.

Table 3.1: Summary of sediment feed regimes used in experimental runs

Run	R1	R2	R3	R4	R5	R6	R7
Sediment feed regime	-	constant	episodic	episodic	episodic	constant	-
Feed rate, $\mathrm{g\,s^{-1}}$	0	2	83	83	83	2	0
Number of pulses	-	-	1	4	2	-	-
Pulse magnitude, kg	-	-	300	75	150	-	-
Pulse recurrence interval, h	-	-	40	10	20	-	-

During the experiment, flow properties, bed elevation, bed-surface particle size, and sediment transport were systematically measured. Water depth was measured along the side of the flume at an interval of 0.5 m and was used to estimate water-surface slope; the mean water depth was 0.077 m. Bed characteristics were measured under no flow. Digital elevation models (DEMs) were obtained from bed scans using a video-camera and a green laser beam. DEM resolution was 2 mm $\times$ 2 mm in the horizontal and 1 mm in the vertical. Bed-surface grain-size distributions were obtained from point counts on bed surface photographs in the center of the flume, 6–8 m upslope from the downstream end. The sample grid superimposed on the photos had a cell size of 65 mm, which was equal to the largest particle size. Grains smaller than 2.8 mm were difficult to recognize, and were grouped in one class. Fractional sediment transport data were generated using the video-based method explained in *Zimmermann et al.* (2008) supplemented by sampling of grains as small as 1 mm (*Elgueta-Astaburuaga and Hassan*, 2017). Additionally, a sediment trap was placed at the downstream end of the flume to check results. Material $<$ 1mm was under-detected by the video-based method, but no correction was applied because trap data had a considerably lower temporal resolution than that of the video-based data and because sediment $<$ 1mm only corresponded to 2–3% of the sediment mixture, so errors were small. More details on the experimental set up and data collection can be found in *Elgueta-Astaburuaga and Hassan* (2017).

3.3.2 Data analyses

The geometric mean diameter D_g was estimated for the bed surface from point counts and for the bedload from video-based light table data. Bed slope was estimated along the thalweg using DEMs. Only data between 4 and 11.8 m were included to avoid backwater effects downstream and the effects of sediment feed upstream. As a reference, critical shear stress for each grain size τ_{ci} was estimated rearranging

$$\tau^*_{ci} = \frac{\tau_{ci}}{\mathrm{D}_i g(\rho_s - \rho_w)} \tag{3.1}$$

where τ^*_{ci} is the critical Shields number (*Shields*, 1936), D_i is grain size, g is acceleration of gravity (9.8 $\mathrm{m\,s^{-2}}$), ρ_s is sediment density (2650 $\mathrm{kg\,m^{-3}}$), and ρ_w is water density (1000 $\mathrm{kg\,m^{-3}}$). We assumed $\tau^*_{ci} = 0.047$ (*Meyer-Peter and Müller*, 1948). The boundary shear stress τ_b was computed as

$$\tau_b = \rho_w g R_h S_w \tag{3.2}$$

where R_h is the hydraulic radius and S_w is the water-surface slope. Grains sizes for which $\tau_b > \tau_{ci}$ were expected to be mobile during the experiment.

Relative sediment mobility was analyzed by computing scaled sediment transport rates as in *Wilcock and McArdell* (1993). Fractional transport rates q_{bi} were scaled by the grain-size distribution of the bed bulk material f_i. We used f_i and not the bed surface to scale q_{b_i} for similar reasons to those argued in *Church and Hassan* (2002): differences in the temporal resolution of sediment transport data (high) and bed photographs (low), difficulties linking transport measurements to specific bed surface conditions (temporally and spatially), and the truncation of bed surface grain-size distributions at 2.8 mm. We analyzed the grain-size composition of large bedload rates with probability of exceedence $p_e < 0.01$ as in *Saletti et al.* (2015) to assess the contribution of coarse partially-mobile grains and the effects that changes in sediment feed could cause in this contribution.

For bedload rate time series, the structure of memory for different grain sizes was analyzed to compare sediment transport patterns with those for total bedload. To assess short memory and evaluate the presence of trends, the sample autocorrelation coefficients ρ_τ were estimated as in *Chatfield* (1975)

$$\rho_\tau = \frac{c_\tau}{c_0} = \frac{\frac{1}{N}\sum_{t=1}^{N-\tau}(Y_t - \overline{Y})(Y_{t-\tau} - \overline{Y})}{\frac{1}{N}\sum_{t=1}^{N}(Y_t - \overline{Y})^2} \tag{3.3}$$

Here, c_τ is the autocovariance at lag τ and c_0 is the autocovariance at lag 0 for time series Y, $\overline{Y}$ is its mean, Y_t and $Y_{t-\tau}$ are values at time t and t minus lag τ respectively, and N is the number of observations. We assumed 95% confidence limits ($\pm 1.96/\sqrt{N}$) as the threshold for significant autocorrelation.

To detect multi-regime fluctuations in bedload, the relationship between variance σ_T^2 and aggregation time scale T was evaluated on log-log scale plots as in *Ma et al.* (2014). We used sediment mass for sediment flux instead of number of particles as in *Ma et al.* (2014) because of the wide range of grain sizes in our mixture. To compare results among different runs we divided the variance for each time scale σ_T^2 by the variance for $T = 1$ s. To assess grain-size dependence, we grouped fractional data in four grain size classes: 0.5–2 mm (sand), 2–8 mm (fine gravel), 8–16 mm (coarse gravel), and 16–64 mm (very coarse gravel). Sediment $<$ 2 mm was grouped together because we wanted to observe the behavior of sand, which was expected to be fully mobile and potentially sensitive to hiding effects and infiltration. The limit of 8 mm for fine gravel was near the limit for partial mobility during the experiment. Grains $>$ 8 mm were grouped in two fractions to observe grain-size dependence on coarse partially-mobile gravels. The limit of 16 mm corresponds to the D_{75} of the bulk sediment and it is similar to the D_g observed for the bed surface when the bed was armored (*Elgueta-Astaburuaga and Hassan*, 2017).

The Hurst exponent H was used to quantify long-term memory in time series (e.g., *Hurst*, 1951; *Shang and Kamae*, 2005; *Koutsoyiannis and Montanari*, 2007; *Saletti et al.*, 2015), and was estimated as

$$H = S + 1 \tag{3.4}$$

where S is the best fit slope on a log-log scale of the standard deviation σ_T against aggregation time scale T. The functional relation between σ_T and T is described as

$$\sigma_T = \frac{\sigma_0}{T^{1-H}} \tag{3.5}$$

Finally, to identify at which T different grain sizes exhibit the strongest memory, the sample autocorrelation coefficient at $\tau = 1$, ρ_1, was computed at different T. Minimum T (1 s) used to compute bedload rate statistics (σ_T^2, σ_T, ρ_{1_T}) was limited by data resolution and maximum T was taken as $N/50$.

3.4 Results

3.4.1 Observations

Bed adjustment and sediment mobility

To summarize bed adjustments to changes in sediment supply regime, bedload transport rate (Figure 3.1a), D_g of the bed surface and bedload (Figure 3.1b), and bed slope (Figure 3.1c) are presented as functions of time. Bedload rate statistics and observations at the end of each run can be found in Table 3.2. As expected, bedload transport rate (Figure 3.1a) and D_g of the bed surface (Figure 3.1b) responded significantly to sediment feed. Without sediment feed as in R1 and R7, bedload rates decreased as the bed surface coarsened. With constant feed as in R2 and R6, bedload rate responded after 7 h with a gradual increase, but D_g of the bed surface did not change significantly. Sediment pulses as in R3, R4, and R5, caused sharp increases of bedload rate, which were related to a more pronounced fining of the bed surface. The increase in bedload was larger by orders of magnitude and much faster than with constant feed. Once the feed stopped, there was a monotonic decrease in bedload rate as the bed surface re-coarsened. The strength of the effects increased with pulse magnitude and the differences with constant feed were less evident in R4 that received smaller, but more frequent pulses. The range of values for bedload rate was similar among the runs, with minimum values near zero and maximum around 10^2 $\mathrm{g\,m^{-1}\,s^{-1}}$, although the mean bedload rate $\bar{q}_b$, standard deviation σ_{q_b}, and 75th percentile were different (Table 3.2). Although, differences in $\bar{q}_b$ were moderate among runs (0.4–1.5 $\mathrm{g\,m^{-1}\,s^{-1}}$ range), differences in σ_{q_b} were large (2–30 $\mathrm{g\,m^{-1}\,s^{-1}}$).

The response of bed slope to sediment feed was not always consistent (Figure 3.1c). Bed slope decreased significantly during the first hour of R1 as a large amount of sediment exited the flume because of the well-mixed initial bed. During the rest of R1, bed slope remained low at $\sim$0.018 m/m and did not change much during R2. In R3, the slope increased significantly with the pulse, but after the feed was stopped, it did not return to the same values previous to the pulse, and remained considerably higher. A cumulative increase in bed slope was observed through R3–R5, until it reached the flume slope ($\sim$0.022 m/m) and remained nearly constant until the end of the experiment. The increased slope was coherent with a net

Table 3.2: Bedload rate statistics and observations at the end of each run

Run	R1	R2	R3	R4	R5	R6	R7
Bedload rate ($gm^{-1}s^{-1}$)							
Mean	1.29	0.65	1.56	0.98	1.19	1.25	0.42
Standard deviation	27.06	5.12	7.64	3.17	10.32	31.32	1.56
25th percentile	0.05	0.14	0.12	0.28	0.22	0.27	0.13
50th percentile	0.14	0.37	0.24	0.50	0.41	0.54	0.22
75th percentile	0.46	0.76	0.63	0.96	0.89	1.00	0.38
Mean water depth (m)	–	0.073	0.08	0.083	0.072	0.075	0.073
Water-surface slope (m/m)	–	0.017	0.019	0.020	0.020	0.020	0.020
Bed slope (m/m)	0.017	0.016	0.018	0.020	0.022	0.022	0.022
D_g surface (mm)	14.5	15.3	14.4	14.3	14.4	13.8	15.7

sediment storage in the order of 10^2 kg, which consisted mainly of coarse grain sizes that were less mobile.

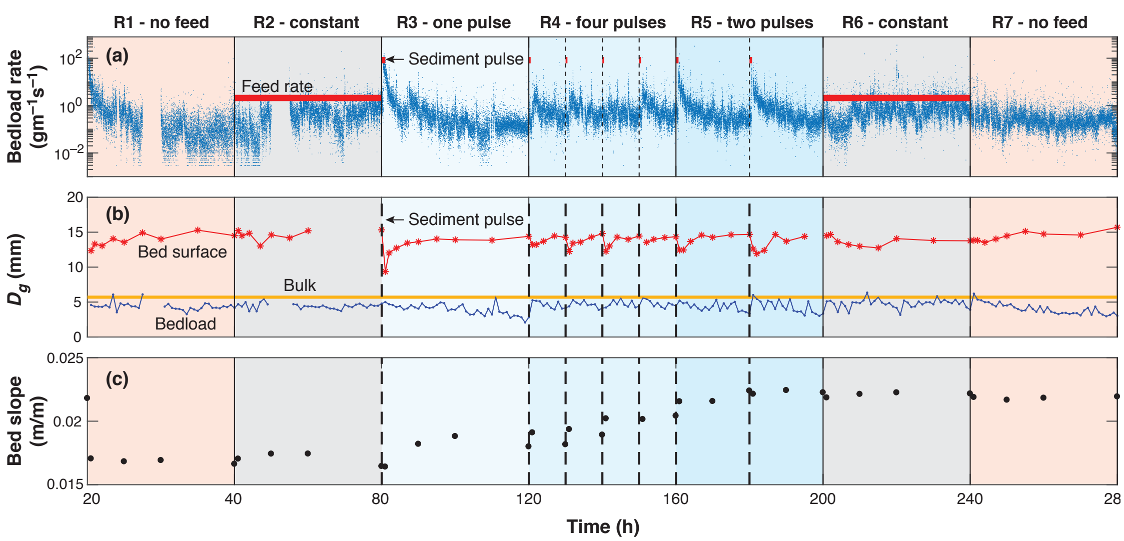

Figure 3.1: Bed adjustments for the entire 280-h experiment. Modified from Figures 3 and 4 in *Elgueta-Astaburuaga and Hassan* (2017) (AGU Usage Permissions). (a) Total bedload transport rate and sediment feed rate (red lines and dots) in logarithmic scale. Gaps in the data are due to technical problems. (b) Geometric mean particle size D_g of the bed surface, bedload, and bulk bed. (c) Slope at the thalweg. Sediment pulses are indicated with vertical dashed lines in (b) and (c).

Mean sediment transport rate varied with grain size over more than two orders of magnitude (Figure 3.2a). Grains up to 45 mm exited the flume throughout the experiment, although $\tau_{ci} > \tau_b$ for grains $>$ 20 mm under average flow conditions, which highlights the importance of variability at small scales (e.g., arrangement of grains, flow turbulence) and that the critical Shields stress for poorly sorted gravel is below the one we assumed from *Meyer-Peter and*

Müller (1948) already noted by *Parker and Klingeman* (1982). Transport rate increased with grain size for sand fractions (< 2 mm), grains between 2 and 8 mm exhibited similar mean rate, but this decreased with size for grains > 8 mm. The decrease in grains < 2 mm could be related to hiding effects limiting the fine material available for transport or to under-detection associated with the light table method (likely for grains < 1 mm). Relative mobility analysis (*Wilcock and McArdell*, 1993) indicated that the limit between partial and full mobility was stable at $\sim$8 mm and was not significantly affected by changes in sediment feed.

The frequency of fractional bedload transport was characterized by measuring the time over which no grains of a given size exited the flume (Figure 3.2b). Even though, coarse particles (> 16 mm) were seen moving through the flume during the experiment, they moved for short distances and in most cases, did not leave the flume. Grain-size fractions < 2 mm were grouped together as sand to avoid the effects of mis-detection noticed for grains < 1 mm. Time immobile was very low for sand and increased with grain size for particles > 2.8 mm. Over the entire 280-h experiment aggregated sand fractions (< 2 mm) exited the flume 97% of the time, fine gravel (2–8 mm) 98%, coarse gravel (8–16 mm) only 8%, and very coarse material (> 16 mm) less than 1%.

Bursts in bedload rates

Regardless of their low frequency, occasional bursts in bedload rates mobilized large amounts of sediment, which in general exhibited a coarser composition than bulk bedload transport. To assess the composition of such spikes in the transport rate, we divided each run into four 10-h intervals and then, within each interval, selected all observations for which bedload rates (in g m^{-1} s^{-1}) had a low probability of exceedance $p_e < 0.01$ as in Figure 3.3. 25% of the total mass transported during the experiment can be attributed to bedload rates with low p_e. Commonly, these large bedload rates had a greater proportion of sediment > 8 mm than the bulk bedload, but exceptions were noted during the first 10 h of R1 or R3 (Figure 3.4). For these exceptions, large spikes in the transport rate were caused by the large availability of fine mobile sediment due to an initial well-mixed bed in R1, and due to a large sediment pulse at the beginning of R3 (Figure 3.3).

Because of their large masses, a few coarse grains could significantly affect the composition of large bursts in bedload rate under low–moderate transport conditions. The percent of bedload observations with $p_e < 0.01$ that involved coarse material was estimated over each 10-h period (Table 3.3) to assess the frequency with which they occurred. Regardless of the variability among analyzed periods, the percentage of large bedload bursts contributed by coarse grains was large. Overall, 77% of the observations included grains > 8 mm, roughly 53% contained material > 11 mm, and 24% included particles > 16 mm.

To visualize variability in the grain-size composition of bedload observations with low p_e, bedload rate of coarse grain sizes (> 8 mm) was plotted against total bedload rate for those cases over all the 10-h intervals. Three examples are presented in Figure 3.5 to describe

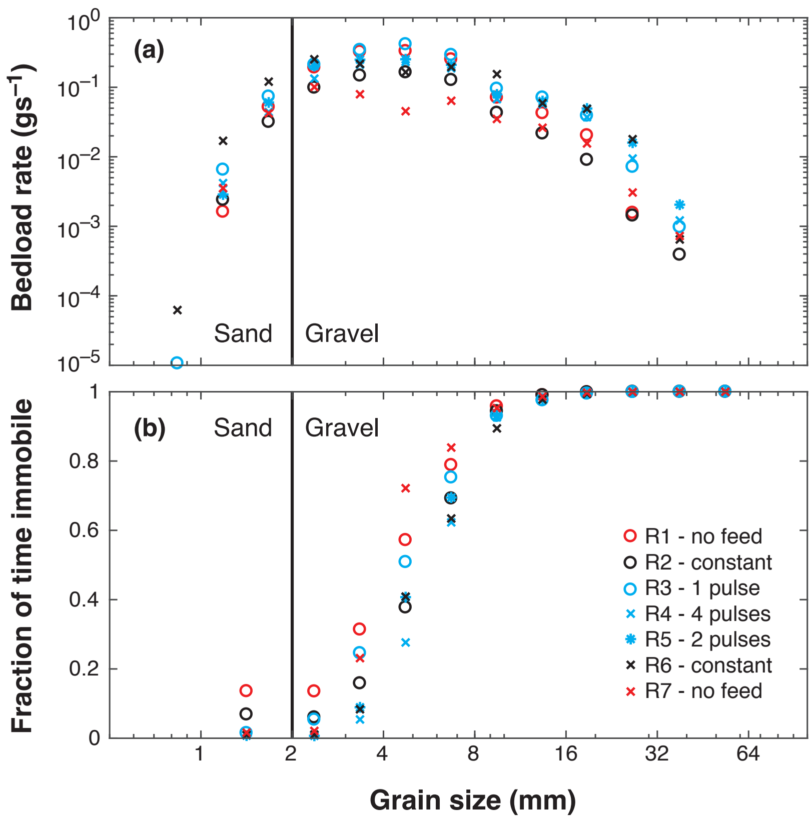

Figure 3.2: Bedload transport intensity by grain size for each run. (a) Mean bedload transport rate. (b) Fraction of time immobile. Time immobile was estimated as the time over which no grains of a specific size exited the flume. Grain-size fractions < 2 mm were grouped together as sand to avoid the effects of mis-detection of grains < 1 mm. Coarse grains were observed to move for short distances, but most of the time did not leave the flume.

observations under different transport intensities. In all three, there were cases that did not include any coarse grains, although a considerable number of them did. Grains coarser than 22 mm contributed least frequently due to their sporadic movement. The range of grain sizes that participated in observations with $p_e < 0.01$ increased with sediment transport rate. Points that fall on or near the 1:1 line represent cases that involved, almost exclusively a specific coarse grain-size. These cases were common during low transport, as in the last 10 h of R1 (Figure 3.5a). They became less abundant and coarser during moderate transport as in the last 10 h of R2 (Figure 3.5b) when large bedload rates included a wider range of sizes. Finally, during very intense transport as in the first 10 h of R3 or R1 (Figure 3.5c), fractional bedload was always significantly lower than total bedload and no points fall near the 1:1 line.

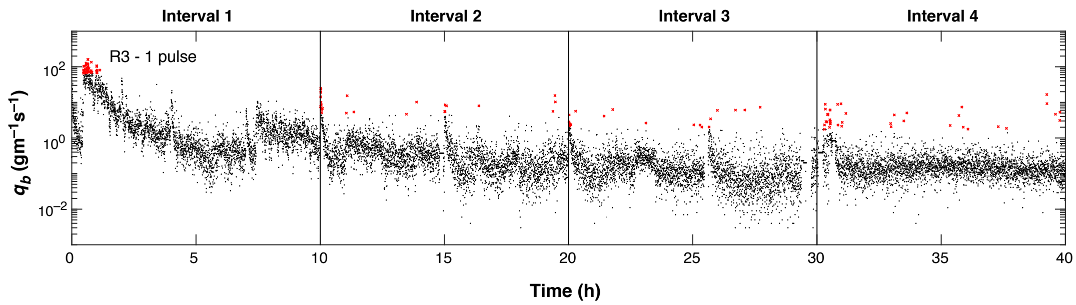

Figure 3.3: Bedload transport rate q_b and large bursts in q_b (displayed in red) during R3. The run was divided in four 10-h intervals (Interval 1–4) and, within each interval, q_b with probability of exceedance $p_e < 0.01$ were selected as large bursts.

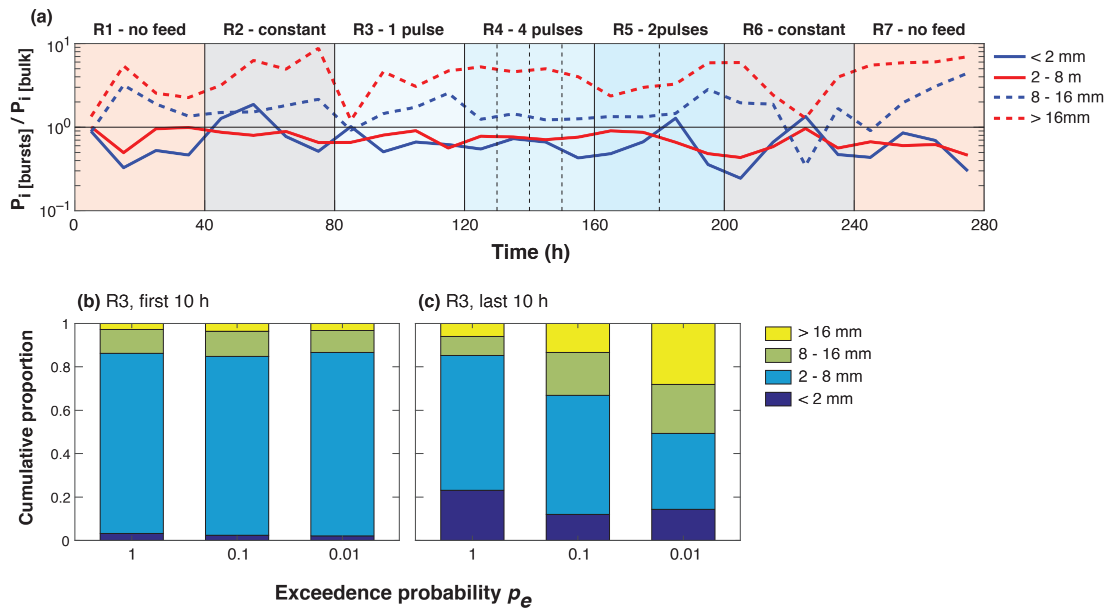

Figure 3.4: (a) Ratios between the proportion of sediment of each grain size class in large sediment bursts $P_{i[bursts]}$ and the proportion of the same grain size class in bulk bedload $P_{i[bulk]}$. For large bursts, p_e< 0.01. (b) Grain-size distribution of bedload rates with p_e< 1, 0.1, and 0.01 over the first 10 h of R3. (c) Grain-size distributions over the last 10 h of R3.

3.4.2 Memory and scaling statistics

Sample autocorrelation coefficients

The sample autocorrelation coefficients ρ_τ were used to identify trends and evaluate short-term memory in sediment transport rate time series. In the presence of a trend, ρ_τ remains significant for large time lags τ. For a completely random process (e.g., white noise), ρ_τ vanishes except at $\tau = 0$. Finally, for short-term correlation, ρ_τ vanishes except for small τ (*Chatfield*,

Table 3.3: Summary statistics for the percent of sediment bursts that included coarse material for all 10-h intervals

Statistic	% events with grains >		
	16 mm	11 mm	8 mm
Minimum	1.1	17.9	35.5
Maximum	58.8	82.7	98.3
Mean	23.7	53.2	76.6
Standard deviation	15.2	18.2	15.5

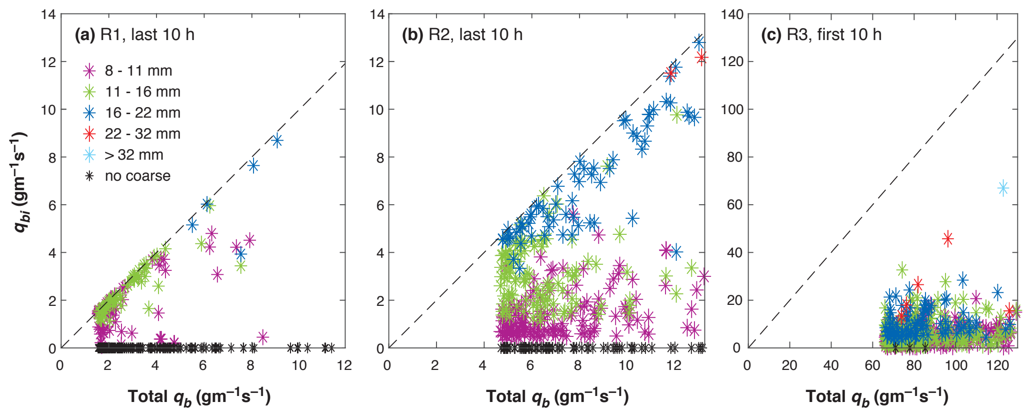

Figure 3.5: Fractional bedload rate q_{bi} of coarse grains against total bedload rate q_b for three 10-h time intervals. Only q_b observations with $p_e < 0.01$ are presented. Dashed line corresponds to $q_{bi} = q_b$. (a) Last 10 h of R1 when the intensity of sediment transport was low after 30 h of no feed. (b) Last 10 h of R2 when the intensity of transport was moderate after 30 h of constant feed. (c) First 10 h of R3 when the intensity of transport was high because of a large sediment pulse.

1975).

For each of the 40-h runs we computed ρ_τ over time periods that ranged from 10–40 h to characterize the effects of changes in feed on the strength and persistence of the bedload rate autocorrelation and found trends in most cases (Table 3.4). To represent the range of results, we provide examples for the three types of correlograms observed: trend, low ρ_τ, and white noise (Figure 3.6). In some cases, strong trends caused ρ_τ to remain very high for large τ as in R3 (Figure 3.6a). Cases where ρ_τ exceeded only slightly 95% confidence limits (< 10% as in Figure 3.6b) are indicated as "low ρ_τ". Seven of the 28 correlograms in Table 3.4 support a white noise process (as in Figure 3.6c). In general, periods that included changes in feed conditions at the beginning exhibited high ρ_τ whereas correlograms that resembled white noise only occurred over periods when sediment feed did not change and the system was more stable.

Table 3.4: Description of correlograms of bedload time series

Run	Time period (h)			
	0–40	10–40	20–40	30–40
R1	trend*	white noise	white noise	white noise
R2	trend (low ρ_τ)*	trend (low ρ_τ)	trend (low ρ_τ)	trend (low ρ_τ)
R3	trend*	trend (low ρ_τ)	white noise	trend (low ρ_τ)
R4	trend*	trend*	trend*	trend*
R5	trend*	trend (low ρ_τ)	trend*	trend (low ρ_τ)
R6	trend (low ρ_τ)*	trend (low ρ_τ)	trend	white noise
R7	trend*	trend (low ρ_τ)	white noise	white noise

* Changes in feed conditions at the beginning of these periods are thought to have influenced the trends.

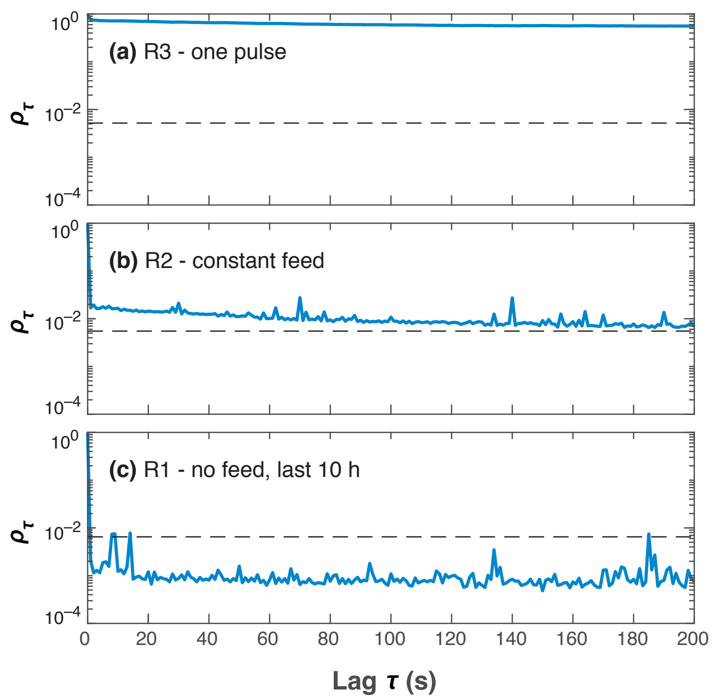

Figure 3.6: Sample autocorrelation ρ_τ against lag time τ. Examples for the three types of correlograms described in Table 3.4. Note logarithmic ordinate. (a) R3 displays persistently high ρ_τ due to strong trend. (b) For R2 ρ_τ is lower, but still significant. (c) For the last 10 h of R1 ρ_τ is only significant at $\tau = 0$, as for white noise. The dashed horizontal line indicates 95% confidence limits.

Variance scaling

To describe multi-regime fluctuation in bedload, the relationship between variance σ_T^2 and time scale T was plotted on a log-log graph (Figure 2.7). *Ma et al.* (2014) observed a decrease of σ_T^2 with -1 slope in the case of independent (non-correlated) fluctuations. This occurred at short T due to intermittency in the signal (intermittent stage) and at very long T, when autocorrelation vanished (memoryless stage). At intermediate T (invariant or memory stage), σ_T^2 became more constant.

In our experiment, only the runs with constant feed (R2, R6) exhibited the three stages of fluctuation described by *Ma et al.* (2014). An intermittent stage was visible for $T < 10$ s, an invariant stage stretched over $10\text{ s} < T < 500$ s, and a memoryless stage over longer T (Figure 3.7a). In all other runs, the invariant stage occurred over a wider range of T and showed stronger fluctuations than with constant feed. The invariant and memoryless stages were not always exhibited. The most extreme case was R3, for which the variance decreased only slightly with T and only the invariant stage was observed. This could be related to the strength and persistence of the trends caused by the large sediment pulse introduced at the beginning of the run.

The decrease in variance σ_T^2 with T was also analyzed for different grain sizes over each run and we found fine gravel (2–8 mm) to be the most representative of total bedload. Although there was considerable variability in the results, total bedload and fine gravel displayed similar patterns in most cases, in contrast to very coarse gravel or sand, which usually exhibited a longer intermittent stage and a more significant decrease in σ_T^2 (for example, R2 in Figure 2.7b).

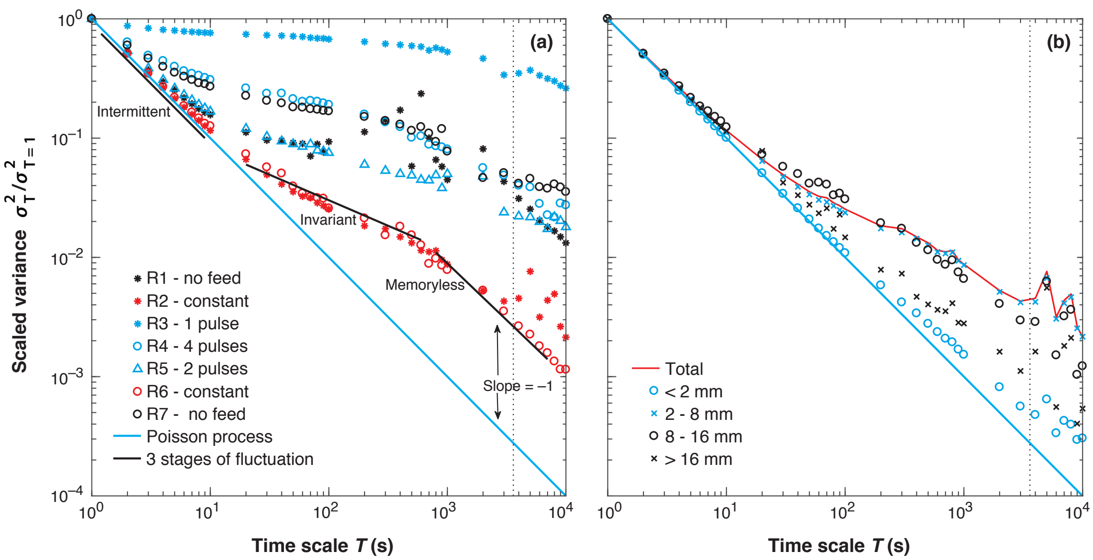

Figure 3.7: Scaled variance vs. aggregation time scale T. The variance σ_T at each T was divided by σ_T when $T = 1$ s. The number of observations N decreases as T increases. T at which $N = 50$ is displayed with a vertical dashed line. (a) Results for individual runs using total bedload rates. (b) Grain-size dependent results for R2.

Hurst exponent H

The Hurst exponent H, which is calculated from the relation between the standard deviation σ_T and time scale T, was used to quantify memory in bedload rate time series. For processes with memory, $0.5 \leqslant H \leqslant 1$ with $H = 0.5$ corresponding to short-term persistence, characteristic of Markov processes, which only have memory of $\tau = 1$. $H = 1$ indicates long-term memory and is characteristic of series with trends, or of series in which observations at each side of the mean cluster into prolonged periods (*Koutsoyiannis and Montanari*, 2007). To identify changes in the memory structure of bedload rates within each run, H was estimated over a 5-h moving window that stepped forward at intervals of 1 h; cumulative H was computed in 1-h increments (Figure 3.8). T ranged between 1 s and 360 s.

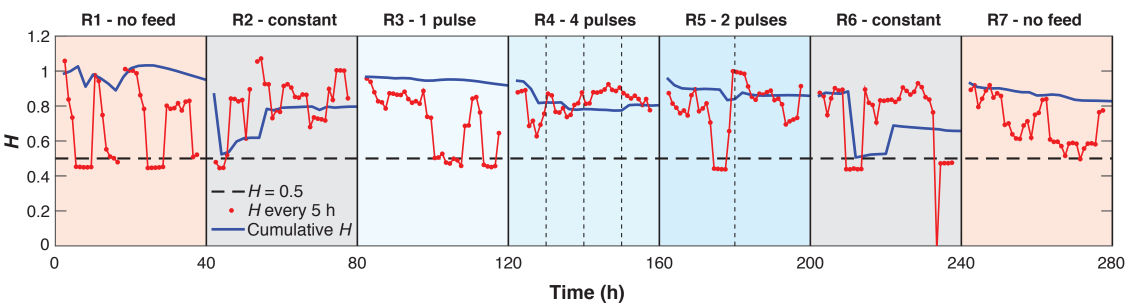

Figure 3.8: Evolution of long-term memory. The Hurst exponent H was estimated for each run over 5-h moving windows and in cumulative 1-h increments.

Only part of the significant variability observed in H could be attributed to effects of sediment feed on sediment transport rates. The inconclusive relationship found between H and mean bedload rate (Figure 3.9) implies that long memory was not exclusively controled by bedload intensity. Large infrequent sediment pulses, as in R3 and R5, clearly influenced memory. The strong trends in bedload rate due to these pulses caused H to approach 1 immediately after the pulse and to decrease as bedload rate stabilized under no feed (Figure 3.8). Strong memory observed over periods with relatively stable mean bedload rates (e.g., last 10 h of most runs) was unlikely to be a consequence of long-term trends caused by changes in sediment feed, but more likely a result of clustered observations that could be related to local changes in bed conditions. Therefore, $H \approx 1$ could result from the dispersion of large infrequent sediment pulses or from significant releases of bed sediment (e.g., from a sediment wedge created by sediment feed upstream).

For each run, H was quantified for different grain size fractions and demonstrated a strong influence of grain size on memory. In general, memory strength decreased with grain size as indicated by a lower mean and shorter range of H (Figure 3.10a). Grains > 32 mm exhibited no long-term memory because they moved very occasionally and only a small proportion of them exited the flume. These grain sizes corresponded to the coarsest 10% of the bed surface (mean surface $D_{90} = 32$ mm). Plots of H for five grain size fractions against H for total bedload are presented in Figure 3.10b. H for fine gravel was very similar to H for total bedload (plot near 1:1 line), which is consistent with our previous results on variance scaling (memory structure of total bedload rate was like that of fine gravel). Sand and coarse gravel had lower H than

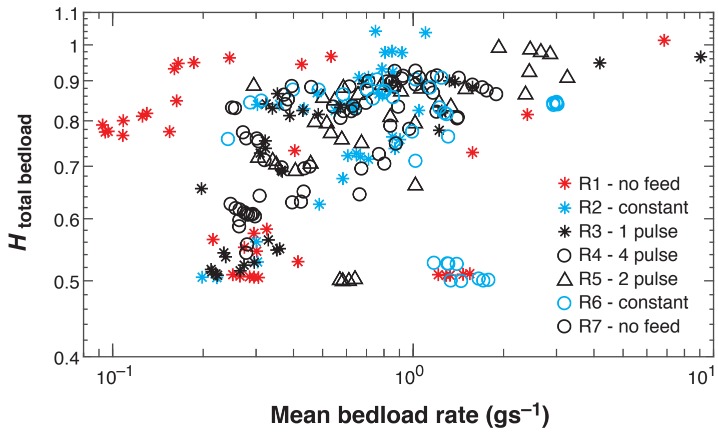

Figure 3.9: Hurst exponent H over 5-h moving window against mean bedload rate.

total bedload, and H was even lower for very coarse gravel.

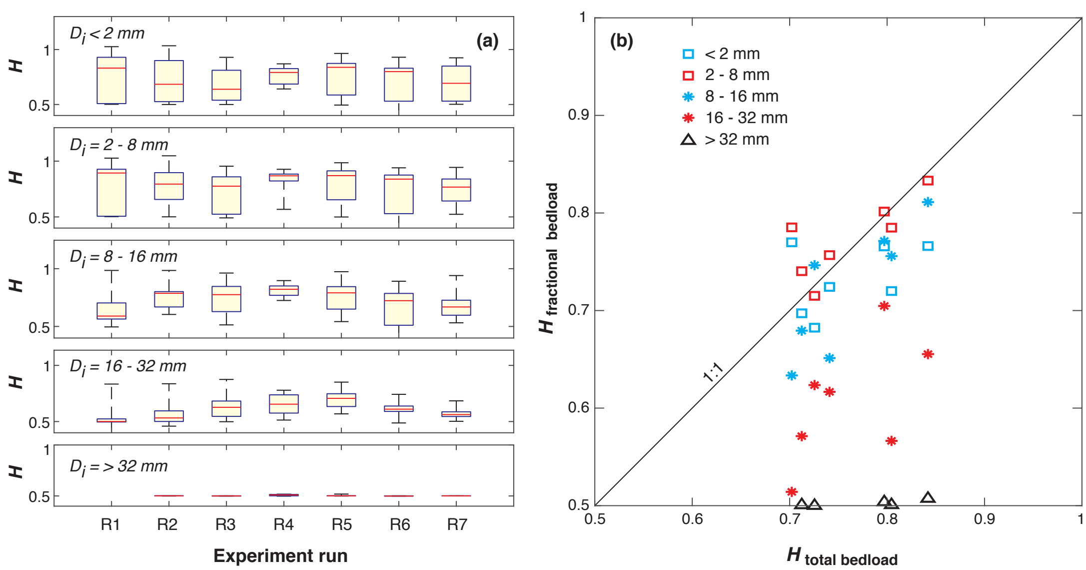

Figure 3.10: (a) Range of H by run for five grain size fractions D_i. (b) H for fractional bedload against H for total bedload by grain size (run averages).

Effects of aggregation time scale T on memory

To analyze the effects of the temporal aggregation scale T on the strength of short memory in total and fractional transport rates, the lag-one autocorrelation coefficient ρ_1 was estimated using T between 1–600 s. Results were very similar among runs, so only R2 (constant) and R3 (one pulse) are presented as examples in Figure 3.11a–b. T with highest autocorrelation was plotted against grain size for each run in Figure 3.11c.

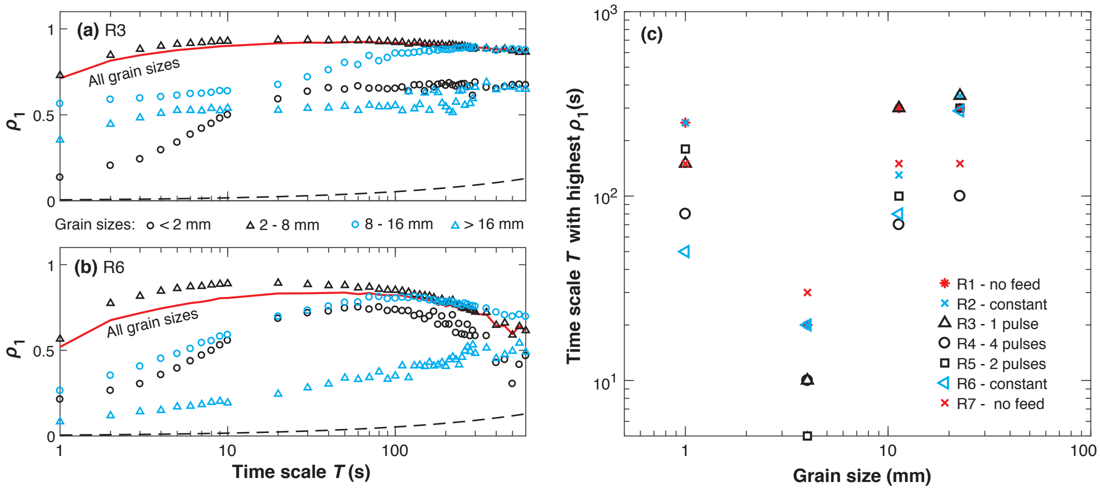

Figure 3.11: Lag-one autocorrelation coefficient ρ_1 against aggregation time scale T for total bedload and four grain size fractions. 95% confidence limits presented in dashed lines. (a) Results for R2. (b) Results for R3. (c) Time scale T with highest lag-one autocorrelation ρ_1 for different grain sizes and runs.

Once more, total bedload follows a similar pattern to that observed for fine gravel: ρ_1 increases rapidly with T for $T < \sim 20$ s and decreases after it reaches a maximum. The decrease can be gradual as in R1 or R3 (Figure 3.11a), or more pronounced as in R2, R4 or R6 (Figure 3.11b). With coarse gravel (8–16 mm), ρ_1 starts lower than for total bedload and peaks at longer T. The increase with T is more gradual and ρ_1 reaches values similar to or higher than that for total bedload at long T. Grains $>$ 16 mm show the lowest ρ_1 and peak at longer T than total bedload. The case of sand is interesting because it does not fit the grain-size dependence pattern observed for gravels ($>$ 2 mm). For sand, ρ_1 usually falls among the coarse size classes and peaks at longer T than for fine gravel.

3.5 Discussion

3.5.1 Controls on sediment mobility and the composition of large bursts in bedload

Sediment supply regime was a first order control on temporal adjustments of bedload rate and bed surface particle size. Constant feed made sediment gradually available, causing slower and weaker responses than the occasional sediment pulses, which made a large amount of sediment suddenly available. Differences among results from runs with the same sediment supply regime indicate that the initial bed conditions influenced the bed response to changes in sediment feed. Differences in the shape and statistics of bedload time series for R1 and R7 (no feed) were mostly because of the contrast between the fine well-mixed bed at the beginning of R1 and the armored bed at the beginning of R7, although differences in bed slope and cumulative storage might had also been important. No textural differences were observed among the initial bed surface of R2 and R6 (constant feed), so diversity among bedload statistics for these runs was likely because of cumulative sediment storage and the overall increase in bed slope that caused a steeper bed in R6 than in R2.

The configuration of the bed surface conditioned the role of coarse grains in the occurrence of large bursts in bedload rate. The role of coarse grains was significant during supply-limited conditions when the bed was well-armored, but it became less relevant during transport-limited conditions when the bed had a less organized structure, as in the beginning of R1 or R3. Over most analyzed periods, the grain-size composition of large bedload rates with low p_e was coarser than the composition of bulk bedload. Most, but not all, large bedload rates included coarse grains. It is important to consider that the role of coarse grains might not have been limited to their evacuation, but also to their interactions with the bed while moving. For example, a large grain that exits the flume might cause the movement of others by exposing fines, or by collisions, or any type of bed disruptions. Our observations are consistent with *Saletti et al.* (2015), although in their case large bedload bursts were even coarser because they were associated with the collapse of steps in their step-pool morphologies. In our experiment, the bed exhibited riffle-pool morphologies, where the movement of coarse grains could be related to the breakup of small bed features like clusters and the evolution of larger bedforms such as bars.

3.5.2 Hypothesis 1: Bedload rate time series for runs with constant sediment feed have weaker memory than those for runs with large infrequent sediment pulses, which can cause pronounced trends in bedload transport

The structure of memory in bedload rate signals was influenced by sediment feed regime, as proposed in our hypothesis, and by bed organization. Runs with episodic feed exhibited higher ρ_τ and more persistent memory than runs with constant feed. The three stages for bedload fluctuation (*Ma et al.*, 2014) were only observed in the total bedload rate of runs with constant feed, which had the same simplified feed regime as the experiments analyzed by *Ma et al.* (2014). For runs that had episodic feed regimes as in mountain streams, the scaling regimes proposed by *Ma et al.* (2014) did not hold. Instability produced by episodic feed caused the autocorrelation to persist over very long T and a longer duration of the invariant stage of fluctuations (memory stage). Without constant feed, a memoryless stage was not present. Constant feed caused a modest increase in bedload rate, a trend that could be obscured by bedload fluctuations caused by changes in bed elevation due to the building and destruction of bed surface structures (e.g., pebble clusters). Episodic feed regimes produced more persistent trends in the sediment transport rate as the system relaxed from the strong increase caused by a sediment pulse. Long-term trends due to large sediment pulses (R3, R5) were pronounced and caused the invariant stage to extend over longer T than under constant feed. For R3, the intermittent stage was not observed. This could be explained by the larger transport rates experienced after the pulse (first $\sim$10 h), which probably induced an increased frequency of sediment movement that could have reduced or erased the intermittency of total bedload signal at $T \leq 1$ s. These results support the idea that sediment supply and changes in sediment storage are a first order control in channel response (e.g., *Hassan et al.*, 2008).

Long-term memory was observed after significant changes in sediment feed, but also during more stable periods. Changes in sediment feed caused trends which appeared as strong memory in the signal (persistently significant ρ_τ, large H). When the processes governing transport were related to bed evolution at small scales (e.g., grain sorting, arrangement of small structures), bedload rate signals could become more stochastic over relatively stable periods, as indicated by correlograms that resemble white noise and $H \approx 0.5$. Over the same periods, bedload signals could show long memory if the governing processes occurred at larger scales (i.e., evolution of bedforms) and caused bedload rate to shift between persistently high and persistently low values. In summary, memory was not exclusively determined by transport regime or sediment feed, but also by local changes in the bed configuration. The inconclusive relationship found between mean transport rate and H supports this idea (Figure 3.9).

3.5.3 Hypothesis 2: The memory structure of total bedload reflects that of fully-mobile grain sizes, which dominate sediment transport and exhibit strong memory in their bedload signals

The memory structure of total bedload was similar to that of fine gravel (2–8 mm), which contributed the most to sediment transport, but was considerably different from those of other grain sizes (Figures 3.10b and 3.11). The strength of memory decreased with grain size except for sand, which exhibited weaker memory than fine gravel. In the gravel fractions, memory weakened with grain size as mean bedload rate decreased (Figure 3.2a) because of the less recurrent entrainment of coarse gravel (Figure 3.2b). Total bedload rate displayed very similar memory structure (H and ρ_{1_T}) to that for fine gravel (Figure 3.10b and 3.11), which was the most mobile fraction during the experiment. As these grain sizes experienced full mobility, their response to sediment feed was expected to be strong, given that sediment feed increased their availability on the bed surface. We found that H was a good proxy for relative sediment mobility of gravel fractions. $H \approx 1$ for fully-mobile gravels and $H < 1$ for coarse gravels under partial mobility, which moved more sporadically and resulted in lower mean bedload rates. For gravels under incipient motion, $H \approx 0.5$. The memory in bedload rate signals weakened with grain size, as the signals gained stochasticity and became more intermittent. Even though sediment transport processes are stochastic in nature, this was obscured by trends caused by changes in sediment feed and by persistent autocorrelated patterns caused by bed evolution.

On the other hand, sand was not affected by grain-size dependence in the same way as gravel fractions. Sand load signals exhibited greater stochasticity (e.g., longer intermittent stage) and weaker memory (decreased H and ρ_1) than fine gravel, although there was considerable variability in their structures (e.g., wide range of H). The greater stochasticity of sand patterns could not be due to increased intermittency because the signal was almost as continuous as for fine gravel (no movement 3% of the time) and very different from coarser fractions ($> 90\%$ time immobile). The sediment fed upstream and the bed itself were sources of sand during the experiment. Flow conditions were well above critical for sand, so a considerable proportion of the sand supplied was expected to exit the flume. This could happen rapidly through pulse dispersion, but as the poorly sorted bed developed armor and bed structures, infiltration and hiding effects were expected to play a significant role in the availability of sand for transport (sand $< \mathrm{D}_g$ of the bulk bed and $\ll \mathrm{D}_g$ of the bed surface). Some of the sand input could get stored in the bed and become available later during the experiment, when the movement of a coarser grain exposed hidden sand. The movement of sand might have been more influenced by these highly stochastic dynamics and less affected by longer scale processes such as bedform evolution that reduced stochasticity in the system.

Grain-size dependence in the statistics and memory structure of bedload rates needs to be considered when studying sediment transport patterns of sediment mixtures under partial transport. This is important because the most effective sampling durations and autocorrelated time scales also depended on grain size. The time scale $T_{\max(\rho_1)}$ with highest autocorrelation $\max(\rho_1)$ can be used as a reference. For $T < T_{\max(\rho_1)}$, the signal gains stochasticity possibly due to intermittent sediment flux; for $T = T_{\max(\rho_1)}$, autocorrelation in the signal becomes stronger and better captures any trends that are lost at smaller T. If sampling duration is shorter than $T_{\max(\rho_1)}$ for a given grain size, the sample might not be representative of that size because sampling duration is within the intermittency of the signal. On the other hand, the stochastic variability of the process is only observable at $T < T_{\max(\rho_1)}$.

Our results are consistent with the observations of *Saletti et al.* (2015). As for these authors, we found a relationship between transport intensity and memory strength, together with grain-size dependence in the memory structure of bedload signals that was reflected in differences in H and ρ_1. They used sediment coarser than 2 mm and did not find any inflection of grain-size dependence patterns in their finest classes (2–5.6 mm) as we did for sand. In contrast with our results, in their study coarser grain sizes (16–45 mm) exhibited a memory structure closer to that for total bedload, which might be related to differences in boundary conditions among the experiments (e.g., flow discharge, sediment feed) and the development of distinct bed morphologies: step-pool in their case, riffle-pool in ours.

3.5.4 Hypothesis 3: Grain-size dependence in bedload transport increases with sediment feed because the movement of fully-mobile sediment is more responsive to feed than that of partially-mobile grain sizes

This hypothesis was not confirmed because the same patterns of grain-size dependence in bedload transport persisted during the experiment regardless of changes in sediment feed. Sediment feed increased the availability of fully-mobile sediment for transport and, as the bed surface became finer and smoother, it increased the frequency of movement of partially-mobile grains too. No matter what the intensity of movement, grain-size selectivity was always evident in gravel bedload rates and the limit between partial and full mobility remained nearly constant. The largest grain size transported was the same in all runs, except for R1 when it was slightly smaller. Grain-size dependence and relative sediment mobility could be more affected by changes in flow strength (e.g., *Wilcock and McArdell*, 1993) or sediment feed texture (e.g., *Curran and Wilcock*, 2005), which were constant through all the experiment.

Sediment feed affected the duration of the invariant stage of bedload fluctuations and the strength of memory, but the observed differences among the patterns of different grain size classes remained the same. We expected grain-size dependence to be stronger in the presence of sediment feed, which significantly increased the intensity of transport for fine gravels. We also expected that during long periods without feed when transport intensity was low, fine gravel would exhibit a more stochastic behavior as for coarser fractions. The results did not support these hypotheses. Coarse gravel signals always had weaker memory and had the strongest autocorrelation ρ_1 at longer time scales T than those for fine gravel.

Initial bed conditions might have influenced patterns of fractional bedload fluctuation in runs that had same sediment feed regime. Whereas patterns of multi-regime fluctuation in total bedload rate were very similar over both runs with constant feed (R2, R6), memory structures of fractional bedload rates exhibited differences in the range and mean of H (Figure 3.10). T with highest ρ_1 was the same for fine gravel in both runs, but differed for other grain sizes (Figure 3.11). Similar types of differences were noticed between the two runs without sediment feed (R1, R7).

3.6 Conclusions

We studied the effects of sediment feed regime on sediment mobility, long-term memory of bedload transport, and grain-size dependence, over an experimental bed with a wide grain-size distribution and extended history. Sediment mobility was affected by sediment feed regime. Fully-mobile gravel (2–8 mm), which dominated sediment transport and strongly influenced the memory structure of total bedload rate, was more significantly affected than other grain sizes. The contribution of coarse material to large bedload rates with low p_e was more important during periods with low sediment transport intensity.

Episodic sediment feed caused more pronounced changes in the transport rate and stronger memory than constant feed, although memory was also controled by local changes in bed characteristics, such as bedform evolution and storage release. Sediment pulses caused different temporal scales of bedload fluctuations than constant feed. We think this relates to differences between the time that it takes for the bed to armor and reach a stable mean bedload rate after a pulse, and the temporal scale of fluctuations related to the largest bedforms present, which probably influenced the duration of memory in runs with constant feed.

The three stages of bedload fluctuation proposed by *Ma et al.* (2014) only held under simplified situations when we used constant feed as they did. The strong trends caused in bedload by occasional sediment pulses like those reported in mountain streams increased long-term memory and the duration of the invariant stage. This caused the intermittent and memoryless stages to vanish.

As expected under partial transport conditions, the patterns of fluctuation observed for total bedload were not representative of all grain size fractions. We observed grain-size dependence in mean bedload rates and the memory structure of bedload signals. Our observations were consistent with *Saletti et al.* (2015), although interesting differences were noticed. In our case, the memory structure for total bedload was like that for fine gravel (2–8 mm), whereas in their case H for total bedload was closer to that for coarser grains (16–45 mm). This could be related to substantial differences in bed morphologies: we developed a riffle-pool morphology, whereas they created step-pools.

The patterns of grain-size dependence found in sediment transport were not significantly affected by sediment feed because we only changed the magnitude and frequency, but not the texture of sediment feed, nor flow discharge. Changes in sediment texture could affect bed surface roughness and entrainment thresholds (*Curran and Wilcock*, 2005; *Venditti et al.*, 2010), and changes in flow could affect the limit between partial and full mobility (*Wilcock and McArdell*, 1993; *Church and Hassan*, 2002). It would be interesting to analyze grain-size dependence of bedload statistics under changing feed texture or flow discharge.

The initial bed was different for each run because of cumulative sediment storage that caused an overall increase in bed slope with sediment feed and because of a different history. A detailed description of the bed morphology and patterns of sediment storage for different grain size fractions could help to relate our observations to processes of erosion and deposition.

Chapter 4

Temporal patterns of sediment storage and spatial variability on a gravel bed under changing sediment supply regimes

4.1 Summary

Patterns of sediment storage and spatial variability on a gravel bed were analyzed using data from a sequence of experimental runs with steady flow discharge, but changing sediment supply regime. All grain sizes exhibited net storage, except for fine gravel, which had an overall negative mass balance. Differences were observed among feed regimes, but also within the same feed regimes, which could be related to an increase in bed slope. The storage of fine gravel (2–8 mm) responded the most to changes in sediment feed and bed conditions, whereas the storage of coarser gravels and sand was nearly stable. More than 60% of the sand fed during each run got stored, probably due to its higher potential for infiltration and for getting caught within larger grains. Hysteresis in sediment transport-storage relations was observed between runs with constant feed and those without feed because of differences in bed state and sediment availability. Sediment pulses also caused hysteresis, although its direction was influenced by the lag time between sediment feed and downstream response in bedload rate. Small cycles of hysteresis were observed during constant feed if the mean bedload rate approached the feed rate. Sediment transport processes and bed characteristics varied considerably in space. The cumulative increase in mean bed elevation was larger upstream due to the preferential storage of coarse material, which also promoted downstream fining on the bed surface. The evolution in the standard deviation of bed elevations σ_η was consistent with the development of bedforms at different scales. σ_η was more stable in the center of the flume, indicating bed roughness was less affected by bedform evolution over that area. Instead, upstream and

downstream the development of lateral bars and larger scales bedforms caused more significant changes in σ_η. The accumulation of sediment upstream due to size-selectivity created a sediment wedge that expanded downstream. The way in which the sediment entered during the first run probably dictated the development of lateral bars due to differences in flow configuration and erosion in the transverse direction. As sediment feed became better spread laterally, a longitudinal sequence of riffle-pool like morphologies developed downstream of the wedge.

4.2 Introduction

Sediment supply has been proposed as a first order control in mountain streams (e.g., *Hassan et al.*, 2006, 2008). Well-armored and structured beds with low intensity of sediment transport have been reported for streams with low sediment supply regimes (sediment supply $\ll$ transport capacity). Instead, finer bed textures and more intense sediment transport have been noticed for streams with high sediment supply regimes (sediment supply $\gg$ transport capacity). Transport capacity can be highly variable at intermedate time scales T (10^0 years $<$ T $<$ 10^3 years) because of changes in sediment supply, storage, and bed surface composition (*Lisle and Church*, 2002). Mountain streams usually receive sediment episodically (e.g., mass movements, bank collapses, disintegration of large wood jams), which depending on its amount and texture, will be either deposited or transported further downstream. For uniform sediment, the difference between sediment supply and transport capacity dictates sediment storage. For poorly sorted sediment, flow transport capacity and flow competence to entrain sediment of specific grain sizes will influence sediment storage significantly (if there is too much sediment or if it is too coarse for the flow, it will be left behind). Under partial transport, gravel beds usually exhibit size-selective mobility in the coarse fractions, which cause their preferential deposition. Even though, there are studies that report on size-selective transport (e.g., *Wilcock and McArdell*, 1993; *Church and Hassan*, 2002), there are still open questions regarding the effects of particle size on sediment storage, sediment mobility, and channel morphology.

Given the limitations for collecting detailed data in the field (e.g., technology, time, and accesibility), flumes are a good alternative to study channel adjustment under controled environments (e.g., *Dietrich et al.*, 1989; *Lisle and Church*, 2002; *Eaton and Church*, 2004; *Curran and Wilcock*, 2005; *Eaton and Church*, 2009; *Pryor et al.*, 2011). For simplicity, most experiments have used constant sediment feed and in only a few of them, sediment was introduced in episodic pulses (*Cui et al.*, 2003; *Sklar et al.*, 2009; *Venditti et al.*, 2010; *Johnson et al.*, 2015). These studies give insights mostly on the importance of the grain-size distribution of sediment feed relative to that of the bed, in terms of pulse–bed interactions (*Venditti et al.*, 2010), mechanisms of pulse propagation (*Cui et al.*, 2003; *Sklar et al.*, 2009), and bed surface texture (*Johnson et al.*, 2015). With the exception of *Elgueta-Astaburuaga and Hassan* (2017), there are still no thorough descriptions of the effects of episodic sediment supply on channel adjustments and the roles of the magnitude and frequency of sediment supply are still an open question. In *Elgueta-*

Astaburuaga and Hassan (2017) we analyzed the effects on the temporal variability of bedload transport. Here, we use data from the same experiment to study temporal and spatial patterns of total and fractional sediment storage and how they relate to bedload transport and bed morphology.

Lisle and Church (2002) pointed out the importance of understanding sediment transport–storage relations for sediment routing models. They proposed that each sediment reservoir is governed by a unique positive relation, which in degrading streams exhibit two phases. In phase I there is significant degradation, whereas in phase II, transport rate decreases as armor developes and counteracts degradation. Later, physical modeling of complete cycles of aggradation–degradation revealed that the relation could become more complex (*Madej et al.*, 2009; *Pryor et al.*, 2011) and that hysteresis developed from differences in the bed state (i.e., bed composition). In the light of these findings, *Lisle* (2012) described two possible scenarios for transport–storage relations: a common relation that persists as the bed aggrades and degrades (scenario I) or a more complex relation that changes as the bed evolves (scenario II). In the last case, bedload transport rates for a given sediment stage depend on bed conditions and there is hysteresis during cycles of aggradation–degradation (as in *Madej et al.*, 2009; *Pryor et al.*, 2011). *Lisle* (2012) explained the occurrence of scenario II by changes in sediment supply that cause variability in channel response and transport capacity. More recently, *Luzi* (2014) showed that hysteresis can also result from the variability of sediment transport rate under dynamic equilibrium when the mean transport rate approaches the feed rate. In this study, we analyze transport–storage relations over a long experiment, in which the bed underwent mutiple cycles of aggradation–degradation caused by changes in sediment feed under steady flow discharge. Besides the complexity achieved in the bed due to the design and duration of the experiment, we included no feed, constant feed, and episodic feed regimes for comparisons.

Spatial variability of sediment transport and storage in a stream responds to the locations where sediment enters the stream and to variability in the channel bed (e.g., morphology, texture) and flow conditions. The wide range of grain sizes in gravel bed rivers promotes sediment sorting processes at different scales and in different directions (vertical, across, and downstream), which influence bed roughness and the availability of in-channel sediment for transport. At small–intermediate scales, sediment sorting results in bed armor (e.g., *Parker and Klingeman*, 1982), bed structures (e.g., *Hassan and Church*, 2000), and the development of fine sediment patches (e.g., *Nelson et al.*, 2009) and sediment sheets (e.g., *Iseya and Ikeda*, 1987). At larger scales, sediment sorting can be appreciated over bars and riffle-pool sequences (e.g., *Chartrand et al.*, 2015) and along step-pools (e.g., *Zimmermann*, 2009). At the largest scale, sediment sorting can result in downstream fining (e.g., *Seal and Paola*, 1995). Channel morphology promotes distinct mechanisms and paths for bedload propagation downstream. These include, but are not limited to the migration of alternate bars (e.g., *Ikeda*, 1989) and discrete jumps between riffles (e.g., *Hassan et al.*, 1991).

Sediment inputs propagate dowsntream by different mechanisms and at different rates, which largely depend on flow conditions, bed morphology, and the texture of sediment supply relative to bed texture. Grain arrangements and bedforms provide resistance to flow under bankfull conditions (e.g., *Millar*, 1999), affecting the spatial variability of transport capacity, which influences the distribution of bedload transport processes. Flume experiments have reported dispersion and translation as the main mechanisms for pulse propagation (*Lisle et al.*, 2001; *Cui et al.*, 2003; *Sklar et al.*, 2009). Dispersion was reported if sediment supply had the same texture as the bed, whereas translation occurred if supply was considerably finer. More recently and based on a field case of gravel augmentation, *Gaeuman et al.* (2017) proposed that pulses propagated by fragmentation into smaller pulses at short-intermediate scales. Also based on field evidence, *Brumer and Montgomery* (2006) observed that poorly sorted sediment delivered to channels could form lag deposits that developed an armored layer, which was driven by size-selective sediment transport and counteracted incision. Our data provides an opportunity to analyze the response of spatial variability to changes in feed over a gravel bed under partial transport. The dimensions of the flume together with a wide range of particle sizes allowed sediment sorting in all directions and the development of bedforms at different scales, which ranged from pebble-clusters to lateral bars. The experiment was long enough for the bed to develop a complex topography as a result of an extended history of flow and sediment supply.

Previously, we analyzed the effects of episodic sediment supply on temporal patterns of bedload transport (*Elgueta-Astaburuaga and Hassan*, 2017) and their dependence on grain size and aggregation scale (*Elgueta-Astaburuaga et al.*, 2017). The goal of this study is to assess the effects of episodic sediment inputs on sediment storage and bed evolution. Fractional transport data provided an opportunity to study the effects of size-selective transport on sediment storage. We used constant flow discharge to isolate the effects of sediment feed and followed a sequence of seven consecutive runs with different supply regimes to test the effects of feed magnitude and frequency. We were able to assess transport–storage relations over multiple cycles of aggradation–degradation, which exhibited different durations depending on feed regime. These cycles included the intercalation between runs without feed and runs with constant feed, as well as short periods of intensive aggradation caused by sediment pulses that were followed by longer periods of degradation. Systematic measurements of bed properties along and across the flume allowed us to assess spatial variability on bed topography and bed surface texture, which were used to explain patterns of aggradation–degradation along the flume and the propagation of sediment feed downstream.

We propose the following hypotheses. (H1) Preferential deposition of coarse partially-mobile gravels near the feed source promotes increased storage upstream and downstream fining on the bed surface. (H2) Constant feed, which makes sediment available more gradually, promotes larger sediment storage than sediment pulses because of a greater probability for sediment being sequestered in the bed. (H3) Hysteresis in sediment transport–storage relations largely depends on differences in bed surface texture and sediment availability.

4.3 Methods

4.3.1 Experiment

The data were collected at the Mountain Channel Hydraulic Experimental Laboratory, University of British Columbia (*Elgueta-Astaburuaga and Hassan*, 2017) in an 18 m long, 1 m wide flume, with a 14 m long working bed and a slope of 0.022 m/m. The bed and feed were composed of poorly sorted sediment (0.5–64 mm), with ∼20% sand, geometric mean $D_g = 5.7$ mm, and percentiles $D_{16} = 1.6$ mm and $D_{90} = 27$ mm. The experiment consisted of a sequence of seven 40-h runs, denoted R1–R7, under constant flow discharge (65 $\mathrm{L\,s^{-1}}$), but changing sediment feed regimes. Only R1 started from a flat and well-mixed bed; all other runs inherited their initial beds from previous runs. For R2–R6, 300 kg of sediment was introduced over each run, but the magnitude and frequency of sediment feed varied. R1 had no feed to condition the bed and R2 received constant feed. R3 received the 300 kg of sediment during the first hour to assess channel adjustments to large infrequent inputs of sediment. R4 and R5 received 75 kg of sediment every 10 h (four pulses) and 150 kg of sediment every 20 h (two pulses) respectively, to test the importance of the magnitude and frequency of sediment inputs. To explore the importance of bed history, the constant feed regime of R2 was repeated in R6, and no feed like in R1 was repeated in R7. All sediment pulses were introduced at the same rate (83 $\mathrm{g\,m^{-1}\,s^{-1}}$), but feed duration d_f differed with pulse size ($d_f = 1$ h for 300 kg, 0.5 h for 150 kg, and 0.25 h for 75 kg).

Flow properties, bed elevation, bed-surface particle size, and sediment transport were systematically measured. Water-surface elevation and depth were measured along the side of the flume at an interval of 0.5 m. Bed elevation was measured under no flow, by video-recording the reflectance of a green-beam laser with a resolution of 2 mm × 2 mm in the horizontal and 1 mm in the vertical. Bed-surface texture was assessed from photographs of the bed surface along the flume. A grid with cell size = D_{max} was superimposed on the photographs for point counts to compute grain-size distributions. Grains smaller than 2.8 mm were grouped in one class because of difficulties in their identification. Fractional sediment transport data were generated using the video-based method explained in *Zimmermann et al.* (2008), which in our case was improved by sampling grains as small as 1 mm (*Elgueta-Astaburuaga and Hassan*, 2017). A sediment trap was placed at the downstream end of the flume to confirm results. A description of the experimental set up and data collection can be found in *Elgueta-Astaburuaga and Hassan* (2017). A summary for each run with mean flow properties, bed characteristics at the end, and bedload transport statistics is presented in Table 4.1.

4.3.2 Data analyses

We analyzed temporal and spatial patterns of sediment storage by computing mass balances using video-based sediment transport data and also by estimating changes in digital elevation models (DEMs) built from laser scans on the bed. Time series of sediment storage Δ_T from

Table 4.1: Mean flow characteristics, bed observations at the end of each run, and bedload rate statistics

	Run	R1	R2	R3	R4	R5	R6	R7
Mean water depth (cm)		–	7.3	8.0	8.3	7.2	7.5	7.3
Water-surface slope (m/m)		–	0.017	0.019	0.02	0.02	0.02	0.02
Bed slope (m/m)		0.017	0.016	0.018	0.02	0.022	0.022	0.022
Bed surface (mm)	D_g	14.5	15.3	14.4	14.3	14.4	13.8	15.7
	D_{16}	6.7	7.7	7.0	7.4	7.2	6.3	7.8
	D_{90}	34.1	33.7	31.5	31.6	31.0	31.7	31.5
	SD_g	2.2	2.0	2.1	2.0	2.0	2.1	1.9
Bedload rate (g s^{-1})	Mean	1.29	0.65	1.56	0.98	1.19	1.25	0.42
	Standard deviation	27.06	5.12	7.64	3.17	10.32	31.32	1.56
	25th percentile	0.05	0.14	0.12	0.28	0.22	0.27	0.13
	50th percentile	0.14	0.37	0.24	0.50	0.41	0.54	0.22
	75th percentile	0.46	0.76	0.63	0.96	0.89	1.00	0.38

mass balances were computed by subtracting output mass estimates (video-based transport data) from the known mass of sediment fed over a specific time interval T as

$$\Delta_T = T \times Q_f - T \times \overline{Q}_b \tag{4.1}$$

where Q_f and $\overline{Q}_b$ are the sediment feed rate and mean bedload transport rate. Cumulative sediment storage was estimated as

$$\text{Cumulative } \Delta_{T_n} = \sum_{1}^{n} \Delta_T; \qquad \text{for } n = 1 : N \tag{4.2}$$

where N is the total number of observations in Δ_T time series. We used $T = 15$ min to reduce noise caused by stochastic variability of bedload transport in the short term, without loosing the responses caused by sediment pulses.

We analyzed sediment storage from mass balances for the bulk sediment and for four grain-size classes: 0.5–2 mm (sand), 2–8 mm (fine gravel), 8–16 mm (coarse gravel), and 16–64 mm (very coarse gravel). Sand was grouped together because it behaved in a distinct way; 8 mm was the limit between partial and full mobility; 16 mm was the D_{75} of the bulk sediment and similar to the D_g on the surface of an armored bed (*Elgueta-Astaburuaga and Hassan*, 2017). Sediment transport–storage relations for bulk sediment were assessed in plots of cumulative Δ_{T_n} vs. $\overline{Q}_b$ (*Pryor et al.*, 2011; *Madej et al.*, 2009; *Luzi*, 2014).

Sediment storage was also analyzed by computing changes in bed elevation $\delta\eta$ between two consecutive DEMs as

$$\delta\eta_{[x,y]} = \eta_{[x,y]_d} - \eta_{[x,y]_{d-1}}; \qquad \text{for } d = 1 : D - 1 \tag{4.3}$$

where $[x, y]$ are DEM coordinates, η is bed elevation, d is the DEM chronological order, and D

is the total number of DEMs available. Mean change in bed elevation $\bar{\delta}\eta$ between two DEMs was computed as

$$\bar{\delta}\eta = \frac{\sum_1^N \delta\eta}{N} \tag{4.4}$$

where N is the number of observations for η in a DEM (columns $\times$ rows). Cumulative mean change in elevation was estimated as

$$\text{Cumulative}\,\bar{\delta}\eta_d = \sum_1^d \bar{\delta}\eta; \qquad \text{for } d = 1 : D \tag{4.5}$$

To assess spatial variability over the bed, we estimated cumulative $\bar{\delta}\eta$ for 1-m^2 sections along the flume. To evaluate differences in bed roughness, we computed the standard deviation of bed elevation σ_η for the same 1-m^2 sections. Elevation data were relative to the floor of the flume. We used DEMs to identify bedforms like bars, sediment wedges, and riffle-pool sequences (i.e., mesoforms and macroforms in *Hassan et al.* (2008)). No objective method for bedform delineation was available (e.g., bars are usually delineated relative to base flow in the field), so we used slope inflections in longitudinal and transverse profiles to guide the delineation of boundaries. To assess textural differences on the bed surface, we estimated grain-size statistics from point counts on seven bed sections between 1–10.5 m from downstream. Each bed section included two bed surface photos (an area of 1.3–1.4 m^2).

4.4 Results

4.4.1 Temporal patterns of sediment storage

All runs with sediment feed had net positive mass balances between sediment feed and sediment outputs from video-based transport data. Significant differences were mainly caused by variability in storage of fine gravel (2–8 mm) because storage of sand and coarse gravel was more stable (Figure 4.1). Within each run, stored sediment was primarily composed of very coarse gravel (> 16 mm), followed by sand. Coarse gravel (8–16 mm) contributed more significantly to storage than fine gravel, except over R2. R3, which received one 300 kg sediment pulse, stored considerably less sediment than all the other runs with sediment feed. It exhibited a negative mass balance for fine gravel of ∼60 kg, which is equivalent to ∼50% of the mass of fine gravel fed (Figure 4.1b). In R5, which received a 150 kg pulse every 20 h, fine gravel also had negative balance, but five times smaller than in R3. In R4, which received a 75 kg pulse every 10 h, fine gravel had a positive mass balance of 10 kg (∼10% mass fed).

Runs with same feed regimes exhibited differences in sediment storage. Runs R2 and R6 received constant feed, but R2 stored a significant amount of fine gravel (37 kg), whereas R6 stored almost none. R2 also stored two times more coarse gravel (8–16 mm) than R6. These differences could relate to the increased bed slope in R6 relative to R2, as a result of cumulative

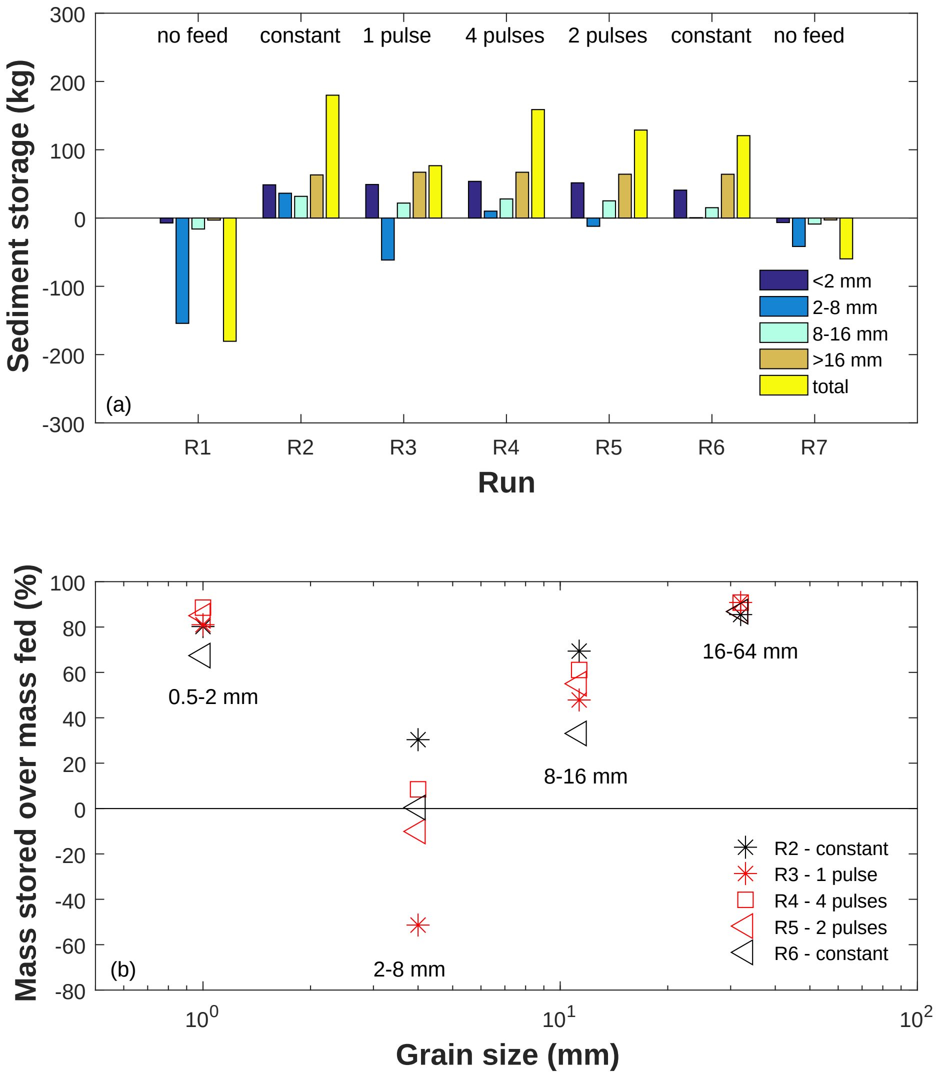

Figure 4.1: (a) Total and fractional sediment storage computed from mass balances over each run. (b) Percent of sediment mass stored over mass fed for different grain size fractions and runs.

sediment storage. Runs R1 and R7 had negative mass balances because of no sediment feed, but the mass of sediment degraded in R1 was three times the mass degraded in R7. Both runs started from the same initial bed slope (0.022 m/m), but the bed surface was considerably coarser at the beginning of R7 with a D_g 2.5 times the D_g at the beginning of R1. The time taken for the bed to armor over each run influenced the strength of bed degradation during no feed. As the initial bed of R1 was well mixed, a lot of sediment exited the flume during the first few hours as the bed armored. Instead, the initial bed of R7 was already armored to some degree, which prevented degradation earlier than in R1.

Except for fine gravel, all grain size fractions exhibited cumulative increase in sediment storage over the experiment (Figure 4.2). The cumulative storage of all grain sizes increased with sediment feed, but only that of fine gravel exhibited pronounced decreases without sediment feed as bed armor counteracted degradation. Instead, the cumulative storage of other grain sizes remained nearly constant under no feed. With constant feed, increases in cumulative storage were gradual and persistent, whereas with episodic feed, increases were sharp and followed by gradual decreases as sediment pulses propagated downstream. Overall the experiment, there was a negative mass balance of $\sim$200 kg of fine gravel, whereas all other size fractions exhibited positive mass balances: $>$ 200 kg for sand, $\sim$100 kg for grains 8–16 mm, and $>$ 300 kg for grains 16–64 mm. The pattern observed for total mass combined the cumulative increase in storage of most grain sizes with fluctuations in storage of fine gravel as a response to changes in sediment feed.

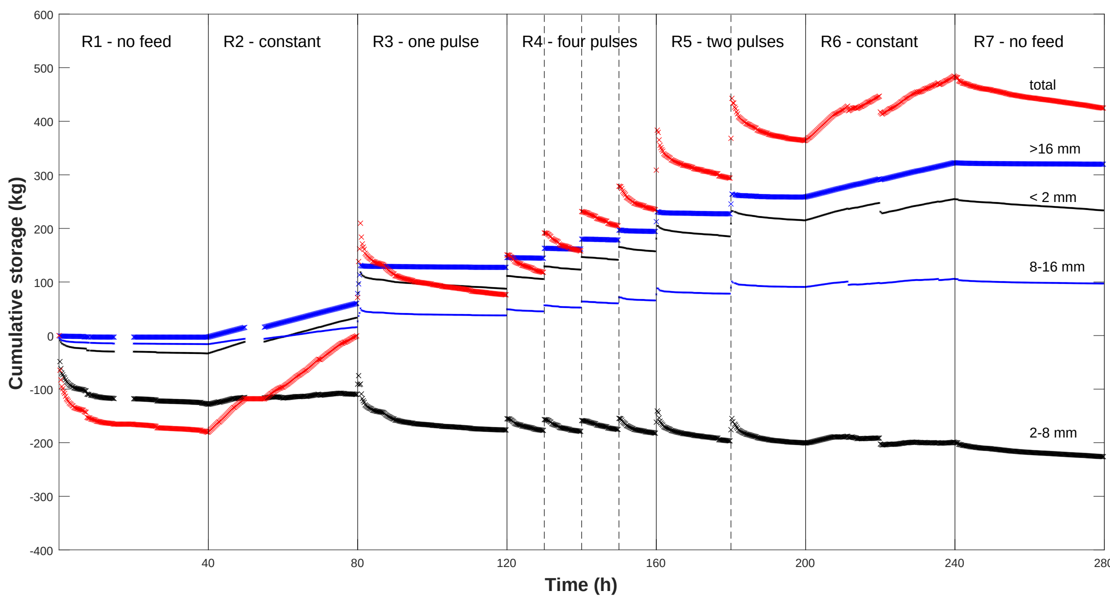

Figure 4.2: Cumulative sediment storage for bulk sediment (total) and four grain size fractions. Mass balances were estimated every 15 min and the cumulative sum is plotted.

4.4.2 Sediment transport–storage relations

To assess sediment transport–storage relations we plot mean total bedload transport rate vs. cumulative sediment storage for the entire 280-h experiment (Figure 4.3). There was considerable variability in mean bedload rate for the same stages of sediment storage (hysteresis) because of differences in sediment availability and bed surface texture. The direction of hysteresis observed within cycles of aggradation–degradation changed over the experiment and depended on bed state. In runs with episodic feed, it also depended on the duration of the aggrading phase relative to the time that it took for bedload rate in the downstream end to respond to sediment feed. In R1, the transport–storage relation was steep because the initial well-mixed bed caused large bedload rates, which decreased as the bed armored slowing down bed degradation. The relation was milder during persistent aggradation caused by constant sediment feed in R2 and for the same levels of cumulative storage, bedload rates were significantly smaller than during degradation in R1 (counter-clockwise hysteresis). The contrast between a well-mixed initial bed in R1 and a conditioned armored bed at the beginning of R2 explains the observed pattern.

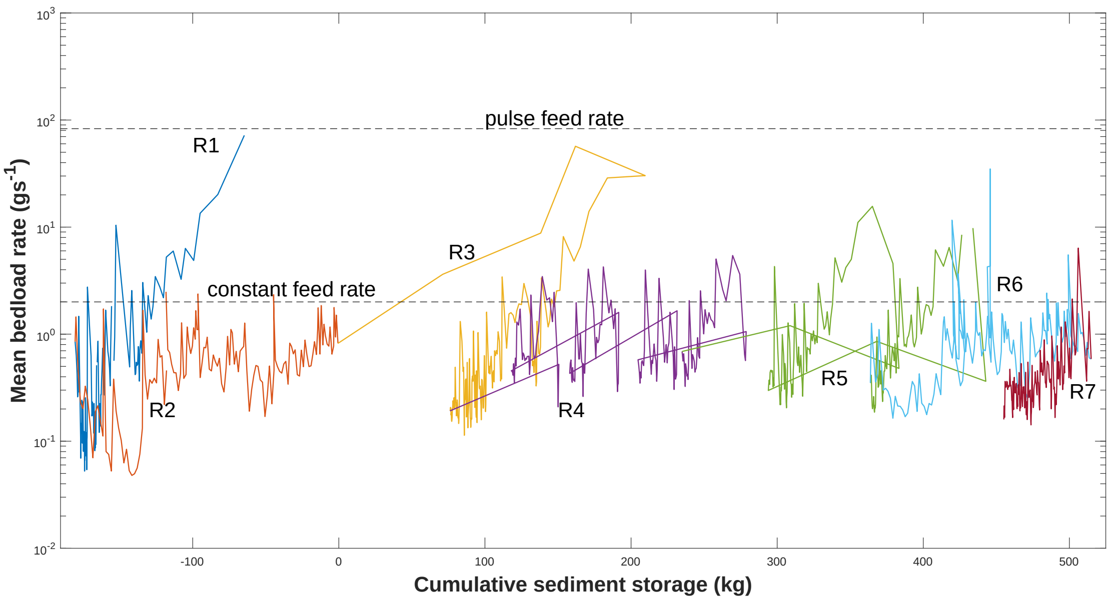

Figure 4.3: Mean bedload transport rate against cumulative sediment storage over the experiment. Seven runs (R1–R7) distinguished by color. Dashed lines indicate sediment feed rates used for constant and episodic feed regimes.

R6, which also received constant sediment feed, exhibited a pattern similar in shape to that of R2, but with larger levels of cumulative sediment storage and a higher range of mean bedload rate (Figure 4.3). In R6, transport rates occasionally exceeded the feed rate, causing cumulative storage to decrease and the development of small aggradation–degradation cycles (Figure 4.4) with larger transport rates during the degrading phase (counter-clockwise hysteresis). These cycles were not present in R2 because mean bedload rate was always below the feed rate. Differences in the intensity of sediment transport among R2 and R6 could be related to cumulative increases in sediment storage and bed slope, but not likely to the initial bed surface D_g, which did not change significantly among them.

R7 had no feed like R1 and exhibited a similar shape for transport-storage relations, but with greater levels of cumulative storage and a narrower range of mean bedload rates (Figure 4.3). Bedload rates were not as large at the beginning of R7 as in R1 because in R7 the bed was armored to some degree, whereas in R1 it was well-mixed. Bedload rates were not as low at the

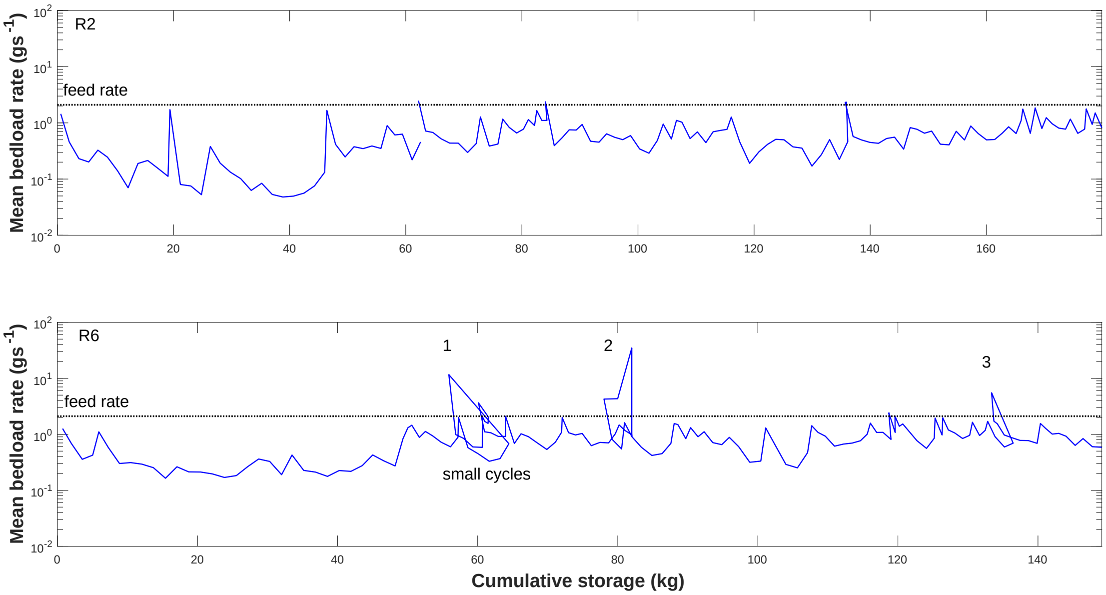

Figure 4.4: Mean bedload transport rate against cumulative sediment storage over runs with constant feed (R2-R6). Dashed lines indicate feed rate. Small cycles of aggradation–degradation occurred in R6 when mean bedload rate exceeded feed rate, which did not happen in R2.

end of R7 as in R1 because R7 started at a greater level of cumulative storage, which implied a steeper bed slope upstream and more sediment available. For same levels of cumulative storage, bedload rates were greater during aggradation in R6 than during degradation in R7 (clock-wise hysteresis), which differs from what we observed between runs R1–R2. Differences in the initial beds of the degrading runs influenced the patterns observed. The initial well-mixed bed in R1 caused intense bedload during degradation, whereas the armored bed in R7 exhibited considerably lower bedload intensity.

Cycles of aggradation and degradation were also observed within runs with episodic sediment supply (Figure 4.3). These runs received large amounts of sediment during short periods of time that alternated with longer periods of no sediment feed. There was a time delay τ of 0.5–1 h between the start of the feed and the response of bedload rate at the downstream end where sediment output was measured. The difference between the delay τ and feed duration d_f influenced the direction of hysteresis found in aggradation–degradation cycles. If $\tau < d_f$, as in R3, bedload rates were larger during aggradation as expected. If $\tau \leq d_f$, as in R4 or R5, transport rates could become larger during degradation. The size of pulses affected the degree of hysteresis. Differences in bedload rate for the same levels of storage were stronger with the larger pulses in R3 and R5 than they were with the small pulses in R4, for which hysteresis was not always clear.

4.4.3 Sediment storage and spatial variability over the channel bed

Mean changes in bed elevation obtained from DEM subtractions were consistent with results of storage computed from mass balances. Despite differences in the temporal resolution, cumulative mean change in bed elevation (Figure 4.5) displayed similar temporal trends to total cumulative sediment storage presented in Figure 4.2. Sediment feed caused positive changes in bed elevation, which were more pronounced with sediment pulses than with constant feed. Instead, the absence of feed first caused slight negative changes in bed elevation and then a more stable behavior as the bed armored. As a DEM for the initial bed in R1 was not available, the strong degradation that occurred during the first hours is not visible in Figure 4.5.

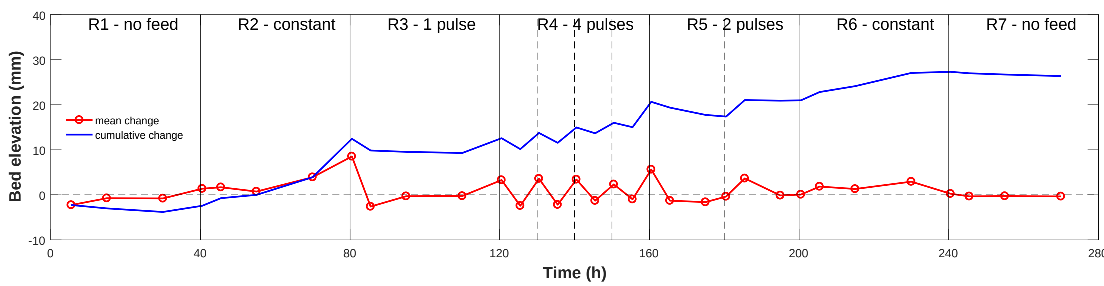

Figure 4.5: Mean change in bed elevation during the experiment. Mean change was estimated by subtracting two consecutive DEMs and computing an average.

To assess differences along the channel, we estimated cumulative mean change in elevation for ten bed sections (Figure 4.6). In all sections, the response to sediment feed consisted of an increase in bed elevation, which occurred faster and was larger towards the upstream end where sediment entered the channel. In sections located more than 10 m from the downstream end, the cumulative change in elevation started to increase after 1–10 h of feed in R2. Instead, in sections located less than 7 m from the downstream end, cumulative change in elevation did not increase until the end of R2. At the end of the experiment, the farthest upstream section exhibited the largest cumulative change in elevation (40 mm at x = 11.5 m), which was probably related to cumulative storage of coarse gravels and sand as shown in Figures 4.1 and 4.2. Near the downstream end (at x = 2.5 m), the increase in elevation with feed was very small and the cumulative mean change curve plots near zero. Stability over this area could be because it was far from the feed source or due to the influence of downstream boundary conditions.

To evaluate bed rugosity and roughness due to the presence of bedforms, we computed standard deviation of bed elevation σ_η for each bed section. We expected to find higher σ_η in the presence of larger bedforms (i.e., bars) and the lowest values in the absence of bedforms when differences in η only occur at the grain scale. The temporal evolution of σ_η varied along the flume (Figure 4.7). In the center of the flume (5–8 m from downstream end), σ_η changed very little. Downstream, short-term changes were not pronounced, but σ_η at the end of the

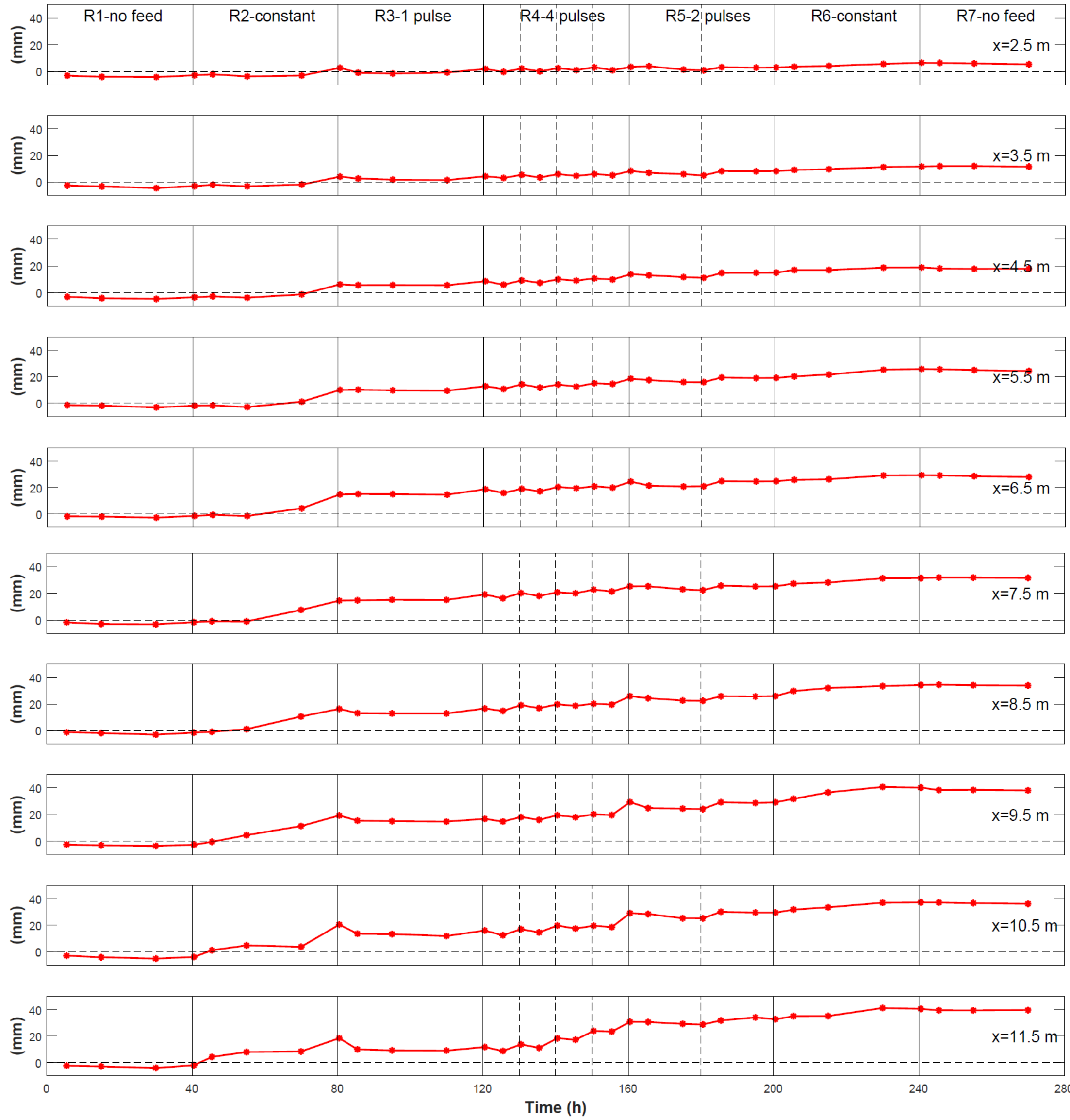

Figure 4.6: Cumulative mean change in bed elevation over different bed sections. DEMs were divided in ten 1-m^2 sections and cumulative changes in elevation were computed for each of them. The downstream end of the flume was at x = 0 m.

experiment was considerably larger than σ_η at the beginning. Upstream, the most dramatic changes occurred between R2–R4 (pulses in R3 and R4 had clear responses) and for sections at x > 10 m, an increase in σ_η was also noticed towards the end.

To link changes in σ_η (Figure 4.7) to the development of bedforms, we summarize the evolution of bed morphology using DEMs for the channel bed at six different times as examples (Figure 4.8). Degradation during no feed in R1 resulted in a straight channel with no large-scale bedforms, but small bed structures (Figure 4.8a). The feed in R2 (constant) entered from the side of the flume and it obstructed the flow causing marked differences in flow and transport patterns in the transverse direction (Figure 4.8b). Upstream, this caused deposition of a

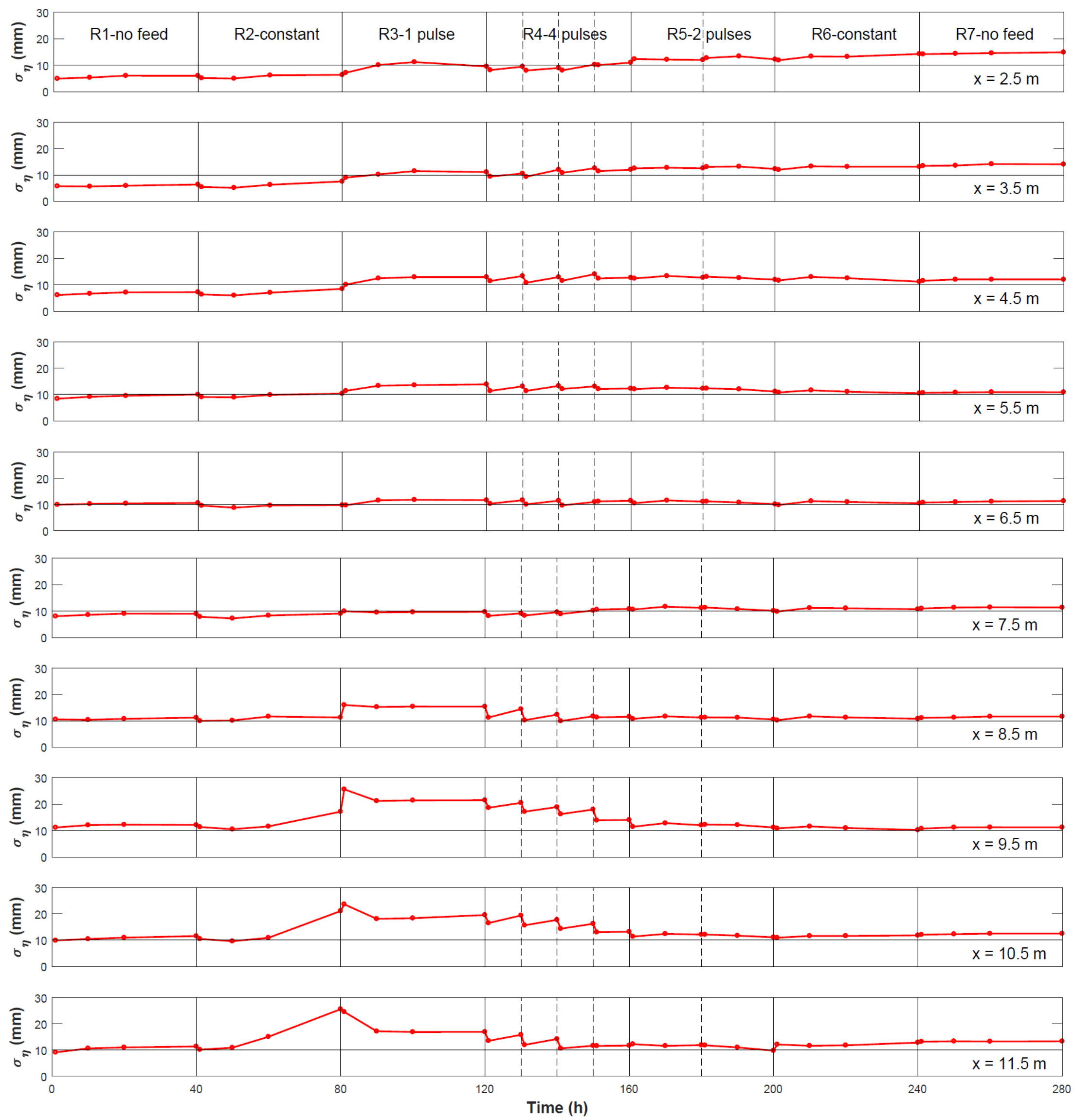

Figure 4.7: Standard deviation for bed elevations σ_η for different bed sections. DEMs were divided in ten 1-m^2 sections and σ_η was computed for each of them. The downstream end of the flume was at x = 0 m.

sediment bar towards one side of the flume and erosion towards the other. The pattern was inverted downstream, which indicated a shift in the thalweg with distance downstream and maybe in the paths of sediment transport. After R3 (large pulse), the main changes in bed morphology occurred upstream where sediment deposited mostly over previously eroded areas (Figure 4.8c). Transverse features developed and pools got excavated, which were evident by the first 10 h of R4 (Figure 4.8d). By the end of R4, the bed had gained considerable elevation, the upstream bar disappeared, transverse features were identified further downstream, and a lateral bar developed downstream (Figure 4.8e). After R5, the upstream bed was undulated and sequences of transverse features and depressions were evident and persisted until the end of the experiment (Figure 4.8f). The bed gained elevation in R6, but channel morphology remained almost unchanged at a large scale, except for the lateral bar downstream that reduced its area but became more prominent. A significant amount of the sediment fed into the channel was not immediately transported and formed a sediment wedge near the upstream end of the bed, which expanded downstream and could have acted as a persistent in-channel source of sediment for transport. Although the wedge started to develop early in R2, it was only evident in DEMs of late runs (Figure 4.8e-f).

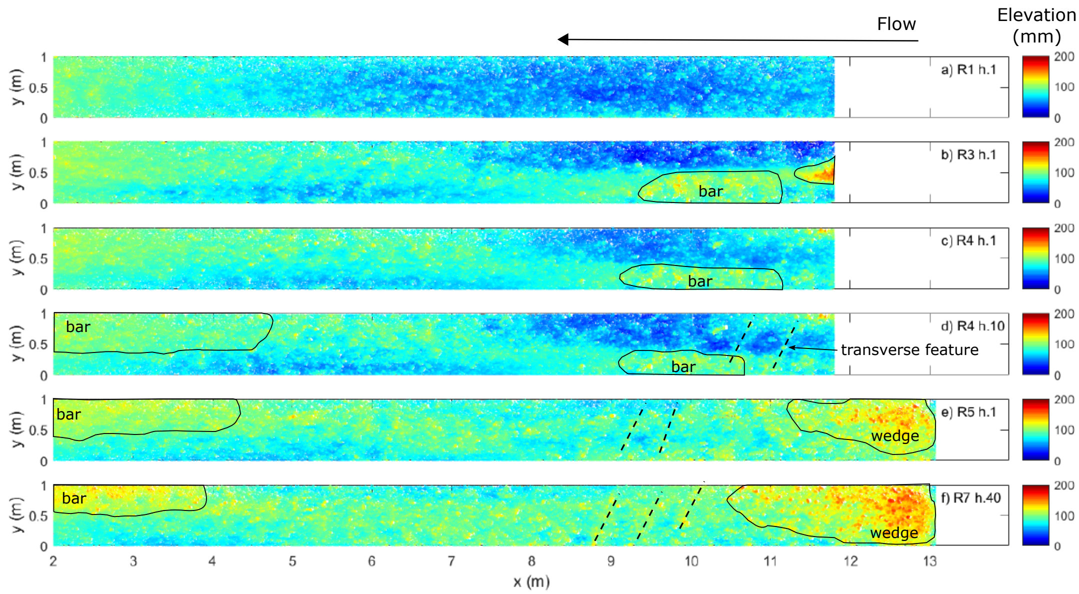

Figure 4.8: Digital elevation models (DEMs) at six different times. We chose these cases from the 34 DEMs collected to summarize the evolution of bed topography at large and intermediate scales. Bed elevations η are relative to the floor of the flume. The downstream end of the flume was at x = 0 m. Lateral bars and upstream sediment wedge are delineated and examples of transverse features that intercalate with pools are indicated.

In general, σ_η was an indicator of bed morphology and it was large at times when the channel developed large-scale bedforms like lateral bars. The large increase in σ_η upstream during R2 was due to the development of a lateral bar, the same as the overall increase in σ_η observed downstream (at $x < 4$ m) through R3–R6. The decrease in σ_η upstream during R3 could relate to the filling of previously degraded areas as sediment feed was transmitted downstream and the wedge expanded. More moderate adjustments of σ_η, as those observed with small sediment pulses in R4, could be related to the evolution of smaller bedforms like transverse features and pools. Bed DEMs for 1 h and 10 h after the first pulse in R4 (Figure 4.8c-d) show the same large-scale bedforms (> 2 channel width) in both of them. Instead, smaller-scale bedforms (< 1 channel width) were more developed after 10 h than they were right after the pulse. We present DEMs for the bed at both times together with bed surface photos at some specific locations (Figure 4.9) to relate changes in bed elevations η with the development of bed structures.

Ten hours after the small pulse, transverse features that were barely visible after one hour became prominent, small pools were scoured, and bed structures became larger. Upstream (at $x > 10$ m), DEMs show a central channel, which developed transverse elevated features intercalated with depressions under no feed (Figure 4.9a-b). Adjustments in the particle size of the bed surface over an upstream transverse feature can be appreciated on photos (Figure 4.9c-d). The feature became considerably coarser after 10 h and the connection between the coarsest grains ($>$ 22 mm, which includes light green, white, and blue) increased. The same photos show the enlargement of a pebble-cluster, which development we suspect was an important mechanism to increase bed roughness at small scales. Bed structures developed further downstream (at $x = 3$–6 m) over a lateral channel (Figure 4.9e–f). Here, a stone line became evident after 10 h because of the deposition or excavation of coarse grains in between other coarse grains, which were already there one hour after the pulse.

To evaluate differences in textural adjustments on the bed surface and grain roughness along the flume, we estimated geometric mean grain size D_g on the surface for different bed sections (Figure 4.10). The bed surface became finer in the downstream direction, probably due to selective transport and preferential storage of coarse sediment upstream. With episodic sediment feed regimes, changes in D_g were consistent with changes in sediment feed, so D_g became finer with sediment pulses and coarsened without feed. Adjustments with constant feed were variable. In R2 some sections became coarser, whereas in R6 they either remained unchanged or became finer.

Although, small changes in σ_η were noticed at $x \approx 6$ m from the downstream end (Figure 4.7), large textural differences on the bed surface for this area can be appreciated in a sequence of photos (Figure 4.11). The bed surface was coarse after 40 h of flow without sediment feed in R1 (Figure 4.11a) and remained coarse after 40 h of constant feed in R2 (Figure 4.11b). By this time, a new cluster had developed, which indicates that the arrangement of grains was not inhibited by constant feed. The bed surface texture became significantly finer one hour after the large pulse in R3 (Figures 4.11c), which shows that fine gravels were rapidly transported downstream when fed in a large pulse. Although, many of the bed structures observed at the end of R2 (Figure 4.11b) were still present one hour after the large pulse (Figures 4.11c), the grains that filled the spaces between them were significantly finer than at the end of R2. After 39 h of no sediment feed, the bed surface re-coarsened with the evacuation of fine gravels and re-arrangement of coarse grains (Figure 4.11d).

4.5 Discussion

4.5.1 Hypothesis 1: Preferential deposition of coarse partially-mobile gravels near the feed source promote increased storage upstream and downstream fining on the bed surface

This hypothesis is supported by an increase in the percent of mass stored from mass fed with grain size within gravel fractions (Figure 4.1b) and by increases in cumulative mean change in bed elevation η (Figure 4.8) and D_g of the bed surface (Figure 4.10) with distance from downstream. During the experiment, the limit between partial and full mobility was stable around 8 mm (*Elgueta-Astaburuaga et al.*, 2017). The storage of gravels > 8 mm was larger than the storage of finer fully-mobile gravels, although the storage of sand was also significant (Figures 4.1 and 4.2). The increase in storage with grain size for gravel fractions is consistent with grain-size dependence observed in their bedload rates (*Elgueta-Astaburuaga et al.*, 2017). Whereas the storage of fine gravel was different among runs, the storage of coarser sediment was more stable. Sediment coarser than 8 mm, for which transport conditions ranged between partial mobility and incipient motion, had positive mass balances. Very coarse gravel (> 16 mm) was near incipient motion and when supplied, it got mostly deposited upstream. These grain sizes moved at very low frequencies and mostly over short distances, so not many of them exited the flume. For example, they exhibited the same output in runs with no feed (R1 and R7), even though, the effects of fines on the surface were expected to be stronger in R1 due to an initial well-mixed bed. This indicates that very coarse grains were mostly deposited and moved at slow virtual velocities (*Einstein*, 1937). Gravel 8–16 mm was more mobile than coarser material, as indicated by larger sediment outputs over runs with no feed and slight decreases in the cumulative storage curve that were not evident for coarser grains. When fed, at least some gravel 8–16 mm was expected to move further downstream. These grains had faster virtual velocities and reached the end of the flume more frequently than coarser grains, but less frequently than fully-mobile gravel. Preferential storage caused an increase in the cumulative change in bed elevation η and D_g of the bed surface with distance from downstream (Figures 4.6 and 4.10).

Sand did not behave in the same way as fully-mobile gravel (Figure 4.1 and 4.2). The output of sand was significantly smaller than the output of fine gravel in runs without feed (R1 and R7) and the percent represented by stored mass from feed mass was considerably larger for sand than for fine gravel. The transport and storage of sand was also more stable and did not change significantly with feed regime like in the case of fine gravel. More than 60% of the sand that entered the flume during each run was deposited on the bed, which can be related to hiding effects and infiltration. We did not measure infiltration rates for sand, but we think infiltration was an active process. The significant storage of coarse gravels and the development of armor on the bed were expected to provide shelter for the finest fractions. We did not observe large areas covered by sand on the bed surface at the end of the experiment, but we did notice the presence of sand (and fines) within larger grains. A significant amount of sand could have also got trapped within the coarse sediment wedge that formed upstream (Figure 4.8e-f). We think fine gravel were entrained more easily because of protruding more and infiltrating less than sand.

Dowsntream fining on the bed surface was clear at the end of the experiment (Figure 4.12). Near the upstream end, a large area of the bed surface was covered with grains under incipient motion (22–45 mm, light green and white particles). Towards the center of the flume, the area of the bed surface covered by white particles (32–45 mm) was considerably less than upstream and more areas were covered by finer, but still partially-mobile material (8–22 mm, which includes yellow, red, and black grains). Near the downstream end, grains under incipient motion were also present, but were less abundant. Instead, areas of the bed covered by fully-mobile gravel (4–8 mm, light blue and dark green grains) became more frequent. Downstream fining have been previously reported over gravel beds under partial transport. *Ferrer-Boix and Hassan* (2015) found that downstream fining was flow dependent and it likely developed during bank-full flows, which promoted some degree of selective transport, and could become less evident after larger floods.

Although found in a considerably larger proportion upstream, coarse grains under incipient motion (e.g., > 22 mm, which includes light green, white, and blue) were found on the bed surface all along the flume. Some of these grains could have been already there at the beginning of the experiment. Others could have been excavated from the bed as finer grains got mobilized (e.g., over R1 that had an output > 150 kg under no feed) or mobilized for short distances and organized into arrangements of grains and bed structures. An example can be appreciated in the sequence of photos at $\sim$6 m from downstream in Figure 4.11. Many of the white (32–45 mm) and all the blue (45–64 mm) particles remained within the area of the photo (< 1 m^2) during R2 (constant feed) and R3 (1 pulse). Apparently, one blue particle that was at the right edge of the photo at the end of R1 (Figure 4.11a) moved over a distance < 1 m and became part of an arrangement of grains identified at the end of R2 (Figure 4.11b). We think the spread of very large grains along the flume during the experiment was defined by their initial spread (they tended to remain close) and by size-selective transport conditions that promoted an increased frequency of coarse material upstream due to feed.

Lag sediment deposits that become armored as a result of poorly sorted sediment supply and size-selective transport have been reported in the field (*Brumer and Montgomery*, 2006), which is consistent with the sediment wedge that developed upstream during our experiment (Figure 4.8). The topography of the wedge was controlled by the way in which the sediment entered the channel. Initially, sediment feed concentrated in a pile, which could have caused the development of lateral bars due to flow obstruction. Later, it spread better across the channel, which might have promoted sequences of transverse features and depressions upstream. There is field evidence that the sediment injection point influences spatial patterns of aggradation–degradation and that the effects of sediment pulses are not restricted to aggradation, which can be localized promoting significant degradation over other areas (*Gaeuman et al.*, 2017) as we observed.

The resulting bed from our experiment was inherited for a subsequent experiment designed to study the effects of larger floods and bankfull flow duration on channel adjustments (*Ferrer-Boix and Hassan*, 2015). Sediment feed was constant at the same rate as in our experiment and they used the same bankfull flow discharge. The flow was ocasionally increased to 1.4 times bankfull and the duration of bankfull flows was varied. In general, large floods caused initial increase in bedload rate, decrease in bed slope, and increases in the amplitude and wavelength of bedforms and in σ_η. Even though grain size statistics for bed surface did not adjust significantly to flow regime (e.g., $D_g = 15$–17 mm), the degree of downstream grain sorting varied with flow and bed history. They explained a decrease in the degree of downstream sorting by partial removal of the upstream wedge.

4.5.2 Hypothesis 2: Constant feed, which makes sediment available more gradually, promotes larger sediment storage than sediment pulses because of a greater probability for sediment being sequestered in the bed

This hypothesis is supported by the large difference in sediment storage noticed between R3 that received one large sediment pulse and runs with constant feed (R2 and R6), although variability in the storage for runs with same feed regime indicates that initial bed characteristics influenced the results. The largest contrast in storage was between R2 and R3 (Figure 4.1). R2 stored almost twice the mass stored in R3 because of larger storage of fine gravel, which instead exhibited significant negative mass balance in R3. Regardless of the presence of large scale bedforms at the beginning of R3, which were absent in R2, differences in bed slope and bed surface texture were small. Instead, these runs received contrasting feed regimes (constant vs. one large pulse), so we think the feed was largely responsible for differences in sediment storage. With constant feed (R2), sediment entered gradually. A significant amount of coarse material was deposited, which created a sediment wedge upstream that probably allowed for the storage of fine sediment within the coarse material. Fully-mobile grains that moved downstream could be deposited before reaching the end of the flume, to be entrained at later stages (i.e., bedload step migration). The time that it took for bedload to respond to constant sediment feed downstream ($\sim$7 h, from *Elgueta-Astaburuaga and Hassan* (2017)) and the gradual adjustments of particle size on the surface (Figure 4.10) support this idea. Under constant feed, sediment transport processes were relatively slow and grains might have remained at rest for longer periods of time (i.e., less interaction between moving grains) or moved for shorter distances in their way downstream. As reported in *vonFlotow* (2013), dynamics of bed structures and clusters were also active during constant feed (i.e., Figure 4.11b) and not exclusively during degradation without feed. Bed structures and clusters could have slowed the movement of fine gravel by forcing grains to deposit more often in their way downstream. These effects might have been reduced by bed surface fining after sediment pulses.

The large pulse made a significant amount of fine gravel available in a short time, which caused significant surface fining (Figures 4.10). The response of bedload rate was also faster than with constant feed (∼0.5 h, from *Elgueta-Astaburuaga and Hassan* (2017)), indicating sediment transport processes occurred faster with the pulse. Fine sediment from the large pulse was transmitted fast downstream and at 6 m from the downstream end (∼7 m from feed location), the bed surface got considerably finer one hour after the pulse (Figure 4.11c). The large pulse caused the development of well-delineated patches of fine sediment upstream, whereas fining was more extensive downstream. We think the large availability of fine gravel decreased the probability of grains getting trapped and could have also decreased the resting periods of grains due to the interaction with other grains. Collective dynamics (i.e., displacement or entrainment due to grain collisions) have been observed to affect bedload transport significantly (*Ancey et al.*, 2006; *Heyman et al.*, 2013). The large pulse in R3 caused intensive sediment transport during an early stage, over which multiple interactions between grains were expected. We think this influenced the large negative mass balance for fine gravel observed for this run.

Net storage decreased with pulse size and in R4 (four small pulses), fine gravel exhibited positive mass balance as in runs with constant feed. In *Elgueta-Astaburuaga and Hassan* (2017) we proposed that feed regimes for which the time required for the channel to reach dynamic equilibrium after a pulse T_r exceeds the recurrence interval of the pulse T_p, could show similar responses to constant feed regimes. These results support this idea because for R4 $T_p < T_r$, whereas for R5 and R3 $T_p > T_r$ (*Elgueta-Astaburuaga and Hassan*, 2017). Even though, in R5 (two pulses) fine gravel exhibited negative mass balance as in R3, it was not as significant and total mass stored in R5 was similar to the mass stored in R6 that received constant feed. This result contradicts the hypothesis (H2) and indicates that bed slope and bed configuration influenced the mass of sediment stored during each run. Large differences in storage over runs with the same feed regimes are evidence of the influence of bed history and initial conditions on the results.

Bed characteristics and configuration could have affected sediment transport and storage in many ways and at a range of scales. Differences in the availability of fully-mobile sediment between R1 that started from a well-mixed bed and R7 that started from an armored bed probably caused larger degradation during the first few hours of R1 (Figure 4.2). Besides the larger availability of fully-mobile sediment at the beginning of R1, the bed surface was significantly finer and did not exhibit bedforms, for which it was expected to be smoother than it was at later stages of the experiment. This could have increased the intensity of movement for coarse gravel (8–16 mm), which output in R1 was twice the output in R7, although in both runs it was very small in comparison to that of fine gravel. Sediment > 16 mm moved very occasionally in both runs.

Differences in storage among runs with constant feed (R2 and R6) were probably related to the increase in bed slope due to preferential storage of coarse sediment. Between R2 and R6, bed slope increased from 0.017 to 0.022 m/m (Table 4.1), which could have increased transport capacity under constant flow discharge. Cumulative storage (Figure 4.2 and 4.6) indicates that R6 started from a higher level of total mass stored than R2, although it started with a larger deficit in fine gravel, which was the most mobile fraction. The D_g of the bed surface was almost the same for both runs and the D_{90} was only slightly finer at the beginning of R6 (Table 4.1), so we think textural differences do not explain patterns of storage observed for these runs. The evolution of D_g (Figure 4.10) shows that at most bed locations, there were no big textural changes between R2 and R6. Bed roughness estimated as σ_η exhibited differences among R2 and R6 for bed sections located at more than 10 m or less than 5 m from downstream. These differences were caused by the development of bars and bed features at a larger scale than those found at the beginning of R2, which had a relatively flat channel with an armored and structured bed. Any increase in roughness due to the development of a more complex topography apparently did not counteract the effects caused by the steeper bed slope in R6, so the channel transported sediment more efficiently during R6. Other studies have also reported the importance of bed history on sediment transport patterns (e.g., *Waters and Curran*, 2012; *Ferrer-Boix and Hassan*, 2015).

4.5.3 Hypothesis 3: Hysteresis in sediment transport-storage relations largely depends on differences in bed surface texture and sediment availability

This hypothesis was supported by differences in the direction and magnitude of hysteresis observed between R1-R2 and between R6-R7. The flat well-mixed bed at the beginning of R1 was responsible for larger bedload rates during degradation for cycle R1-R2. Bedload rates were larger during aggradation for cycle R6-R7 because of the increase in sediment availability caused by the feed and maybe also because of bed surface smoothing. Differences in bedload rate between aggradation and degradation stages were significantly smaller for cycle R6-R7 because the bed texture was similar in both runs. Over a short range of storage, bedload rates were the same during aggradation and degradation as in the first scenario proposed by *Lisle* (2012). These occurred over a period of time when the bed surface texture and sediment availability did not change significantly (between a few hours before the end of R6 and a few hours after the start of R7) and could be related to the time delay τ in downstream bedload response to changes in feed. We think that cycle R6-R7 was more representative of natural streams because it started from a more complex and armored bed than cycle R1-R2, for which the initial well-mixed bed conditioned results. We think that bedload rates should be larger during aggradation than during degradation, unless large differences on the bed texture and sediment availability change this situation. Our results support the idea that the state of the bed influences transport-storage relations (*Madej et al.*, 2009; *Pryor et al.*, 2011).

The large pulse in R3 also caused larger bedload rates during aggradation as the bed surface became finer and more fine gravel was available for transport. The short duration of sediment feed d_f in smaller pulses relative to time delay τ, caused variability in the observed patterns of hysteresis. Despite the large increase in sediment availability caused by pulses, bedload rates were larger during degradation after some of the small pulses in R4 because $d_f \leq \tau$. A similar situation was observed for the two pulses in R5. In our experiment, τ mostly depended on feed regime (smallest with large pulses, largest with constant feed), but changes in the bed state, slope, and morphology could have also influenced τ. Flow conditions, distance from feed location to flume output, and sediment texture could also affect τ, but were held constant during the experiment. Small cycles of hysteresis during constant feed were observed within R6, which is consistent with *Luzi* (2014) that reported similar cycles for runs at dynamic equilibrium. In our case, large occasional bedload rates that exceeded the feed rate caused degradation over a relatively short period of time.

The two-phase transport–storage relation proposed for degrading channels by *Lisle and Church* (2002) was not always observed under no feed. The relation proposed by *Lisle and Church* (2002) consists of an initial phase were bedload rate remains high as the bed degrades followed by a phase in which armor development prevents degradation causing bedload rate to decrease. In our experiment, sediment transport–storage under no feed could either exhibit a two-phase relation like that following the pulses in R5, transition directly into the second phase as in R1 , or remain in the first phase for a long time like after the third pulse in R4 (i.e., bedload rate was nearly constant for all levels of storage). Deviation from the two-phase relation proposed for transport–storage in degrading channels have been noticed (*Madej et al.*, 2009; *Pryor et al.*, 2011) and explained by differences in the bed state.

Size-selective sediment transport promoted the deposition of coarse material upstream, which caused a general increase in cumulative storage over the experiment. In previous studies (*Madej et al.*, 2009; *Pryor et al.*, 2011), sediment storage after cycles of aggradation–degradation did not return to the same level it had before the cycle, but remained at higher levels. The effects of aggradation at a large scale (e.g., development of bedforms, the upstream wedge, overall increase in bed slope, cumulative mass balance, and mean change in bed elevation) were persistent. This is probably related to bed armoring and structuring in poorly sorted beds under partial mobility, which counteracts bed degradation by stabilizing the bed surface.

4.6 Conclusions

We found that patterns of sediment storage were significantly affected by partial mobility, sediment feed regime, and bed characteristics. Partial mobility caused size-selective storage of coarse material and sand within it. Evidence of this was an increased bed elevation by the end of the experiment that was larger upstream and downstream fining on the bed surface. Sediment supply regime affected the mass of sediment stored in each run, which was larger during constant feed. Bed characteristics significantly influenced the temporal response of sediment storage, especially for fine gravel that was the more responsive size fraction. Sediment transport–storage relations were also influenced by sediment supply regime. Whereas constant feed produced a very mild relationship that could (or could not) exhibit small cycles of hysteresis, sediment pulses caused large cycles. Differences in the direction of hysteresis in bedload rates respond to differences in bed surface texture and sediment availability. Spatial patterns of sediment storage and the evolution of large-scale bedforms were not explained by feed regime. We think they responded to the topography of a sediment wedge created upstream due to size-selective transport and storage.

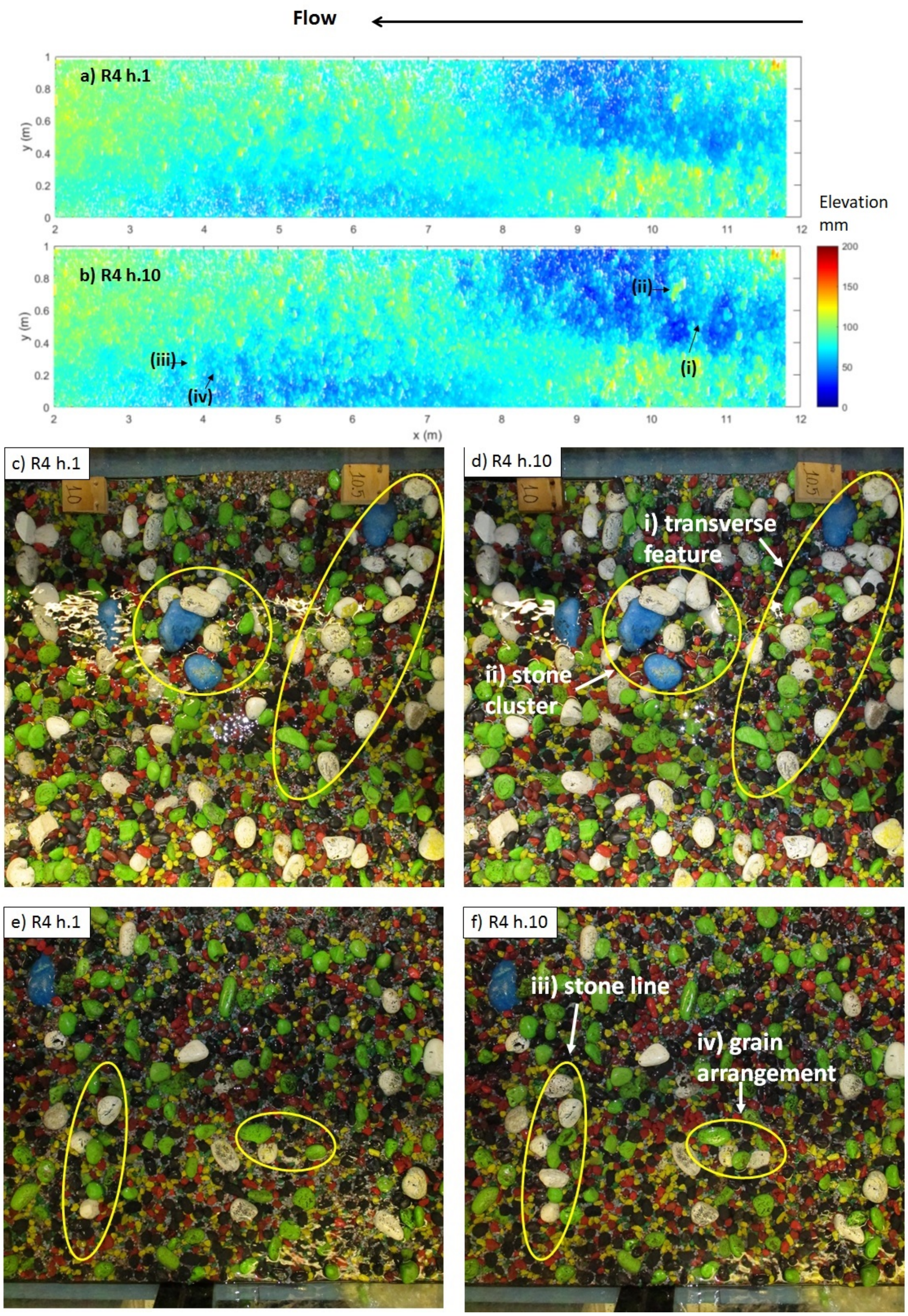

Figure 4.9: Evolution of small-intermediate scale bedforms after the first small pulse in R4. (a) DEM of the bed one hour after the first small pulse in R4. (b) DEM ten hours after the pulse. Examples of bed features are presented with roman numbers: (i) transverse feature, (ii) stone cluster, (iii) stone line, and (iv) small arrangement of grains. The downstream end of the flume was at $x = 0\,\mathrm{m}$. (c–f) Bed surface photographs showing the evolution of bed features i–iv between 1–10 h after the pulse.

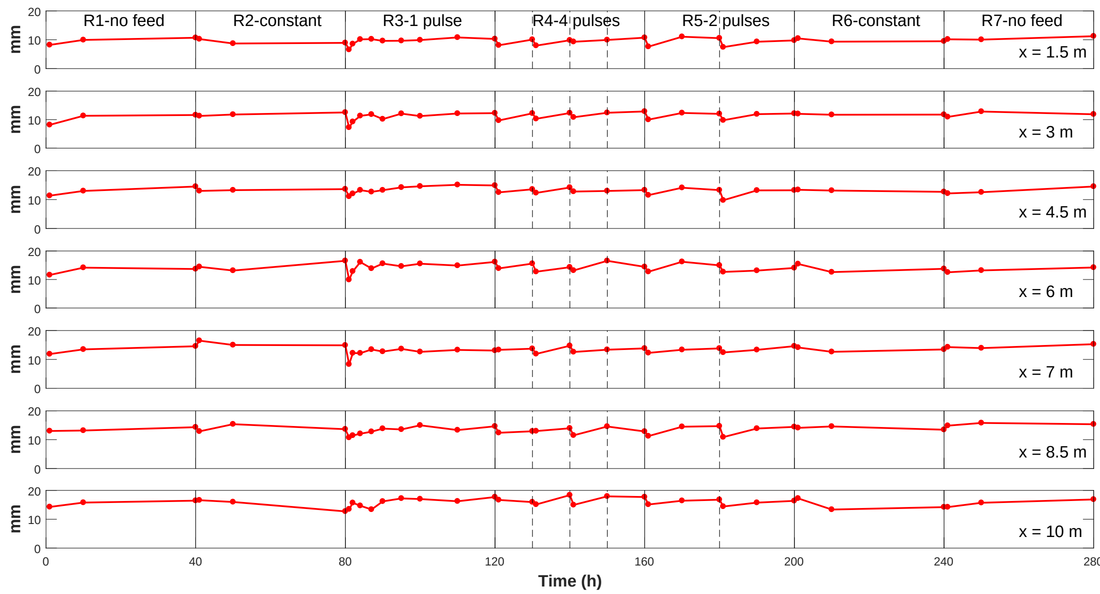

Figure 4.10: Evolution of geometric mean particle size D_g on the bed surface for seven bed sections along the flume. The downstream end of the flume was at $x = 0\,\mathrm{m}$.

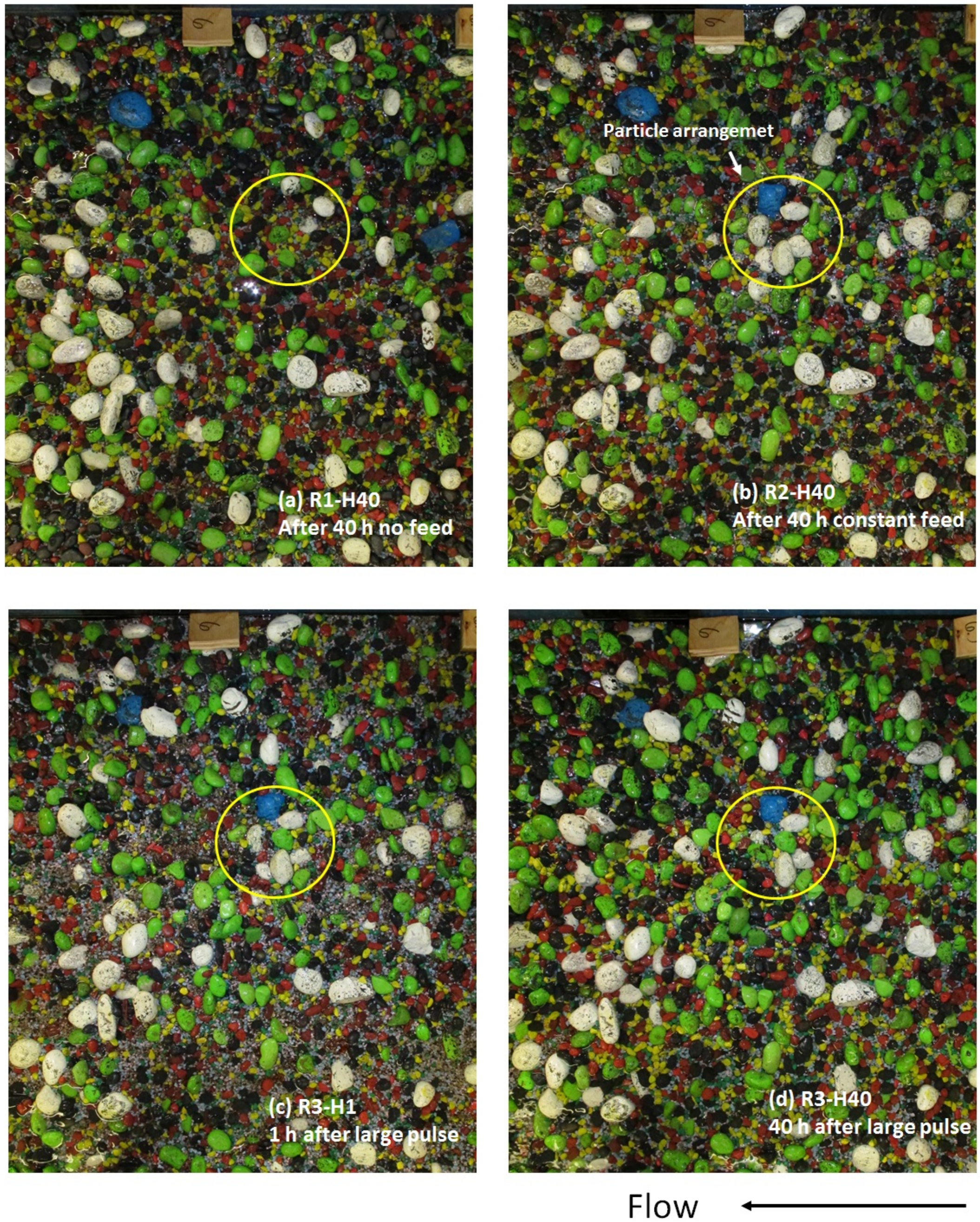

Figure 4.11: Evolution of bed surface texture at ∼6 m from downstream between the end of R1 and the end of R3. (a) The bed surface was coarse by the end of R1 that had no feed. (b) After 40 h of constant feed in R2, there was no significant fining on the surface. (c) In contrast, one hour after the large pulse of R3, significant fining was observed. (d) Forty hours after the large pulse, the bed surface was coarse again.

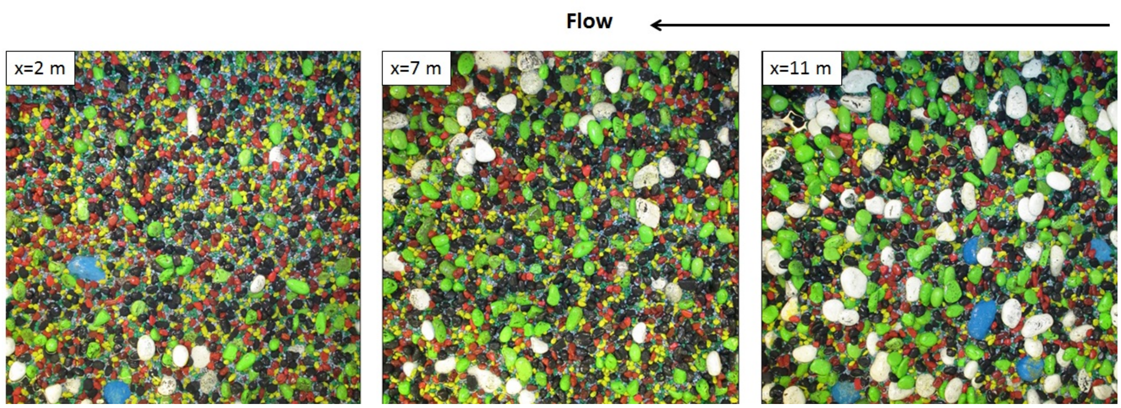

Figure 4.12: Downstream fining at the end of the experiment. Photos of the bed surface at three locations. The downstream end of the flume was at x = 0 m.

Chapter 5

Concluding remarks

The goal to study the effects of episodic sediment supply on channel adjustment was accomplished by analyzing an extensive data set on bedload transport and bed properties, collected systematically by the author during a 280-h long flume experiment with constant flow, but changing sediment feed. The long duration of each run allowed assessing the effects of feed regime on bedload transport statistics at a wide range of time scales. The use of a wide range of grain sizes allowed the effects of the feed on size-selective bedload transport and storage to be studied. To collect fractional sediment transport data the video-based method presented in (*Zimmermann et al.*, 2008) was improved by increasing the resolution considerably to accurately detect grains as small as 1 mm. Obtaining representative grain-size distributions of the bed surface was possible by systematically taking photographs of the bed surface along the flume, which alllowed an accurate identification of gravel grain sizes. Research was directed by the following questions, for which summarized answers are provided in the next subsections: (1) which episodic sediment feed regimes could be represented by constant feed and at which time scales?, (2) how do bed history and bed state affect channel reponse to changes in sediment feed regime?, and (3) what are the consequences of size-selective bedload transport on this response?

The results support the idea that sediment supply is a first order control in mountain streams, for which evidence had been provided in previous experiments and field studies (e.g., *Hassan et al.*, 2006, 2008). The variables that responded more consistently to sediment feed regime were bedload transport rate and bed surface texture. Sediment feed promoted bed surface fining and increased bedload rates as described in previous studies (*Lisle and Madej*, 1992; *Madej et al.*, 2009), whereas no feed caused bed surface coarsening and decreased bedload rates (e.g., *Dietrich et al.*, 1989).

Cumulative storage of sediment, which had been observed under partial transport (e.g., *Brumer and Montgomery*, 2006), caused an overall increase in bed slope over the experiment. Bed slope response did not necessarily coincide with changes in feed and thalweg slope became nearly stable by the fifth run in a sequence of seven runs, despite changes in feed rate. The poorly sorted sediment and near bank-full flow discharge promoted partial sediment transport, which resulted in bed surface armoring and preferential storage of coarse material. The effects of cumulative storage and bed slope increase on channel response to changes in feed were tested by comparing the results for runs with the same feed regimes but started from different initial conditions.

5.1 Which episodic sediment feed regimes could be represented by constant feed and at which time scales?

The assumption of constant feed might not be suitable to model streams that are subjected to large, infrequent sediment episodes as in R3 and R5, but could be appropriate to study channels that receive more frequent pulses as in R4. As verified, channel adjustment to changes in sediment supply regime was affected by the magnitude and frequency of sediment feed. Sediment pulses caused significant fining on the bed surface, which resulted in larger and faster increases in bedload transport rate dowsntream than with constant feed. As fully-mobile sediment evacuated, the bed surface re-coarsened, which limited bedload transport decreasing bedload rate as in runs without sediment feed. Larger sediment pulses produced stronger responses in bedload rate, but the time it took for bedload rate to stabilize around a low constant mean after the pulse (relaxation time T_r) did not depend on pulse size. If T_r exceeded the time between pulses T_p as for R4, the response exhibited similarities to the response for constant feed, especially at large time scales ($2T_p$ to run scale). This was supported by similar spans in the variability of cumulative departures from mean bedload rate and the lack of statistical differences in bedload rate signals for runs with constant feed and R4, which was indicated by results from L-ratio tests for temporal resolution ≥ 30 min. At short timescales ($< T_p$), the effects of each sediment pulse were evident and very different from those of constant feed (i.e., faster response, trend inflection caused by no feed).

The memory structure for total bedload rate was also affected by sediment feed regime. Pronounced trends in bedload rate caused by episodic feed increased long-term memory. The three stages of fluctuation proposed by *Ma et al.* (2014) were only observed for runs with constant feed. Episodic feed caused an increase in the range of scales with long-term memory (invariant stage of fluctuation) and the absence of a memoryless stage. Another difference between constant and episodic feed regimes was that constant feed promoted larger sediment storage, although changes in the initial bed conditions significantly influenced the results.

5.2 How do bed history and bed state affect channel reponse to changes in sediment feed regime?

Bed state and bed slope conditioned channel adjustments to changes in sediment feed significantly. This was supported by differences in temporal patterns of bedload rate between runs with the same feed regimes or after pulses with same size. R1 and R7 had the same feed regimes and initial bed slope, but started from very different bed states that dictated sediment availability (well-mixed and armored bed respectively). This caused significant differences in the patterns of bedload transport and storage among them. R2 and R6 had same feed regimes and initial armored beds, but started from very different bed slope and levels of cumulative sediment storage. Even though, no statistically significant differences were found with L-ratios between them at 5 min resolution, the range of bedload rates was higher during R6, bedload scaling statistics (i.e., H) indicated stronger memory, and patterns of sediment storage indicated that the channel transfered fully-mobile gravel more efficiently during this run. Transport–storage relations indicated R6 was closer to mass equilibrium as bedload rate occasionally exceeded feed rate causing small cycles of hysteresis as those described in *Luzi* (2014).

The evolution of bed morphology was dictated by the way in which sediment entered the channel. This was more localized at the beginning, but became better spread in the cross-section later during the experiment. This caused the development of lateral bars early in the experiment, followed by the appearance of smaller transverse features intercalated with depressions. Mean changes in bed elevation responded to sediment feed, although in all runs a large amount of sediment was stored near the feed source because of size-selectivity in flow competence. The cumulative storage of sediment upstream increased bed slope, which increased the intensity of bedload transport towards the end of the experiment. These effects were likely to inluence relaxation times T_r.

5.3 What are the consequences of size-selective bedload transport on this response?

Grain-size dependence in patterns of bedload transport and storage was almost the same regardless of sediment feed regime. Gravel fractions were affected by size-selective transport and the limit between relative partial and full mobility (*Wilcock and McArdell*, 1993) remained nearly unchanged around 8 mm. The memory structure for total bedload reflected that for fully-mobile gravel (2–8 mm), which dominated bedload transport. Memory strength decreased with grain size, except for sand that behaved more stochastically than fine gravels. The decrease in memory for partially-mobile gravel was related to their occasional movement, which resulted in preferential storage of coarse grains near the feed source upstream as in coarse lag formations reported in the field (*Brumer and Montgomery*, 2006). These conditions promoted increased storage upstream and downstream fining on the bed surface throughout the experiment.

Although sand was fully-mobile, it behaved differently from fine gravel, which was probably related to the higher potential for sand to be affected by hiding effects and infiltration. The movement of sand was more stochastic, but this cannot be explained by a lack of movement because transport rate time series at 1 s exhibited little intermittency for sand. Mass balances revealed more than 60% of the sand fed got stored, which could have got trapped in the upstream wedge or within larger grains and structures along the bed. Stored sand could become available later, if the movement of coarse grains exposed it to the flow. The movement of sand might have been more influenced by these highly stochastic dynamics and less affected by longer scale processes such as bedform or pulse evolution.

5.4 Limitations of the study

The experimental design was complex in comparison to many flume experiments (we used a poorly sorted gravel bed with relatively long and varied history of sediment feed), but in comparison to natural rivers, flumes are always a simplified case. Here, I provide some examples of factors that increase complexity in natural streams, but were neglected in the experiment. Streams are subjected to variations in flow discharge, which affect channel response to sediment inputs (*Sutherland et al.*, 2002), but in the experiment flow was held constant to isolate the effects of feed. The flume had a fixed width, whereas many stream have erodable banks. The work of (*Eaton and Church*, 2004) shows that in unconstrained channels variations in width can be important (even more important that the adjustments of particle size). The glass walls of the flume were also very different from stream banks, which can be irregular and provide different types of roughness elements (e.g., vegetation). The presence of large wood (see *Montgomery and Piégay* (2003) for examples) and channel constrictions (*Chartrand*, 2017), which can significantly influence channel morphology and spatial variability of flow and sediment transport, was also disregarded. Natural rivers are very complex environments, where even living organisms can be responsible for changes in sediment supply and channel morphology. Examples of this are salmons that mobilize a significant amount of gravel for spawning (*Hassan et al.*, 2008) and beavers that build dams (*Naiman et al.*, 1986).

The main limitations of the experimental design were the lack of replicates and the differences in the initial bed among runs that challenged comparisons. We only repeated constant feed and no feed regimes. If we had repeated all sediment feed regimes, we could have got an idea of the variability within them increasing the certainty of comparisons among them. For statistical tests among bedload rate signals, the lack of replicates made it impossible to apply paired t-tests, so a general least-squares model and likelihood L-ratio tests were used. The sequence of runs caused differences in the initial bed that challenged comparisons, but as it allowed for a more realistic bed to develop and to compare among same feed regimes that started from different initial conditions, this limitation was also a strength. We were careful to consider the influence that these differences had in the results and used them to explain them.

Regarding data collection, limitations included the relatively low temporal resolution of bed data relative to transport data, misdetection of grains < 1 mm with video-based transport method, and inability to distinguish among grain sizes < 2.8 mm on bed photographs. As the intensity of bed adjustments decreased with time from changes in sediment feed, bed data was collected more often when adjustments to changes were more active to optimize results. Misdetection of small grains might have affected results for sand, although errors were expected to be small because grains < 1 mm comprised only 2–3% of the sediment mixture. Grain-size distributions for the bed surface were truncated at 2.8 mm, which was expected to cause only a small systematic error that would not affect the temporal patterns of textural adjustment.

5.5 Future research directions

This study increases the understanding of the role of sediment feed regime on channel adjustment, but there are still topics that remain unexplored. As mentioned, not all feed regimes were replicated and those that were, started from different initial beds. Repeating the exact sequence of runs followed in the experiment would give a good idea of how much variability should be attributed to feed regime and how much of it is intrinsic to the stochastic nature of sediment transport processes. It would also allow the use of more formal statistical tests for differences in bedload and bed characteristics among feed regimes. Another possibility would be to use the same feed regimes, but organized in a different sequence, which would give a better idea of the role of bed history and how important are initial bed conditions. One could test, for example, whether a large pulse mobilizes more sediment when introduced towards the end of the experiment when cumulative effects of feed on bed slope and storage were the largest.

Although the effects of sediment feed texture relative to bed texture have been analyzed (*Curran and Wilcock*, 2005; *Venditti et al.*, 2010), it would be interesting to run the same experiment, but with a finer sediment feed texture than bed texture to see how this affects channel response to changes in feed, grain-size dependence, and downstream fining on the bed surface. One could expect the permanent introduction of finer sediment to result in more intense sediment transport and less sediment storage, as the bed surface becomes smoother and the proportion of partially mobile sediment is reduced. Or, it could be expected for the bed surface to coarsen even more after finer sediment pulses as observed by *Johnson et al.* (2015).

As described in *Gaeuman et al.* (2017) and observed in this experiment, the sediment injection point influences the spatial patterns of bed aggradation and degradation, which condition changes in bed morphology. It would be interesting to study these effects in an experiment were sediment feed location is varied. Feed location could vary in the transverse direction (e.g., localized vs. well-spread, at one side vs. the other). Two contrasting feed regimes could be used to compare between the effects of feed location and feed regime. One could expect that differences in feed location would influence the development of large-scale bedforms, whereas feed regime would dictate the overall intensity of changes and their temporal signal. The location of sediment feed could also be varied along the flume (i.e., upstream vs. center) to also discuss the effects of changes in feed upstream of feed location.

Although results supported that constant feed promoted larger sediment storage, they were likely influenced by the cumulative increase in bed slope. It would be interesting to test this hypothesis starting each run from the same initial bed conditions. For simplicity, the experiment could first use uniform sediment and only two contrasting feed regimes (i.e., constant vs. one large pulse), which could be replicated. The same experiment could be done using a poorly sorted mixture, like the one used here, to test the effects of sediment sorting in the results.

To isolate the effects of feed regime, the experiment was conducted under steady flow conditions, which are not likely found in nature. Flow discharge varies within a flood, seasonally, and from year to year. Previous studies have shown that hydrologic regime influences the degree of armor (e.g., *Hassan et al.*, 2006) and that flood recurrence interval influences the degree of downstream sediment sorting (*Ferrer-Boix and Hassan*, 2015). Hysteresis in bedload rate is commonly observed with hydrographs (e.g., *Hassan et al.*, 2006; *Mao*, 2012) because of differences in bed state and sediment availability between the falling and rising limbs. It would be interesting to study the effects of sediment feed under unsteady flow, but a simple design might be more suitable to start and separate the effects of feed from those of flow. One possibility would be to use a simple unsteady hydrograph and repeat it, but using feed regimes that contrast in their magnitude and frequency as the ones used in this study (i.e., constant vs. one large pulse). Another possibility would be to study the effects of the timing of sediment feed on channel adjustments under unsteady flow. In this case one could use the same hydrograph and besides constant feeding and introducing one large pulse in the rising limb, the large pulse could be introduced instead during the falling limb in some runs for comparisons. *Ferrer-Boix and Hassan* (2015) studied channel response to water pulses under constant feed and how flood recurrence interval affected these results. They inherited the bed from this experiment and subjected it to constant feed, but increased the flow occasionally changing the recurrence interval. It would be interesting to further explore the influence of flood recurrence interval, but using also episodic feed regimes. One could explore, for example, which combinations of flood magnitude-duration and recurrence interval are more effective in removing the signal of a large sediment pulse in bed storage.

Changes in land cover due to human activities influence sediment sources and sediment supply to streams from local to basin scales. The construction and removal of dams affect sediment supply to downstream reaches (e.g., *Smith and Mohrig*, 2017). Forest activities, which include construction of roads and deforestation near stream banks, can provide additional sources of sediment to channels (e.g., *Croke et al.*, 1999; *Reid and Hassan*, 2016). Physical modeling is a good alternative to explore the effects of human activities on river systems, especially considering that economic development is usually accompanied by changes on land uses and creates new challenges for river management. For example, the impact of construction and maintenance of major oil pipeline projects on sediment supply regimes to streams could be an interesting future research topic.

Bibliography

Akaike, H. (1974), A new look at the statistical model identification, *IEEE T. Automat. Contr.*, *19*(6), 716-723, doi:10.1109/TAC.1974.1100705.

Ancey, C., and J. Heyman (2014), A microstructural approach to bed load transport: Mean behaviour and fluctuations of particle transport rates, *J. Fluid Mech.*, *744*, 129–168, doi:10.1017/jfm.2014.74.

Ancey, C., T. Böhm, M. Jodeau, and P. Frey (2006), Statistical description of sediment transport experiments, *Phys. Rev. E*, *74*, 011302, doi:10.1103/PhysRevE.74.011302.

Benda, L., and T. Dunne (1997), Stochastic forcing of sediment supply to channel networks from landsliding and debris flow, *Water Resour. Res.*, *33*(12), 2849–2863, doi:0.1029/97WR02388.

Brummer, C. J. , and D. R. Montgomery (2006), Influence of coarse lag formation on the mechanics of sediment pulse dispersion in a mountain stream, Squire Creek, North Cascades, Washington, United States, *Water Resour. Res.*, *42*, W07412, doi:10.1029/2005WR004776.

Campagnol, J., A. Radice, and F. Ballio (2012), Scale-based statistical analysis of sediment fluxes, *Acta Geophys.*, *60*(6), 1744–1777, doi:10.2478/s11600-012-0028-6.

Chartrand, S. (2017), Pool-riffle dynamics in mountain streams: implications for maintenance, formation and equilibrium, Phd thesis, Univ. of B. C, Vancouver, Canada.

Chartrand, S., M. A. Hassan, and V. Radic (2015), Pool-riffle sedimentation and surface texture trends in a gravel bed stream, *Water Resour. Res.*, *51*, 8704-8728, doi:10.1002/2015WR017840.

Chatfield, C. (1975), *The Analysis of Time Series. An Introduction*, CRC Press Company.

Church, M., and M. A. Hassan (2002), Mobility of bed material in Harris Creek, *Water Resour. Res.*, *38*(11), 1237, doi:10.1029/2001WR000753.

Church, M., M. Hassan, and J. Wolcott (1998), Stabilizing self-organized structures in gravel-bed stream channels: Field and experimental observations, *Water Resour. Res.*, *34*(11), 3169–3179, doi:10.1029/98WR00484.

Croke, J., P. Hairsine, and P. Fogarty (1999), Sediment transport, redistribution and storage on logged forest hillslopes in south-eastern Australia, *Hydrol. Process.*, *13*, 2705–2720, doi:10.1002/(SICI)1099-1085(19991215)13:17<2705::AID-HYP843>3.0.CO;2-Y.

Cui, Y., G. Parker, T. Lisle, J. Gott, M. Hansler-Ball, J. Pizzuto, N. Allmendinger, and J. Reed (2003), Sediment pulses in mountain rivers: 1. Experiments, *Water Resour. Res.*, *39*(9), 1239, doi:10.1029/2002WR001803.

Curran, J., and P. Wilcock (2005), Effect of sand supply on transport rates in a gravel-bed channel, *J.Hydraul.Eng.*, *131*, 961–967, doi:10.1061/(ASCE)0733-9429(2005)131:11(961).

Dadson, S., N. Hovius, H. Chen, W. Dade, J. Lin, M. Hsu, C. Lin, M. Horng, T. Chen, J. Milliman, and C. Stark (2004), Earthquake-triggered increase in sediment delivery from an active mountain belt, *Geology*, *32*(8), 733–736, doi:10.1130/G20639.1.

Dietrich, W., J. Kirchner, H. Ikeda, and F. Iseya (1989), Sediment supply and the development of the coarse surface-layer in gravel-bedded rivers, *Nature*, *340*(6230), 215–217, doi:10.1038/340215a0.

Eaton, B., and M. Church (2004), A graded stream response relation for bed load-dominated streams, *J. Geophys. Res.*, *109*(F3), F03011, doi:10.1029/2003JF000062.

Eaton, B., and M. Church (2009), Channel stability in bed load-dominated streams with nonerodible banks: Inferences from experiments in a sinuous flume, *J. Geophys. Res.*, *114*, F01024, doi:10.1029/2007JF000902.

Einstein, H. A. (1937), Bed load transport as a probability problem, PhD thesis, ETH Zurich, Zurich, Switzerland.

Einstein, H. A. (1950), The bed-load function for sediment transportation in open channel flows, *Tech. Bull*, 1026, U.S. Dep. of Agric., Washington, D. C.

Elgueta, M. (2014), Channel adjustment of a gravel-bed stream under episodic sediment supply regimes, *MSc Thesis*, The University of British Columbia, B.C., Canada, doi:10.14288/1.01658472.

Elgueta-Astaburuaga, M. A., and M. A. Hassan (2017), Experiment on temporal variation of bed load transport in response to changes in sediment supply in streams, *Water Resour. Res.*, *53*, doi:10.1002/2016WR019460.

Elgueta-Astaburuaga, M. A., M. A. Hassan, M. Saletti, and G. C. Clarke (2017), The effect of sediment supply regime on bedload scaling and sediment mobility, *Manuscript submitted to Water Resour. Res.*

Fenton, J. D., and J. E. Abott (1977),Initial movement of grains on a stream bed: The effect of relative protrusion , *Pr. Soc. London A*, *352*, 523–537, doi:10.1098/rspa.1977.0014.

Ferrer-Boix, C., and M. A. Hassan (2015), Channel adjustments to a succession of water pulses in gravel bed rivers, *Water Resour. Res.*, *51*, 8773–8790, doi:10.1002/2015WR017664.

Foufoula-Georgiou, E., and C. Stark (2012), Introduction to special section on Stochastic Transport and Emergent Scaling on Earth's surface: Rethinking geomorphic transport–Stochastic theories, broad scales of motion and nonlocality, *J. Geophys. Res.*, *115*, F00A01, doi:10.1029/2010JF001661.

Furbish, D. J., P. K. Haff, J. C. Roseberry, and M. W. Schmeeckle (2012), A probabilistic description of the bed load sediment flux: 1. Theory, *J. Geophys. Res.*, *117*, F03031, doi:10.1029/2012JF002352.

Gaeuman, D., R. Stewart, B. Schmandt, and C. Pryor (2017), Geomorphic response to gravel augmentation and highflow dam release in the Trinity River, California, *Earth Surf. Processes Landforms*, *42*, 2523–2540, doi:10.1002/esp.4191.

Ganti, V., A. Singh, P. Passalacqua, and E. Foufoula-Georgiou (2009), Subordinated brownian motion model for sediment transport, *Phys. Rev. E*, *80*, 011111, doi:10.1103/PhysRevE.80.011111.

Ghilardi, T., M. J. Franca, and A. J. Schleiss (2014), Bed load fluctuations in a steep channel, *Water Resour. Res*, *50*, doi:10.1002/2013WR014449.

Goff, J., and P. Ashmore (1994), Gravel transport and morphological change in braided Sunwapta River, Alberta, Canada, *Earth Surf. Processes Landforms*, *19*(3), 195–212, doi:10.1002/esp.3290190302.

Hassan, M. A., and M. Church (2000), Experiments on surface structure and partial sediment transport on a gravel bed, *Water Resour. Res.*, *36*(7), 1885–1895, doi:10.1029/2000WR900055.

Hassan, M. A., M. Church, and A. P. Schick (1991), Distance of movement of coarse particles in gravel bed streams, *Water Resour. Res.*, *27*, 503–511, doi:10.1029/90WR02762.

Hassan, M. A., R. Egozi, and G. Parker (2006), Experiments on the effect of hydrograph characteristics on vertical grain sorting in gravel bed rivers, *Water Resour. Res.*, *42*(9), W09408, doi:10.1029/2005WR004707.

Hassan, M. A., D. Tonina, and T. H. Buxton (2015), Does small-bodied salmon spawning activity enhance streambed mobility? *Water Resour. Res.*, *51*(9), 7467–7484, doi:10.1002/2015WR017079.

Hassan, M. A., B. J. Hogan, S. A. Bird, C. L May, T. Gomi and D. Campbell (2008), Spatial and temporal dynamics of wood in headwater streams of the Pacific Northwest, *J. Am. Water Resour. As.*, *41*(4), 899–919, doi:10.1111/j.1752-1688.2005.tb04469.x.

Hassan, M. A., B. J. Smith, D. L. Hogan, D. S Luzi, A. E. Zimmermann and B. C. Eaton (2008), Sediment storage and transport in coarse bed streams: scale considerations, in *Gravel-Bed Rivers VI: From Process Understanding to River Restoration*, edited by H. Habersack, H. Piegay and M. Rinaldi, 473–496, Elsevier.

Hassan, M. A., A. S. Gottesfeld, D. R. Montgomery, J. F. Tunnicliffe, G. K. C. Clarke, G. Wynn, H. Jones-Cox, R. Poirier, E. MacIsaac, H. Herunter, and S. J. Macdonald (2008), Salmon-driven bed load transport and bed morphology in mountain streams, *Geophys. Res. Lett.*, *35*(4), L04405, doi:10.1029/2007GL032997.

Heyman, J., F. Mettra, H. B. Ma, and C. Ancey (2013), Statistics of bedload transport over steep slopes: Separation of time scales and collective motion, *Geophys. Res. Lett.*, *40*, 128–133, doi:10.1029/2012GL054280.

Heyman, J., H. B. Ma, F. Mettra, and C. Ancey (2014), Spatial correlations in bed load transport: Evidence, importance, and modeling, *J. Geophys. Res.*, *119*, 1751–1767, doi:10.1002/2013JF003003.

Hovius, N., and C. P. Stark (2006), Landslide-driven erosion and topographic evolution of active mountain belts, in *Landslides From Massive Rock Slope Failure*, edited by S. G. Evans, G. S. Mugnozza, A. Strom, and R. L. Hermanns, 573–590, Springer, Dordrecht, Netherlands, doi:10.1007/978-1-4020-4037-5_30.

Hurst, H. E. (1951), Long-term storage capacity of reservoirs, *Trans. Am. Soc. Civ. Eng*, *116*, 770–808.

Ikeda, H. (1989), Sedimentary controls on channel migration and origin of point bars in sandbedded meandering rivers, *American Geophysical Union Water Resources Monograph*, *12*, 51–69.

Iseya, F. and H. Ikeda (1987), Pulsations in bedload transport induced by a longitudinal sediment sorting; a flume study using sand gravel mixtures, *Geogr. Ann. A*, *69*, 15–27, doi:10.2307/521363.

Jackson, W., and R. Beschta (1982), A model of 2-phase bedload transport in an Oregon coast range stream, *Earth Surf. Processes Landforms*, *7*(6), 517–527, doi:10.1029/2005WR004707.

Johnson, J. P. L., A. C. Aronovitz, and W. Kim (2015), Coarser and rougher: Effects of fine gravel pulses on experimental step-pool channel morphodynamics, *Geophys. Res. Lett.*, *42*(20), 8432–8440, doi:10.1002/2015GL066097.

Jones, J. (2012), The impact of fine sediment on macro-invertebrates, *River Res. Appl.*, *28*(8), 1055–1071, doi:10.1002/rra.1516.

Kondolf, G. M., and M. G. Wolman (1993), The sizes of salmonid spawning gravels, *Water Resour. Res.*, *29*(7), 2275–2285, doi:10.1029/93WR00402.

Koutsoyiannis, D., and A. Montanari (2007), Statistical analysis of hydroclimatic time series: Uncertainty and insights, *Water Resour. Res*, *43*, W05429, doi:10.1029/2006WR005592.

Lancaster, S. T. (2008), Evolution of sediment accommodation space in steady state bedrock-incising valleys subject to episodic aggradation, *J. Geophys. Res.*, *113*(F4), F04002, doi:10.1029/2007JF000938.

Lane, S., K. Richards, and J. Chandler (1995), Morphological estimation of the time-integrated bed-load transport rate, *Water Resour. Res.*, *31*(3), 761–772, doi:10.1029/94WR01726.

Lisle, T.(2012), Transport capacity, bedrock exposure, and process domains, in *Gravel-bed Rivers: Processes, Tools, and Environments*, edited by M. Church, P. Biron, and A. Roy, 419–423, Wiley-Blackwell, doi:10.1002/9781119952497.ch30.

Lisle, T.(2008), The evolution of sediment waves influenced by varying transport capacity in heterogeneous rivers, in *Gravel-bed Rivers VI: From Process Understanding to River Restoration*, edited by H. Habersack, H. Piegay and M. Rinaldi, 443–469, Elsevier., doi:10.1016/S0928-2025(07)11136-6.

Lisle, T., and M. Church (2002), Sediment transport-storage relations for degrading, gravel bed channels, *Water Resour. Res.*, *38*(11), 1219, doi:10.1029/2001WR001086.

Lisle, T., and M. Madej (1992), Spatial variation in armoring in a channel with high sediment supply, in *Dynamic of Gravel Bed Rivers*, edited by P. Billi, R. D. Hey, C. R. Thorne, and P. Tacconi, 277–291, John Wiley, New York.

Lisle, T. E., F. Iseya, and H. Ikeda (1993), Response of a channel with alternate bars to a decrease in supply of mixed-size bed load a flume experiment, *Water Resour. Res.*, *29*(11), 3623–3629, doi:10.1029/93WR01673.

Lisle, T., Y. Cui, G. Parker, J. E. Pizutto, and A. M. Dodd (2001), The dominance of dispersion in the evolution of bed material waves in gravel-bed rivers, *Earth Surf. Process. Landforms*, *26*(13), 1409–1420, `doi:10.1002/esp.300`.

Luzi, D.S. (2014), Sediment transport and morphological response of a semi-alluvial channel. Insights from a Froude scales laboratory model, Phd thesis, Univ. of B. C., Vancouver, Canada.

Ma, H., J. Heyman, F. M. X. Fu, C. Ancey, and G. Parker (2014), Bedload transport over a broad range of time scales: Determination of three regimes of fluctuations, *J. Geophys. Res.*, *119*, 2653–2673, `doi:doi:10.1002/2014JF003308`.

Mackenzie, L. G., and B. C. Eaton (2017), Large grains matter: contrasting bed stability and morphodynamics during two nearly identical experiments, *Earth Surf. Processes Landforms*, *42*, 1287–1295, `doi:10.1002/esp.4122`.

Madej, M., and V. Ozaki (1996), Channel response to sediment wave propagation and movement, Redwood Creek, California, Usa, *Earth Surf. Processes Landforms*, *21*(10), 911–927, doi:10.1002/(SICI)1096-9837(199610)21:10<911::AID-ESP621>3.0.CO;2-1.

Madej, M. A., D. G. Sutherland, T. E. Lisle, and B. Pryor (2009), Channel responses to varying sediment input: A flume experiment modeled after Redwood Creek, California, *Geomorphology*, *103*(4), 507–519, `doi:10.1016/j.geomorph.2008.07.017`.

Mao, L. (2012), The effect of hydrographs on bed load transport and bed sediment spatial arrangement, *J. Geophys. Res.*, *117*, F03024, `doi:10.1029/2012JF002428`.

Mathers, K. L., S. P. Rice and P. J. Woods (2017), Temporal effects of enhanced fine sediment loading on macroinvertebrate community structure and functional traits, *Sci. Total Environ.*, *599–600*, 513–522, `doi:10.1016/j.scitotenv.2017.04.096`.

Meyer-Peter, E., and R. Müller (1948), Formulas for bed-load transport, *Proc.*, 2nd Meeting, IAHR, Stockholm, Sweden, 39–64.

Millar, R. (1999), Grain and form resistance in gravel-bed rivers, *J. Hydraul. Res.*, *37*(3), 303–312, `doi:10.1080/00221686.1999.9628249`.

Montgomery, D., and J. Buffington (1997), Channel-reach morphology in mountain drainage basins, *Geol. Soc. Am. Bull.*, *109*(5), 596–611, doi:10.1130/0016-7606(1997)109<0596:CRMIMD>2.3.CO;2.

Montgomery, D., and H. Piégay (2003), Wood in rivers: Interactions with channel morphology and processes, *Geomorphology*, *51*, 1–5, `doi:10.1016/S0169-555X(02)00322-7`.

Nelson, P. A., J. G. Venditti, W. E. Dietrich, J. W. Kirchner, H. Ikeda, F. Iseya, and L. S. Sklar (2009), Response of bed surface patchiness to reductions in sediment supply, *J. Geophys. Res.*, *114*, F02005, `doi:10.1029/2008JF001144`.

Naiman, R. J., J. M. Melillo, and J. E. Hobbie (1986), Ecosystem alteration of boreal forest streams by beaver (Castor canadensis), *Ecology*, *67*, 1254–1269, `doi:10.2307/1938681`.

Paola, C. and R. Seal (1995), Grain size patchiness as a cause of selective deposition and downstream fining, *Water Resour. Res.*, *31*(5), 1395–1407, `doi:10.1029/94wr02975`.

Parker, G. (1992), Some random notes on grain sorting, in *International Seminar on Grain Sorting, Ascona, Switzerland*, Mitteilungen 117 der Versuchsanstalt für Wasserbau, Hydrologie und Glaziologie, ETH Zurich, 19–76.

Parker, G. (2008), Transport of gravel and sediment mixtures, in *Sedimentation Engineering ASCE Manual 54*, edited by M. Garcia, 165–251, Reston, VA, `doi:10.1061/9780784408148.ch03`.

Parker, G. and P. C. Klingeman (1982), On why gravel bed streams are paved, *Water Resour. Res.*, *18*(5), `doi:1409-1423.10.1029/WR018i005p01409`.

Parker, G., S. Dhamotharan, and H. Stefan (1982), Model experiments on mobile, paved gravel bed streams, *Water Resour. Res.*, *18*(5), 1395–1408, `doi:10.1029/WR018i005p01395`.

Powell, D. (1998), Patterns and processes of sediment sorting in gravel-bed rivers, *Prog. Phys. Geog.*, *22*(1), 1–32.

Pryor, B. S., T. Lisle, D. S. Montoya, and S. Hilton (2011), Transport and storage of bed material in a gravel-bed channel during episodes of aggradation and degradation: a field and flume study, *Earth Surf. Process. Landforms*, *36*(15), 2028–2041, `doi:10.1002/esp.2224`.

Recking, A, F. Liébault, C. Peteuil, and T. Jolimet (2012), Testing bedload transport equations with consideration of time scales, *Earth Surf. Process. Landforms*, *37*(7), 774–789, `doi:10.1002/esp.3213`.

Reid, L. M., and T. Dunne (2003), Sediment budgets as an organizing framework in fluvial geomorphology, in *Tools in Fluvial Geomorphology*, 463–500, John Wiley & Sons, Ltd, `doi:10.1002/0470868333.ch16`.

Reid, D., and M. Hassan (2016), Reach-scale contributions of road-surface sediment to the Honna River, Haida Gwaii, BC, *Hydrol. Process.*, *30*, 3450–3465, `doi:10.1002/hyp.10874`.

Riebe, C., L. S. Sklar, B. T. Overstreet, and J. K. Wooster (2014), Optimal reproduction in salmon spawning substrates linked to grain size and fish length, *Water Resour. Res.*, *50*, 898–918, `doi:10.1002/2013WR014231`.

Ryan, S. (2001), The influence of sediment supply on rates of bedload transport: A case study of three streams on the San Juan National Forest, in *Proceeding of the Seventh Federal Interagency Sedimentation Conference*, III, 48–54, Reno, Nevada.

Saletti, M., P. Molnar, A. Zimmermann, M. A. Hassan, and M. Church (2015), Temporal variability and memory in sediment transport in an experimental step-pool channel, *Water Resour. Res*, *51*, `doi:10.1002/2015WR016929`.

Seal, R. and C. Paola (1995), Observations of downstream fining on the North Fork Toutle River near Mount St. Helens, Washington, *Water Resour. Res.*, *31*(5), 1409–1419, `doi:10.1029/94wr02976`.

Shang, P., and S. Kamae (2005), Fractal nature of time series in the sediment transport phenomenon,, *Chaos Soliton. Fract.*, *26*(3), 997–1007, `doi:10.1016/j.chaos.2005.01.051`.

Shields, A.(1936), Anwendung der Aehnlichkeitsmechanik und der Turbulenzforschung auf die Geschiebebewegung, *Mitt. Preuss. Versuch. Wasserbau und Schiffbau*, *26*, Berlin, Germany.

Singh, A., F. Porte-Agel, and E. Foufoula-Georgiou (2010), On the influence of gravel bed dynamics on velocity power spectra, *Water Resour. Res.*, *46*, W045099 doi:10.1029/2009WR008190.

Singh, A., K. Fienberg, D. J. Jerolmack, J. Marr, and E. Foufoula-Georgiou (2009), Experimental evidence for statistical scaling and intermittency in sediment transport rates, *J. Geophys. Res*, *114*, F01025, doi:10.1029/2007JF000963.

Sklar, L. S., J. Fadde, J. G. Venditti, P. Nelson, M. A. Wydzga, Y. Cui, and W. E. Dietrich (2009), Translation and dispersion of sediment pulses in flume experiments simulating gravel augmentation below dams, *Water Resour. Res.*, *45*, W08439, doi:10.1029/2008WR007346.

Smith, V., and D. Mohrig (2017), Geomorphic signature of a dammed Sandy River: The lower Trinity River downstream of Livingston Dam in Texas, USA , *Geomorphology*, *297*, 122–136 doi:10.1016/j.geomorph.2017.09.015.

Sutherland, D., M. Ball, S. Hilton, and T. Lisle (2002), Evolution of a landslide-induced sediment wave in the Navarro River, California, *Geol. Soc. Am. Bull.*, *114*(8), 1036–1048, doi:10.1130/0016-7606(2002)114<1036:EOALIS>2.0.CO;2

Turowski, J. M. (2010), Probability distributions of bed load transport rates: A new derivation and comparison with field data, *Water Resour. Res.*, *46*, W08501, doi:10.1029/2009WR008488.

Venditti, J., P. Nelson, and W. Dietrich (2008), The domain of bedload sheets, in *Marine Sandwave and River Dune Dynamics III*, edited by D. Parsons, J. Best, and A. Trentesaux, 315–321, Leeds University, Leeds.

Venditti, J. G., W. E. Dietrich, P. A. Nelson, M. A. Wydzga, J. Fadde, and L. Sklar (2010), Effect of sediment pulse grain size on sediment transport rates and bed mobility in gravel bed rivers, *J. Geophys. Res.*, *115*, F03039, doi:10.1029/2009JF001418.

vonFlotow, C. (2013), Temporal adjustments of a streambed following an episodic sediment supply regime, MS thesis, Univ. of B. C., Vancouver, Canada.

Waters, K. A., and J. C. Curran (2012), Investigating step-pool sequence stability , *Water Resour. Res.*, *48*, W07505, doi:10.1029/2011WR011436.

Wilcock, P. R. (1992), Experimental investigation of the effect of mixture properties on transport dynamics, in *Dynamics of Gravel-Bed Rivers*, edited by P. Billy, R. D. Hey, C. R. Thorne and P. I. Taccon, 109–131, John Wiley & Sons.

Wilcock, P., and J. Crowe (2003), Surface-based transport model for mixed-size sediment, *J. Hydraul. Eng-ASCE*, *129*(2), 120–128, doi:10.1061/(ASCE)0733-9429(2003)129:2(120).

Wilcock, P. R. and B. T. DeTemple (2005), Persistence of armor layers in gravel-bed streams, *Geophys. Res. Lett.*, *32*(8), 1–4, doi:10.1029/2004GL021772.

Wilcock, P., and B. McArdell (1993), Surface-based fractional transport rates - mobilization thresholds and partial transport of a sand-gravel sediment, *Water Resour. Res.*, *29*(4), 1297–1312, doi:10.1061/(ASCE)0733-9429(2003)129:2(120).

Wong, M., and G. Parker (2006), Reanalysis and correction of bed-load relation of Meyer-Peter and Muller using their own database, *J. Hydraul. Eng-ASCE*, *132*(11), 1159–1168, doi:10.1061/(ASCE)0733-9429(2006)132:11(1159).

Yager, E. M., M. Kenworthy, and A. Monsalve (2015), Taking the river inside: Fundamental advances from laboratory experiments in measuring and understanding bedload transport processes, *Geomorphology*, *244*, 21–32, doi:10.1016/j.geomorph.2015.04.002.

Zimmermann, A. (2009), Experimental investigations of step-pool channel formation and stability, Phd thesis, Univ. of B. C, Vancouver, Canada.

Zimmermann, A. (2010), Flow resistance in steep streams: An experimental study, *Water Resour. Res.*, *46*, W09536, doi:10.1029/2009WR007913.

Zimmermann, A. E., M. Church, and M. A. Hassan (2008), Video-based gravel transport measurements with a flume mounted light table, *Earth Surf. Processes Landforms*, *33*(14), 2285–2296, doi:10.1002/esp.1675.